Geotechnical Investigation

BergerABAM
1111 Main Street, Suite 300
Vancouver, WA 98660-2958

Tesoro Savage Vancouver Energy Distribution Terminal – Dock Facility Port of Vancouver, USA

Prepared by

GRI
Washington & Oregon

September 5, 2014

EX 0188-TSS

TABLE OF CONTENTS

Page

INTRODUCTION 1
PROJECT DESCRIPTION 1
Overview 1
SITE CONDITION AND BACKGROUND 2
Topography, Bathymetry, and Site Background 2
Geology 2
SUBSURFACE CONDITIONS 2
General 2
Soils 3
Groundwater 3
CONCLUSIONS AND RECOMMENDATIONS 4
General 4
Seismic Considerations 4
Slope Grading and Protection 9
Pile Support 9
Trestle Abutment Earth Pressures 13
Design Review and Construction Services 14
LIMITATIONS 15

Figures
Figure 1: Vicinity Map
Figure 2: Site Plan
Figure 3: Liquefaction Hazard Analysis – Contingency Level Earthquake
Figure 4: Liquefaction Hazard Analysis – Design Earthquake
Figure 5: Berth 13 Trestle and Dock Profile
Figure 6: Lateral Spreading Loads Trestle and Dock Piles
Figure 7: Surcharge-Induced Lateral Pressure

Appendix A: Field Explorations and Laboratory Testing

Appendix B: Site-Specific Seismic Hazard Study

INTRODUCTION

At your request, GRI has completed a geotechnical investigation at the Port of Vancouver (Port) Berth 13 dock and trestle as part of the Tesoro Savage Vancouver Energy Distribution Terminal (TSVEDT). The Vicinity Map, Figure 1, shows the general location of the project. The investigation was conducted to evaluate subsurface conditions at the site and provide our conclusions and recommendations for design and construction of the proposed modifications. Our investigation has included a review of available geotechnical information, subsurface explorations, laboratory testing, and engineering analyses.

The following geotechnical information has been reviewed for this investigation:

> GRI, December 2013, Geotechnical Report, Tesoro Savage Vancouver Energy Distribution Terminal - Upland Facility, Port of Vancouver, USA; prepared for BergerABAM
>
> Dames and Moore, March 31, 1993, Geotechnical Investigation, Proposed T-Docks/Dolphins, Port of Vancouver, Washington; prepared for URS Consultants
>
> GRI, May 18, 2011, Geotechnical Report, NW Gateway Avenue Rail Bridge and Access to Terminal 5, Port of Vancouver, USA; prepared for HDR, Inc.
>
> Goble, Rauche, Likins and Associates, Inc., 1993, Dynamic Pile Measurements, October 11, 1993, T1 and T2 Dock, Port of Vancouver, Vancouver, Washington

PROJECT DESCRIPTION

Overview

Modifications to the existing Berth 13 dock and trestle are being designed to update the facility to current seismic design standards. Berth 13 consists of a T-shape dock and trestle, as shown on Figure 2. Proposed modifications will be primarily located between an area of proposed ground improvement on the riverbank and the Columbia River channel. We have assumed the area of ground improvement will include the trestle abutment. BergerABAM has indicated the channel depth in front of the dock is a minimum of elevation -43 ft Columbia River Datum (CRD). All elevations within this report reference NGVD29 datum, which is the project datum. Elevations can be converted to NGVD29 by adding approximately 1.78 ft to CRD.

Modifications include reconstruction of the existing deck; strengthening the existing dock, trestle, and mooring structures; and installation of ground anchors inside existing dock and dolphin piles. Landward of the Ordinary High Water Mark (OHWM), there will be two new dolphin pile structures located on the riverbank, new pile structures to support walkways that access existing dolphins, and new piles for the trestle abutment foundation. Additional improvements in the dock area (Area 400) are described in our above-referenced December 2013 report for the upland facility.

Seismic design of the dock modifications is intended to meet the requirements of the upcoming American Society of Civil Engineers (ASCE) standard, *Seismic Design of Pile-Supported Piers and Wharves*.

The proposed riverbank ground improvement is being designed by Hayward Baker, Inc., a ground improvement specialty contractor, to meet specified seismic performance criteria. The ground

improvement design will affect the performance of the proposed Berth 13 modifications along the shore. We anticipate the impact of ground improvement on design of the dock elements will be further evaluated as the ground improvement design is developed.

SITE CONDITION AND BACKGROUND

Topography, Bathymetry, and Site Background

The existing site topography and bathymetry in the vicinity of Berth 13 is shown on Figure 2. The ground surface in the upland area located behind the trestle abutment is relatively flat at about elevation +27 ft and is typically surfaced with AC pavement, gravel, or grass. Two shallow stormwater infiltration swales with a bottom elevation of about +21 to +22 ft are located north of the paved areas and are mantled with grass and shrubs. The riverbank is protected with riprap and slopes down at about 2H:1V to a sandy beach at about elevation +17 ft. The sandy beach is relatively flat and slopes down at about 6H:1V to elevation +3 ft. Below elevation +3 ft, the slope increases to about 2.5H:1V. The existing mudline at the face of the dock is in the range of elevation -35 to -38 ft.

Geology

Based on our understanding of the geology at the site, our experience with nearby sites, and the available exploration data, the upland portion of the project area is mantled by fill that is underlain by recent alluvial soils. The fill typically consists of fine- to coarse-grained sand with silt, silty sand, sandy silt, and gravel. The alluvial soils beneath the fill and the mudline in the river typically consist of loose to medium dense sand and very soft to medium stiff silt. Gravel ranging from gravel in a matrix of sand to open-graded gravel with cobbles and possible boulders is present below elevations ranging from about -50 to -60 ft. Geologic investigations for the proposed Interstate 5 bridge replacement, about 3 miles upstream from the project site, indicate the alluvial gravels on the Washington side of the Columbia River can be up to 100 ft thick.

Available geologic information indicates the alluvial gravels are underlain by the Troutdale Formation, a Pliocene-age unit of well-consolidated or cemented conglomerate and sandstone (Beeson et al., 1991).

SUBSURFACE CONDITIONS

General

Subsurface materials and conditions at the dock site were investigated between July 29 and October 29, 2013, with four borings, designated B-23 through B-26, and one cone penetration test (CPT) probe, designated CPT-6. The borings were advanced to depths of 80 to 104 ft, and the probe was advanced to a depth of about 83 ft. The locations of the borings and CPT probe are shown on Figure 2.

The field exploration and laboratory testing programs completed for this investigation are described in Appendix A. Logs of the borings and CPT probe are shown on Figures 1A through 5A. The terms used to describe the soils encountered in the borings and CPTs are defined in Tables 1A and 2A.

In addition to the borings and CPT probe for this investigation, GRI also reviewed and utilized the logs of previous explorations made by GRI and others for other nearby projects. The soils encountered in the explorations for this investigation are consistent with previous investigations.

Soils

For the purpose of discussion, the materials disclosed by the explorations have been grouped into three units based on their physical characteristics, geologically significant features, and engineering properties. Listed as they were encountered from the ground surface downward, the units are:

1. **FILL**
2. **SAND**
3. **GRAVEL**

1. FILL. Fill was encountered at the ground surface in the upland explorations (Borings B-23 through B-25 and CPT-6) and extends to depths ranging from about 20 to 25 ft (about elevation +7 to +2 ft). Asphaltic-concrete pavement between 4 and 12 in.-thick over 10 to 24 in. of crushed rock base course was encountered at the ground surface in boring B-23 and B-25. Below the pavement and base course in boring B-23 and B-25, and at the ground surface of the other upland explorations, the fill consists of fine to coarse-grained sand with a trace of silt and scattered gravel and organic debris. Interbedded layers of silt and sandy silt up to about 4 in. thick were encountered in the fill. Based on N-values of 9 to 36 blows/ft and CPT tip resistances of about 50 to 240 tsf, the relative density of the fill ranges from loose to dense and is more typically medium dense. The moisture content of fill ranges from 7 to 27% and generally increases with increasing silt content.

2. SAND. Sand was encountered below the fill in the upland borings and at the ground surface in boring B-26. The sand extends to depths ranging from 64 to 87 ft (elevation -51 ft to -60 ft). The sand is fine to coarse grained and contains a trace to some silt. Interbedded layers of sandy silt and silt ranging from 1 in. to 5-ft-thick are present in the sand. The sand contains scattered a trace of gravel in all of the borings except boring B-24. Scattered wood debris was encountered below a depth of 25 ft in boring B-26. Based on N-values of 6 to 33 blows/ft and CPT tip resistances of about 50 to 150 tsf, the relative density of the sand typically ranges from loose to dense. More typically, the sand is medium dense with the exception of the sand in boring B-26 which has N-values of 2 to 10 blows/ft in the upper 40 ft indicating the upper 40 ft of sand is relatively loose. The moisture content of the sand ranges from 21 to 39%. The moisture content of silt layers ranges from 41 to 46%.

3. GRAVEL. Gravel was encountered beneath the sand in all four new borings. The gravel has a matrix of sand and silt and contains scattered cobbles and possible boulders. Loss of drilling fluid and caving of the borehole in Boring B-26 indicates that there are open-graded gravels. Based on N-values of 38 blows/ft and 50 blows for less than 6 in. of penetration, the relative density of the gravel ranges from dense to very dense.

Groundwater

Groundwater levels in the project area fluctuate in response to seasonal river levels, precipitation, and daily tidal fluctuations in the river. It should be anticipated the groundwater level in the project area will reflect the water levels in the Columbia River. Shallow perched groundwater conditions can develop above the less-permeable silty deposits at the site and approach the ground surface during periods of prolonged or intense rainfall.

The Columbia River level is lowest in late summer and early fall and is highest during winter storm events and the spring freshet, when snowmelt runoff causes high river flows. Historical low water in the last 20 years is about elevation +2.5 ft. The 100-year flood and OHWM is about elevation +27 and +17 ft, respectively.

CONCLUSIONS AND RECOMMENDATIONS

General

The borings and CPT probe completed for this investigation indicate the upland area is mantled with about 20 to 25 ft of sand fill that is underlain by alluvial sand and gravel that extend into the Columbia River. The top of a dense gravel unit ranges from about elevation -51 to -60 ft. Groundwater levels at the site will fluctuate in response to precipitation and levels in the nearby Columbia River. Shallow perched groundwater conditions may develop in the fill and approach the ground surface during periods of prolonged precipitation.

The primary geotechnical considerations for the Berth 13 modifications include axial and lateral capacity of proposed and existing piles and seismic hazard considerations. As discussed with BergerABAM, we understand new piles or foundation elements will be installed landward of the OHWM.

The loose to medium dense sand below the water table is liquefiable for the larger seismic hazard levels evaluated. Liquefaction of these soils will result in settlement, a reduction of soil strength, and significant lateral spreading near the riverbank. Lateral spreading is the horizontal displacement of large volumes of soil toward the river as a result of the liquefaction of underlying layers. Lateral ground movement will cause lateral loading and deformation of piles located within the zone of movement. Ground improvement is planned along the riverbank to mitigate the impacts of liquefaction-induced settlement and lateral spreading deformation on the TSVEDT facility improvements near the river. Although the ground improvement design is under development, we have assumed ground improvement will be completed upland of the trestle abutment to limit deformation of the abutment. Ground improvement will not be completed waterward of the OHWM; therefore, seismic-induced ground deformations will impact design of the riverside dock and trestle piles. Further evaluation of the dock modifications may be required as the ground improvement design is developed.

The following sections of this report provide our conclusions and recommendations for design and construction of the proposed modifications.

Seismic Considerations

General. The upcoming ASCE standard, *Seismic Design of Pile-Supported Piers and Wharves* (ASCE SSDPW), defines ground motions for three seismic hazard levels: the Operating Level Earthquake (OLE), the Contingency Level Earthquake (CLE), and the Design Earthquake (DE).

> OLE is defined by 50% probability of exceedance in 50 years, which corresponds to an earthquake with an expected recurrence interval of 72 years and represents a performance level with minimal structural damage.

CLE is defined by 10%probability of exceedance in 50 years, which corresponds to an earthquake with an expected recurrence interval of 475 years, and represents a performance level of controlled and repairable structural damage.

DE is defined per ASCE 7-05 which develops the response spectra based on ground motions associated with the Maximum Considered Earthquake (MCE), which is generally represented by a probabilistic earthquake with a 2% probability of exceedance in 50 years (return period of about 2,500 years), except where subject to deterministic limitations (Leyendecker et al., 2000). The design-level response spectrum that represents the DE is obtained by taking two-thirds of the MCE level ground motions.

The bedrock earthquake motions for each of the hazard levels were selected from the 2008 U.S. Geologic Survey (USGS) probabilistic seismic hazard maps for the coordinates of 45.65° N latitude and 122.71° W longitude. The code-based spectra are developed using two spectral response coefficients, S_S and S_1, corresponding to periods of 0.2 and 1.0 second. These bedrock spectral ordinates are adjusted for Site Class with the short- and long-period site coefficients, F_a and F_v, based on subsurface conditions or with a site-specific response analysis. A summary of the OLE, CLE, and DE hazard level S_S and S_1 coefficients for the dock are tabulated below.

SUMMARY OF SEISMIC DESIGN PARAMETERS

Hazard Level	Ss	S1
Operating Level Earthquake (OLE)	0.11	0.03
Contingency Level Earthquake (CLE)	0.45	0.16
Design Earthquake (DE)	0.94	0.41

The site is generally designated as Site Class D based on the average shear wave velocity (V_s100) in the upper 100 ft per Section 20.4 of ASCE 7-05. Based on our evaluation, the seismic shaking from the OLE is insufficient to cause liquefaction, and the code-based Site Class D is recommended to estimate the ground response spectral acceleration. However, our analysis has identified a potential risk of liquefaction for the CLE and DE hazard levels. In accordance with ASCE SSDPW, sites with subsurface conditions identified as vulnerable to failure or collapse, such as liquefiable soils, shall be classified as Site Class F. For Site Class F sites, ASCE SSDPW Section 4.3.2 requires completion of a site-specific ground motion analysis for structures with a fundamental period of vibration greater than 0.5 second. BergerABAM has indicated the fundamental period of the dock is between 0.5 and 1.0 second. Due to these anticipated longer periods, a site-specific seismic ground motion analysis was completed for CLE and DE hazard levels at the dock and trestle area. The ground motion analysis was completed with the aid of the computer software D-MOD2000, a non-linear seismic soil response software developed by GeoMotions, LLC. The D-MOD2000 analyses are further discussed in Appendix B.

The site-specific response modeling results were compared with both Site Class D and E spectra due to the liquefaction considerations. The modeling indicates that 80% of code-based Site Class E spectral accelerations provide an appropriate estimate of the CLE hazard level in accordance with the ASCE SSDPW. The site-specific response modeling indicates the MCE hazard level spectral accelerations are greater than Site Class D spectral accelerations at periods less than 1.8 seconds. However, based on the

research by Youd and Carter (2005), Site Class D is likely conservative for structures with a period less than 1 second. In this regard, the code-based Site Class D is recommended to estimate the spectral accelerations at short periods ($T < 0.89$ second). At periods between 0.89 and 1.8 seconds, we conservatively recommend the design spectrum include an increase above Site Class D and E to transition to longer periods and envelop the estimated site-specific ground surface response. At periods greater than approximately 1.8 seconds, the site-specific response spectrum is less than 80% of Site Class E, which is the minimum spectral amplification allowed by ASCE 7-05 for liquefied conditions. The DE is determined by taking two-thirds of the MCE. The results of our site-specific ground motion analysis, including plots of the spectral amplification ratio and recommended response spectra, are provided in Appendix B.

Liquefaction. Liquefaction is a process by which saturated, granular materials, such as sand, and non-plastic silts, temporarily lose strength during and immediately after a seismic event. Liquefaction occurs as seismic shear stresses propagate through a saturated soil and distort the soil structure causing loosely packed groups of particles to contract or collapse. If drainage is impeded and cannot occur quickly, the collapsing soil structure increases the pore water pressure between the soil grains. If the pore water pressure increases to a level approaching the weight of the overlying soil, the granular layer temporarily behaves as a viscous liquid rather than a solid. As strength is lost, there is an increased risk of settlement, lateral spread, and/or slope instability, particularly along waterfront areas. Liquefaction-induced settlement occurs as the elevated pore water pressures dissipate and the soil consolidates after the earthquake.

The potential for liquefaction at the site was evaluated with the simplified method based on two methodologies. The first methodology is based on the simplified procedure by Youd, et al. (2001). The analysis was completed with the aid of the computer software LiquefyPro, a seismically induced liquefaction and settlement analysis software developed by CivilTech Corporation. The second methodology is based on the simplified procedure by Idriss and Boulanger (2008). Both methodologies utilize the peak ground acceleration (PGA) adjusted for site amplification to estimate the cyclic shear stress ratio (CSR) experienced by the soil and in situ test data from the borings or CPTs to estimate the cyclic resistance ratio (CRR) of the soil. The factor of safety (FS) against liquefaction is estimated as the CRR divided by the CSR. The OLE PGA was based on the USGS 2008 interactive deaggregations. The CLE and DE PGAs were based on the results of site-specific ground motion analyses. The earthquake magnitudes chosen to represent the earthquake hazard levels for our liquefaction studies were based on the 2008 USGS interactive deaggregations for the OLE, CLE, and DE return intervals as well as the results of our site-specific ground motion analysis for the CLE and DE hazard level. The input values used for our liquefaction studies are tabulated below.

Hazard Level	PGA, g	Earthquake Magnitude, M
Operating Level Earthquake (OLE)	0.07	5.8
Contingency Level Earthquake (CLE)	0.26	8.4
Design Earthquake (DE)	0.28	9.0

For the purpose of liquefaction studies, we have conservatively assumed a groundwater level at elevation +12 ft, which corresponds to the seasonal high average daily river level. Based on our liquefaction studies, we estimate the risk of liquefaction for the OLE hazard level is low, i.e., the FS against liquefaction is greater than 1. The output from our liquefaction studies indicates the loose to medium dense sands

below the groundwater level have a factor of safety against liquefaction less than 1 and could liquefy during the CLE and DE hazard level. A maximum free-field seismic settlement of about 24 in. was estimated for both the CLE and DE hazard levels based on the existing unimproved soil profile at boring B-26. The factor of safety against liquefaction for the CLE and DE hazard levels is summarized on Figures 3 and 4.

Lateral Spreading. Lateral spreading involves the horizontal displacement of large volumes of soil as a result of the liquefaction of underlying soil layers. Ground displacement occurs in response to the combination of gravitational forces and inertial forces generated by an earthquake acting upon the soil mass. Lateral spread can develop on shallow sloping ground or as a flow slide moving toward a moderately steep to steep free face, such as a river channel or lake bottom. Differential internal movement within the spreading mass usually creates surface features, such as ground cracks or fissures, scarps, and/or grabens, in overlying unsaturated or non-liquefied soils. Lateral displacement may range from a few inches to many feet depending on soil conditions, the steepness of the slope, and the magnitude and epicentral distance of the earthquake. Associated differential vertical movements, or ground surface subsidence, may range up to about half of the total horizontal movement.

The method of analysis summarized in Idriss and Boulanger (2008) were used to estimate lateral spreading deformations in free-field conditions. The methodology utilizes the same inputs as the simplified method for liquefaction hazard evaluation. Additionally, lateral spreading deformations were estimated using the methods of Youd et al. (2002). The basic inputs for Youd et al. (2002) include a characterization of the soil profile in terms of grain size, fines content (silt and clay), and Standard Penetration Test N-values; the overall geometry of the riverfront slope; and the magnitude and epicentral distance of the design-basis earthquakes. The risk of liquefaction at the OLE hazard level was estimated to be very low and therefore lateral spreading was not evaluated for the OLE. The range of estimates of lateral deformation for the CLE and DE hazard levels are tabulated below.

LATERAL SPREADING ESTIMATES
(without ground improvement)

Hazard Level	Earthquake Magnitude, M	Epicentral Distance, km	Estimated Range of Lateral Deformation, ft
Contingency Level Earthquake (CLE)	8.4	86	5 to 12
Design Earthquake (DE)	9.0	86	12 to 20

The methods used to estimate the seismically induced horizontal and vertical ground displacement at the site are largely based on empirical methods and, consequently, do not provide a precise estimate of the actual ground movement that may occur. Seismic events of a lesser magnitude, or of the same magnitude but occurring at a greater epicentral distance from the site, would be expected to produce lesser horizontal and vertical ground displacements.

Design Estimates for Lateral Displacement Forces. Earthquake-induced damage to waterfront structures at sites with liquefiable soils is well documented. Stresses induced on piles are typically generated from the inertial mass of the structure and lateral soil loading from both the lateral spreading liquefied soils and the non-liquefied crust of soil generally present above the groundwater table. Case histories have shown that the forces or displacements induced by the non-liquefied soil crust are generally significantly larger than

the forces generated from the liquefied soils with reduced strengths. Design for the lateral spreading soils is typically completed by either applying estimates of soil displacements or forces to the structure. The displacement approach is commonly applied if the structure is somewhat flexible and can accommodate some deformation. The force approach is applied if the structure is more rigid and cannot accommodate the estimated movement. Based on discussions with BergerABAM, we understand the evaluation of the dock and trestle piles will likely be based on a force-based approach. Because the seismic lateral movements of the trestle abutment will be mitigated by ground improvement, we understand the abutment will be evaluated based on a displacement-based approach. The magnitude of displacement at the abutment will depend on the ground improvement design and should be evaluated as the design is developed. Preliminary earth pressures for the abutment are provided in the Trestle Abutment Earth Pressures section of this report.

A schematic cross section of the trestle alignment with the estimated lateral spreading failure surface is shown on Figure 5. The failure surface shown on Figure 5 assumes that sufficient ground improvement will be installed to limit lateral spreading at the trestle to the area below the OHWM at the CLE and DE hazard levels, which is discussed subsequently. Based on the soil profile and bathymetry, it should be assumed that lateral spreading will occur to a depth of about 35 ft below the mudline or ground surface, but no deeper than elevation -48 ft, for the CLE and DE hazard levels.

For the purpose of lateral spreading studies, we have assumed a groundwater level at elevation +7.5 ft that corresponds to the average level of the Columbia River. Based on our assumptions, the estimated soil movements will result in two different pressures acting on the trestle and dock piles: 1) unsaturated sand moving against the piles, and 2) saturated loose, liquefied sand moving against the piles. For the unsaturated sand above the ground water table, a lateral earth pressure based on an equivalent fluid unit weight of 400 pcf may be assumed to act against the trestle piles in the direction of the river for the CLE and DE hazard levels. Where the sand is saturated, a uniform rectangular pressure distribution of 250 psf may be assumed to act against the trestle piles in the direction of the river. In non-liquefied soils, passive lateral earth pressures tend to "arch" or develop a larger tributary area against piles. In this regard, we recommend assuming the lateral earth pressure against piles in the unsaturated sand material will act over an equivalent of two pile diameters. The lateral pressure against piles in the saturated liquefied sand material will act over one pile diameter. The recommended seismically induced lateral pressures are summarized on Figure 6. The extents of lateral spreading and the lateral spreading forces should be further evaluated as the ground improvement design is developed.

As noted in the ASCE SSDPW peak inertial forces do not necessarily occur at the same time as the peak soil (kinematic) loading on the structure. For this reason, consideration can be given to applying only a portion of the peak inertial loading at the same time as the kinematic loads. Design methods for evaluating combined inertial and kinematic loads are not well documented in the available literature, and ASCE SSDPW does not provide a recommended loading combination. However, another marine structures code, the Marine Oil Terminal Engineering and Maintenance Standards (MOTEMS), includes recommended load combinations for inertial and kinematic loading. In our opinion, it is reasonable to use inertial and kinematic load combinations similar to those provided in MOTEMS to evaluate the dock design.

Ground Improvement. Lateral spreading is often mitigated by constructing a zone, or buttress, of improved soil along the riverbank that will not liquefy. The buttress needs to be of sufficient width and extend to adequate depth to maintain stability following ground shaking and minimize or prevent lateral displacement toward the river of the upland portion of the site behind the buttress.

Due to the potential for large lateral spreading deformations, ground improvement will be designed and constructed to mitigate the impact of large seismic lateral displacements on the proposed transfer pipeline and structures located near the river.

Other Seismic Considerations. In our opinion, the potential for earthquake-induced fault displacement and ground rupture at the site is low unless occurring on a previously unknown or unmapped fault. Due to the topography of the site, it is our opinion the risk of damage by seiche is low. We are not aware of rigorous tsunami modeling for the Columbia River in available literature. However, based on the paper, "Tsunami Hydrodynamics in the Columbia River" (Yeh, 2012), the amplitude of potential tsunami waves at the Port is anticipated to be small at this distance from the Pacific Ocean.

Slope Grading and Protection

We understand the existing riprap and concrete debris slope protection will be left in place wherever possible. We anticipate this slope protection will have to be removed and replaced in the vicinity of the new piles to minimize the risk of obstructions during installation. Depending on the degree of disturbance and the subgrade conditions underlying the existing slope protection, a graded filter material may need to be placed prior to replacing the slope protection. GRI should observe the subgrade conditions during construction to recommend and appropriate filter gradation.

Pile Support

General. New 24-in.-diameter pipe piles (plumb and battered) are being considered for two proposed landside mooring dolphins, the reconstructed abutment, and walkway support piles. New driven piles will be located landward of the OHWM. Some strengthening of the existing 18-in.-diameter dock, trestle, and dolphin pipe piles is planned that includes installing grouted anchors or micropiles through the pipe piles into the gravel, and filling the piles with concrete. Based on discussions with the team, we understand the installation and testing of micropiles or grouted anchors will be through an assumed 10½-in.-diameter hole in the plate at the tip of the existing pipe pile. Our recommendations regarding axial and lateral capacity of the new and existing piles are summarized below.

Proposed Dolphin Piles. The locations of two proposed landside mooring dolphins are shown on Figure 2. At the request of BergerABAM, GRI evaluated 24-in.-diameter pipe piles at the proposed dolphin locations. We anticipate the piles will be driven open-end into the underlying gravel unit. We estimate 24-in.-diameter pipe piles driven with sufficiently large hammers to adequate penetration resistance can develop an ultimate compression capacity of at least 750 kips. The explorations and our experience in the area indicate the sand content and the relative density of the underlying gravel unit tend to be highly variable. As a result, it is difficult to accurately predict the actual penetration of piles into the gravel to develop the estimated ultimate capacities. However, based on our experience, we anticipate the piles will develop the design capacity at a depth of about 15 ft into the gravel plus or minus 10 ft. Assuming penetration of 15 ft into the dense gravel, the resulting pile tips will be at about elevation -68 to -70 ft based

on the available explorations. Due to the variation in subsurface conditions we recommend the piles are ordered at least 10 ft longer than the estimated tip elevation to limit the risk of splices.

Since a significant portion of the estimated ultimate compression pile capacity is derived from end-bearing resistance, the uplift capacity of the piles will be significantly less than the compressive capacity. For preliminary purposes, we estimate the 24-in.-diameter piles can develop an ultimate vertical uplift capacity of about 300 kips assuming the piles will penetrate a minimum of 15 ft into relatively dense gravel.

As discussed in the Liquefaction section of this report, the sand below the groundwater level is subject to liquefaction and/or seismically induced strength loss during the two larger hazard level events. Liquefaction-induced settlements will result in downdrag loads on the piles. In this regard, we recommend assuming a downward skin friction acting along the outside perimeter of the piles of 250 psf above elevation +12 ft and 150 psf from elevation +12 ft to the top of the gravel unit. The top of the gravel unit is estimated at about elevation -57 ft. For seismic conditions the ultimate axial capacities estimated above should be reduced to 280 kips in compression, and 170 kips uplift to account for seismically-induced loss of strength. For piles located within the zone of ground improvement, the depth of liquefaction and magnitude of the downdrag loads will depend on the ground improvement design. The effects of ground improvement on the potential for downdrag induced loads should be evaluated as the ground improvement design is developed.

Recommended factors of safety for allowable capacity are discussed in the Recommended Factor of Safety section of this report.

Trestle Abutment Piles. As currently planned, new 24-in.-diameter pipe piles are being considered at the reconstructed trestle abutment to resist seismic inertial loads from the dock and trestle structure. We have assumed that ground improvement will be designed to extend around the abutment piles to a sufficient depth to mitigate liquefaction and lateral spreading. In this regard the non-seismic axial capacity estimates presented in the previous section for dolphin piles can be used to preliminarily design abutment piles for the non-seismic and seismic loading conditions. The pile capacities at the abutment should be reevaluated as the ground improvement design is developed.

Existing Trestle, Dock, and Dolphin Piles. The existing piles are 18-in.-diameter pipe piles with 3/8-in.-thick walls. The piles were reportedly fitted with a type of endplate that included a 10 1/2-in.-diameter center cut-out. The trestle piles are all plumb piles. The dock and dolphin piles are a combination of plumb and batter (5H:12V and 6H:12V) piles. The total embedded length of the piles typically ranged from about 34 to 100 ft depending primarily on the mudline elevation at the pile location. The piles at the dock typically have the least embedment and range from about 34 to 52 ft. The length of pile embedment into the gravel unit is typically in the range of 10 to 25 ft.

GRI evaluated the axial capacity of the existing piles based on available geotechnical data including pile driving logs and results of Pile Driving Analyzer (PDA) re-strike testing completed when the piles were installed. The PDA results are summarized in the above-referenced report by GRL (1993). The ultimate capacity computed from restrike PDA tests ranges from 435 to 550 kips. The PDA estimated skin friction resistance values of 210 kips and 225 kips for piles 91 and 96, respectively. Pile 91 and 96 were

embedded 36 and 48 ft, and it is our opinion that the estimated ultimate skin friction is representative for the range of pile embedment at Berth 13.

Based on the wide variation in pile embedment depths we recommend an ultimate compression capacity of 435 kips. We estimate the pile tip provides about 200 kips of resistance and the skin friction on the outside of the pile provides the remaining resistance. Since a significant portion of the estimated ultimate compression pile capacity is derived from end-bearing resistance on the partially closed-end plate, the uplift capacity of the piles will be significantly less than the compressive capacity. To consider decreased skin friction values for tension piles relative to compression piles (FHWA, 2006), we recommend an ultimate uplift capacity of about 150 kips for the range of pile embedments at Berth 13.

As discussed in the Liquefaction section of this report, the sand below the groundwater level is subject to liquefaction and/or seismically induced strength loss. Liquefaction-induced settlements will result in downdrag loads on the piles. For the existing dock and trestle piles, we recommend assuming a downward skin friction of 100 psf acting along the outside perimeter of the piles from the mudline to the top of the gravel unit. The top of the gravel unit can be estimated at about elevation -57 ft for this purpose. For seismic conditions, the ultimate axial capacities estimated above should be reduced to 400 kips (compression) and 100 kips (uplift) to account for seismically induced loss of strength.

Recommended Factor of Safety. We recommend applying a factor of safety to the ultimate pile capacities provided above based on soil support properties. A minimum FS of 2 is recommended for typical non-seismic conditions. For seismic conditions we recommend a factor of safety of 1 in accordance with the ASCE SSDPW. For extreme moorage loading combinations such as flood and extreme wind conditions a FS of 1.5 is appropriate for dolphin piles.

Pile Installation. The new dolphin piles should be driven with a pile hammer of sufficient energy to develop the pile ultimate capacity and obtain adequate penetration into the gravel. During installation, we anticipate the top of the gravel can be identified by a noticeable increase in penetration resistance. Based on our experience on adjacent sites with similar soils, a vibratory hammer will likely not be effective in penetrating the gravel layer to the design embedment. In this regard, the contractor should assume final installation of steel pipe piles will require an air, steam, or diesel, impact hammers.

As discussed previously, our experience in the area indicates the driving resistance in the gravel tends to be highly variable. There is some risk that piles may encounter practical refusal before reaching the planned tip elevations.

We recommend an indicator-pile installation program as the initial step in the installation of production piles. The purpose of the program would be to evaluate the contractor's equipment and develop terminal pile driving resistance criteria. We recommend dynamic pile testing of two or three piles with the PDA during initial driving. As a guide, if 24-in.-diameter piles are being considered for the pile program, we recommend using a pile hammer with rated energy of at least 100,000 ft-lbs. The contractor should provide an impact hammer submittal and installation plan for the project team to review at least 2 weeks prior to pile driving.

We understand the pipe piles will likely have a 0.5-in. wall thickness. All piles should be fitted with commercially available tip protection that fit flush with the outside wall of the pile.

Lateral Pile Capacity. Lateral structural loads can be resisted by the piles in bending. The lateral load behavior of the piles can be analyzed using the computer program L-Pile 5.0 by Ensoft, Inc. We recommend using the input parameters summarized in the following tables to model the soils at the site.

SOIL PROPERTIES FOR L-PILE ANALYSIS [1]
Berth 13 Dock, Trestle, and Riverbank Dolphin Piles

Static, Frequently Applied Live Loads, and Operating Level Earthquake (72-year Return Interval)[2]

Soil Unit	Elevation, ft	L-Pile Soil Type	Condition	Soil Properties				
				K, pci	γ′, pci	ϕ′	c, psi	ε_{50}
Fill: SAND	Above +17	Sand (Reese)	Non-Liquefied	25	0.067	32	N/A	N/A
Submerged Fill: SAND	+17 to +2	Sand (Reese)	Non-Liquefied	20	0.03	32	N/A	N/A
Submerged SAND	+2 to -38	Sand (Reese)	Non-Liquefied	20	0.030	32	N/A	N/A
Submerged SAND	-38 to -57	Sand (Reese)	Non-Liquefied	60	0.030	35	N/A	N/A
Submerged GRAVEL	Below -57	Sand (Reese)	Non-Liquefied	125	0.040	40	N/A	N/A

Contingency Level and Design Level Earthquakes (475-year and 2/3 MCE Return Intervals, respectively) [3] [4]

Soil Unit	Elevation, ft	L-Pile Soil Type	Condition	Soil Properties				
				K, pci	γ′, pci	ϕ′	c, psi	ε_{50}
Fill: SAND	Above +7.5	Sand (Reese)	No Lateral Resistance	N/A	0.067	N/A	N/A	N/A
Submerged Fill: SAND	+7.5 to +2	Sand (Reese)	Liquefied	10	0.030	6	N/A	N/A
Submerged SAND	+2 to -38	Sand (Reese)	Liquefied	10	0.030	6	N/A	N/A
Submerged SAND	-38 to -57	Sand (Reese)	Liquefied	10	0.030	12	N/A	N/A
Submerged GRAVEL	Below -57	Sand (Reese)	Non-Liquefied	125	0.040	40	N/A	N/A

Notes:

1) Applicable for the river side of the trestle abutment.
2) Design groundwater level assumed at OHWM Columbia River Elevation +17 ft (NGVD).
3) Design groundwater level assumed at Average Columbia River Elevation +7.5 ft.
4) Lateral spreading occurs to depths/elevations shown on Figure 5.
5) Submerged soils are below the design groundwater level.

For preliminary planning we have assumed that ground improvement will be installed around the abutment and will be sufficient to mitigate liquefaction. In this regard, the lateral resistance of abutment piles can be estimated based on the static L-Pile parameters presented in the above table. Ground slope effects can be taken into consideration with the input of an appropriate slope angle.

It should be noted that L-Pile provides isolated, single-pile capacities. Depending on the direction of the loading and orientation of the piles, group effects should be considered for spacings less than eight (8) pile diameters. This reduction is often applied as a group efficiency or a p-multiplier. L-Pile uses a p-multiplier as a reduction of the k_h value for pile spacing less than eight pile diameters. The following table provides a summary of p-multipliers and reported group efficiencies in sand.

LATERAL PILE GROUP ANALYSIS

Center-to-Center Pile Spacing	Calculated p-multipliers for Rows 1, 2, and 3	Reported Group Efficiency
3d	0.80, 0.40, 0.30	0.75
5d	1.0, 0.85, 0.70	0.95
8d	1.0, 1.0, 1.0	1.0

Caution should be used when applying the reported group efficiencies to pile groups with significantly more than three rows of piles. Additional design methodology of laterally loaded pile groups is provided in the Federal Highway Administration (FHWA) publication entitled, "Design and Construction of Driven Pile Foundations."

Micropiles or Ground Anchors. Micropiles or ground anchors drilled through the tip of the existing piles are being considered to increase the existing pile capacity. We estimate micropiles or ground anchors in the gravel may develop ultimate capacities on the order of 350 kips. Larger capacities may be possible but could be limited by structural design considerations. The micropiles or ground anchors would be drilled and installed through the existing pipe piles and into the underlying gravel.

Drilling through the gravel at the tip of the existing pipe piles will alter the pile tip resistance. For preliminary planning purposes, we recommend considering no tip resistance for the existing pipe piles if micropiles or ground anchors are installed through the pile tip. Installation of micropiles or ground anchors will not reduce the skin friction of the existing pipe piles.

Grouted micropiles or ground anchors are typically designed by specialty contractors to meet specified performance criteria. As a general guideline, we recommend a minimum bonded length of 30 ft into the relatively dense gravel. Micropiles or ground anchors should be designed with a minimum factor of safety of 1.5 in compression and 2 in tension, based on soil support properties.

Micropile or ground anchor capacities should be evaluated by field testing which will be challenging because the existing piles are supporting the dock structure. The maximum test loads and the number of test anchors will depend on the total number and design of the micropiles or ground anchors. The testing program should be developed with the final plans and specifications. The unbonded and bonded lengths may need to be modified based on the actual gravel conditions encountered during drilling and the contractor's equipment and procedures. Micropiles and ground anchors should be provided with permanent corrosion protection.

Trestle Abutment Earth Pressures

Design lateral earth pressures for the trestle abutment depend on the type of construction, i.e., the ability of the abutment to yield. For static conditions, we anticipate the trestle abutment will be relatively rigid and

can be designed to resist an at-rest lateral earth pressure computed on the basis of an equivalent fluid having a unit weight of 50 pcf. Additional lateral earth pressures due to surcharge loadings may be estimated using the guidelines presented on Figure 7.

Additional lateral loads due to seismic forces on retaining walls will be dependent on design of the ground improvement around the abutment and the seismic hazard level. Our studies indicate that liquefaction induced seismic deformations are not likely for the OLE hazard level. Based on this assumption, the abutment may be designed on the basis of static at-rest earth pressure plus an additional seismic load increment during the OLE seismic event. The additional load due to seismic forces can be evaluated based on a rectangular lateral earth pressure distribution with a uniform pressure equal to $H*\gamma$, where H is the height of the wall and γ is an equivalent unit weight of 2 pcf for the OLE.

We have assumed that ground improvement will be designed around the trestle abutment to mitigate liquefaction and lateral spreading loads and deformations at the CLE and DE hazard levels to meet a specified ground movement performance criteria. We understand that the final seismic performance criteria have not yet been selected. Seismic lateral ground deformations toward the river will cause lateral spreading loads on the abutment wall and foundations. Lateral spreading loads should be applied to the wall and piles until the wall has displaced the amount specified by the performance criteria. For preliminary planning, lateral spreading loads can be estimated based on an equivalent fluid unit weight of 400 pcf for the unsaturated sand above elevation 7.5 ft. Below elevation 7.5 ft where the sand is saturated and susceptible to liquefaction, a uniform rectangular pressure distribution of 250 psf may be assumed to act in the direction of the river. The depth of seismic deformation and lateral spreading loads will depend on the ground improvement design and the seismic design of the abutment should be re-evaluated once the ground improvement design is complete. We recommend assuming the lateral earth pressure against piles in the unsaturated sand material will act over an equivalent of two pile diameters due to arching. The lateral pressure against piles in the saturated liquefied sand material will act over one pile diameter. Once the seismic deformation has occurred, the earth pressures can be estimated based on the static at-rest earth pressures provided above.

Based on our discussion with the project team, we understand lateral loads at the trestle abutment may be resisted by battered piles or tieback anchors. Anchor capacities can be provided during final design if needed.

The above criteria assume drained conditions and that the abutment is backfilled with relatively clean, granular material, i.e., medium sand, sand and gravel, or well-graded gravel, with not more than 5% passing the No. 200 sieve (washed analysis). We recommend that this material be compacted to about 95% of the maximum dry density as determined by ASTM D 698. Heavy compaction equipment should not operate within 5 ft of the abutment.

Design Review and Construction Services

We welcome the opportunity to review and discuss construction plans and specifications for this project as they are being developed. In addition, GRI should be retained to review all geotechnical-related portions of the plans and specifications to evaluate whether they are in conformance with the recommendations provided in our report. Additionally, to observe compliance with the intent of our recommendations, design concepts, and the plans and specifications, we are of the opinion that all construction operations

dealing with pile installation should be observed by a GRI representative. Our construction-phase services will allow for timely design changes if site conditions are encountered that are different from those described in this report. In our opinion, this is of particular importance during pile-driving operations. If we do not have the opportunity to confirm our interpretations, assumptions, and analyses during construction, we cannot be responsible for the application of our recommendations to subsurface conditions that are different from those described in this report.

LIMITATIONS

This report has been prepared to assist BergerABAM and the design team in the design of this project. The scope is limited to the specific project and location described herein. Our description of the project represents our understanding of the significant aspects of the project relevant to the design and construction of the trestle, platform, dolphins, and other supports. In the event that any changes in the design and location of the facilities, as outlined in this report, are planned, we should be given the opportunity to review the changes and to modify or reaffirm the conclusions and recommendations of this report in writing.

The analyses and recommendations submitted in this report are based on the data obtained from the borings made at the locations indicated on the Site Plan and from other sources of information discussed in this report. In the performance of subsurface investigations, specific information is obtained at specific locations at specific times. However, it is acknowledged that variations in soil conditions may exist between the boring locations, and groundwater levels fluctuate seasonally. This report does not reflect any variations that may occur between these explorations. The nature and extent of variations may not become evident until construction. If, during construction, subsurface conditions different from those encountered in the exploratory holes are observed or encountered, or appear to be present beneath or beyond foundations, we should be advised at once so that we can observe these conditions and reconsider our recommendations where necessary.

Submitted for GRI,

Expires 4/2016

Matthew S. Shanahan, PE
Associate

Scott M. Schlechter, PE
Principal

References

ASCE 7-05, 2005, Minimum design loads for buildings and other structures: American Society of Civil Engineers.

ASCE, Proposed Seismic Design of Pile-Supported Piers and Wharves

Beeson, M.H., Tolan, T.L., and Madin, I.P., 1991, Geologic map of the Portland quadrangle, Multnomah and Washington counties, Oregon and Clark County, Washington: Oregon Department of Geology and Mineral Industries, Geologic Map Series GMS-75.

FHWA, 2006, Design and Construction of Driven Pile Foundations Reference Manual, Volume I FHWA-NHI-05-042

FHWA, 2006, Design and Construction of Driven Pile Foundations Reference Manual, Volume II FHWA-NHI-05-043

Idriss, I.M., and Boulanger, R.W., 2008, Soil liquefaction during earthquakes: Earthquake Engineering Research Institute (EERI), MNO-12 p. 226.

Personius, S.F., Dart, R.L., Bradley, L.A., and Haller, K.M., 2003, Map and data for Quaternary faults and folds in Oregon: U.S. Geological Survey Open File Report OFR 03-095.

U.S. Geological Survey, 2013, Probabilistic hazard lookup by latitude, longitude, accessed 7/17/13, from USGS website: https://geohazards.usgs.gov/deaggint/2008/

Yeh, Harry; Tolkova, Elena; Jay, David A.; Talke, Stefan A.; and Fritz, Hermann, 2012, Tsunami Hydrodynamics in the Columbia River, Journal of Disaster Research, Vol. 7, No. 5.

Youd, T.L., and. Carter, B.L., 2005, Influence of Soil Softening and Liquefaction on Spectral Acceleration, Journal of Geotechnical and Geoenvironmental Engineering, 131, 811–825.

Youd, T.L., Hansen, C.M., and Bartlett, S.F., December 2002, Revised multilinear regression equations for prediction of lateral spread displacement, ASCE Journal of Geotechnical and Geoenvironmental Engineering, Vol. 128, No. 12.

Youd, T.L., Idriss, I.M., Andrus, R.D., Arango, I., Castro, G., Christian, J.T., and others, October 2001, Liquefaction resistance of soils: summary report from the 1996 NCEER and 1998 NCEER/NSF workshops on evaluation of liquefaction resistance of soils: in Journal of Geotechnical and Geoenvironmental Engineering.

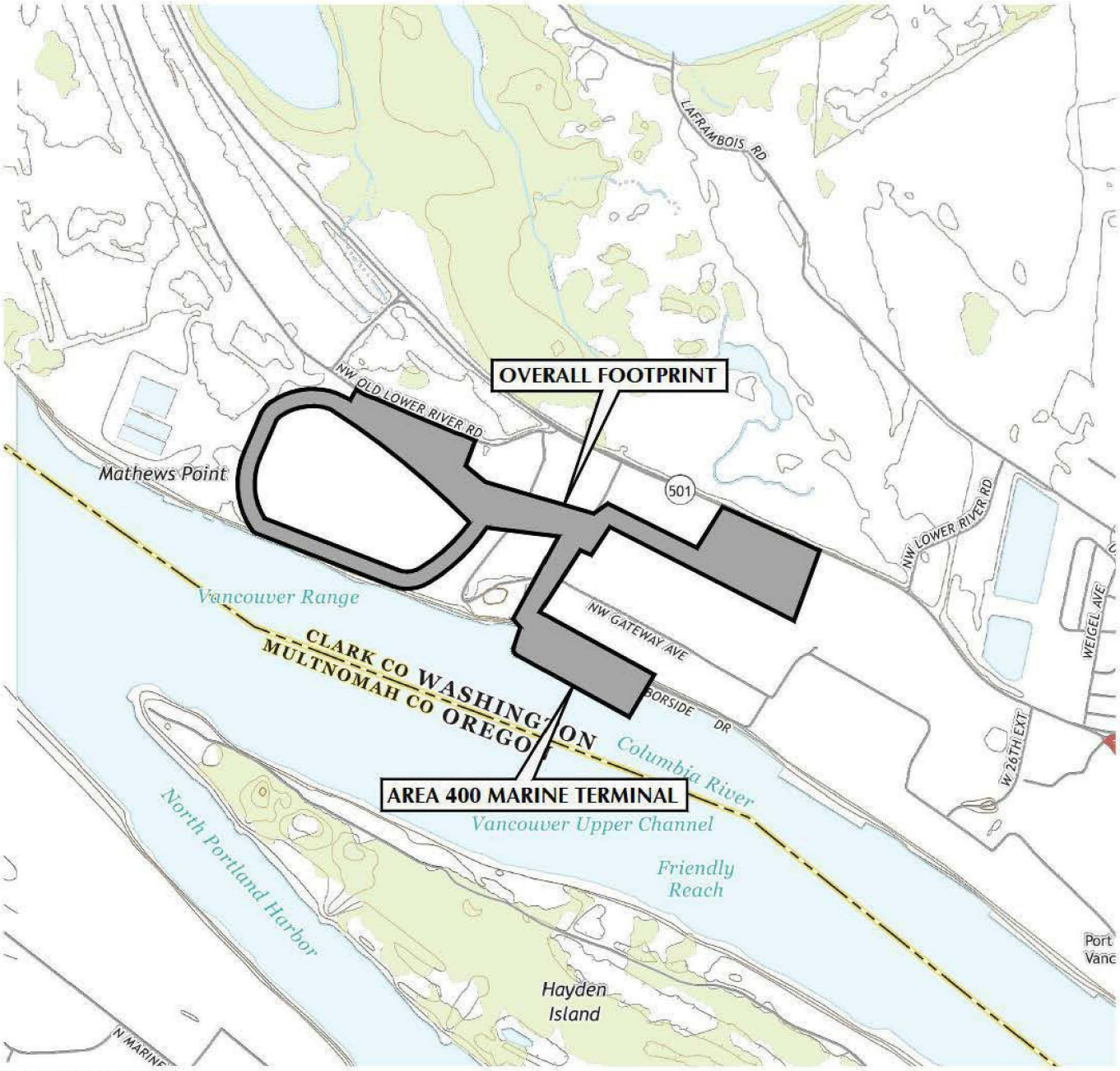

USGS TOPOGRAPHIC MAP
VANCOUVER, WASHINGTON (2011)

North

0 1/2 1 MILE

GRI BERGERABAM
TSVEDT DOCK STRUCTURE

VICINITY MAP

SEP. 2014 JOB NO. W1114-T3 FIG. 1

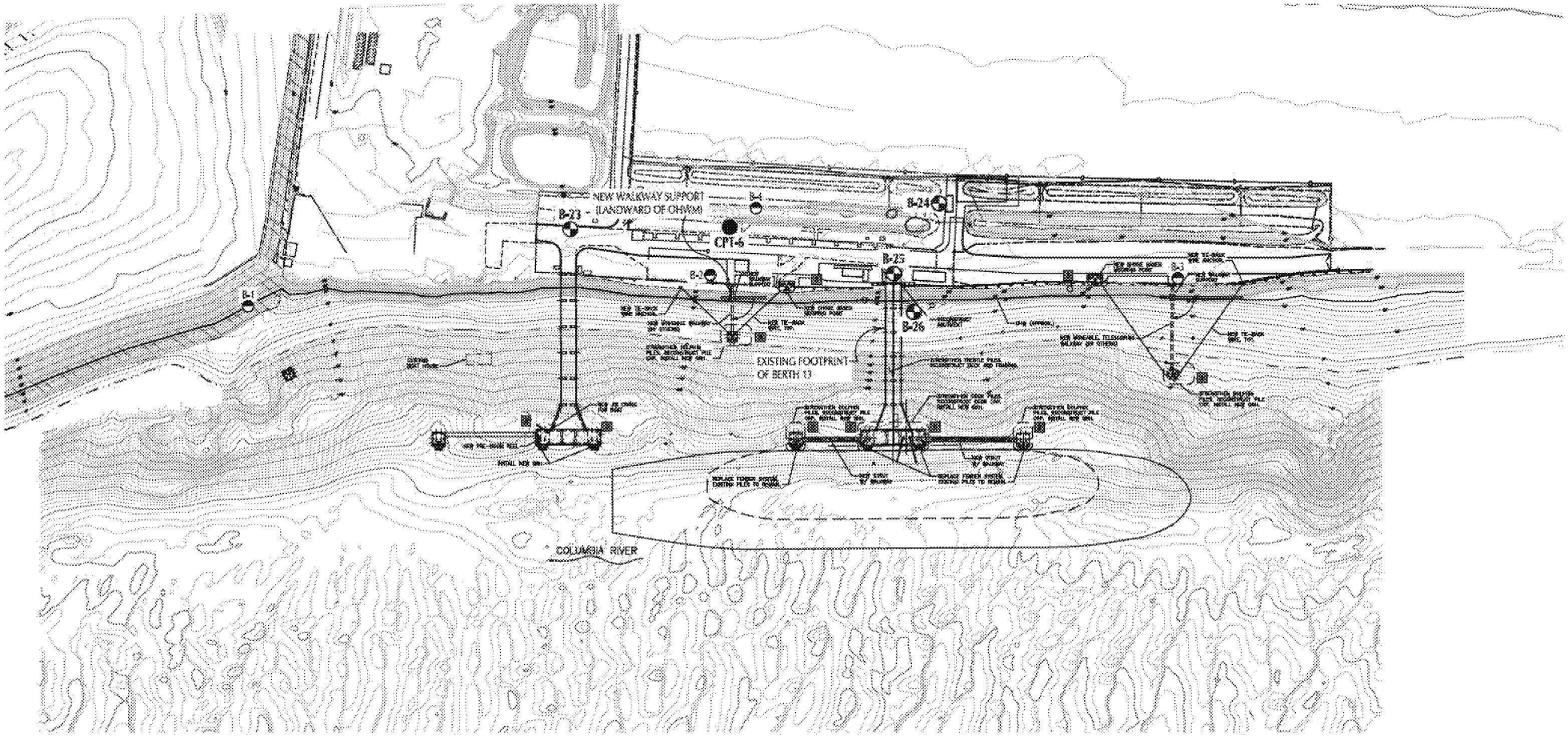

North

0 150 300 FT

BORING MADE BY GRI
(JULY 29 - OCTOBER 29, 2013)

CONE PENETRATION TEST MADE BY GRI
(JULY 29 - AUGUST 5, 2013)

BORING MADE BY DAMES & MOORE
(1993)

SITE PLAN FROM FILE BY MACKAY + SPOSITO

GRI BERGERABAM
TSUGT DOCK STRUCTURE

SITE PLAN

SEP. 2014 JOB NO. W1314-73 FIG. 2

LIQUEFACTION ANALYSIS

Tesoro Savage Vancouver Energy Distribution Terminal

Hole No.=B-26 Water Depth=0 ft Surface Elev.=7

Magnitude=8.4
Acceleration=0.26g

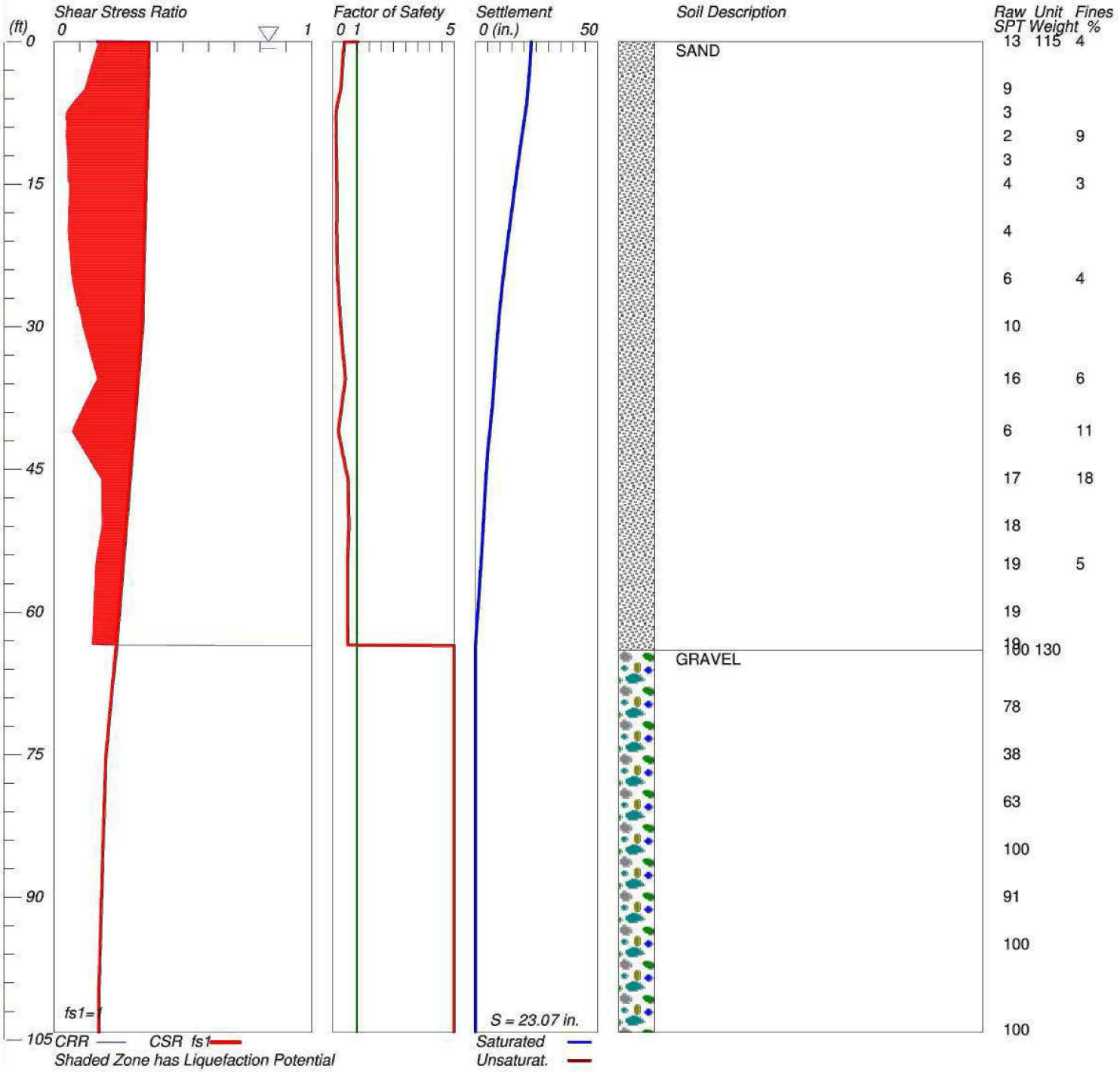

Contingency Level Earthquake (CLE)

GRI BERGERABAM
TSVEDT DOCK STRUCTURE

LIQUEFACTION HAZARD ANALYSIS

SEP. 2014 JOB NO. W1114-T3 FIG. 3

LIQUEFACTION ANALYSIS

Tesoro Savage Vancouver Energy Distribution Terminal

Hole No.=B-26 Water Depth=0 ft Surface Elev.=7

Magnitude=9.0
Acceleration=0.28g

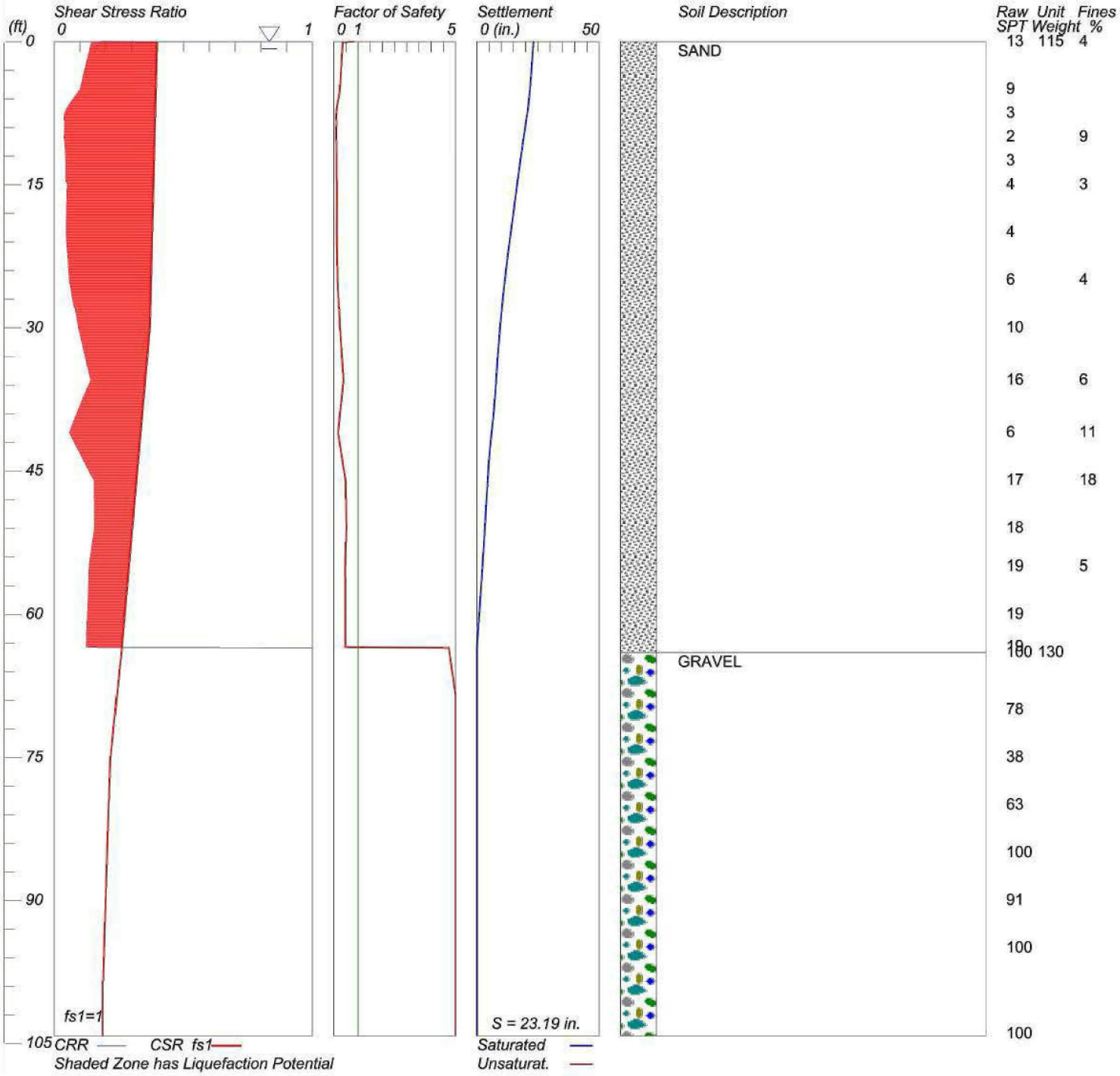

Design Earthquake (DE)

GRI BERGERABAM
TSVEDT DOCK STRUCTURE

LIQUEFACTION HAZARD ANALYSIS

SEP. 2014 JOB NO. W1114-T3 FIG. 4

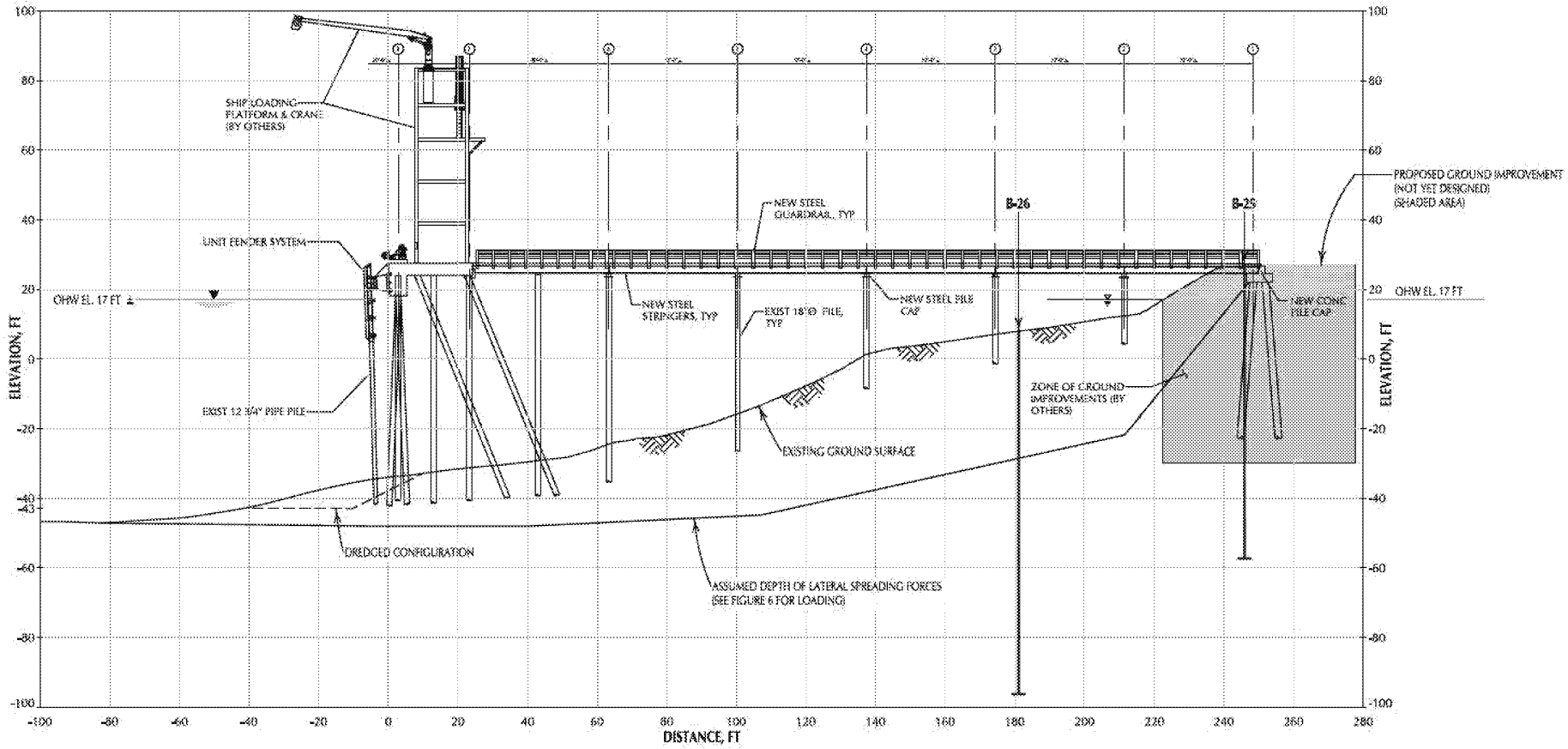

ELEVATION LOOKING WEST

NOTES:

1) THE EXTENT OF LATERAL SPREAD SHOULD BE FURTHER EVALUATED AS THE GROUND IMPROVEMENT DESIGN IS DEVELOPED.

2) DATUM IS NGVD29.

3) EXISTING PILE TIPS ESTIMATED TO RANGE FROM ELEVATION -69 TO -93 FT BASED ON AVAILABLE PILE DRIVING RECORDS.

GRI BERGERABAM TSVEDT DOCK STRUCTURE

BERTH 13 TRESTLE AND DOCK PROFILE

SEP. 2014 JOB NO. W1114-73 FIG. 5

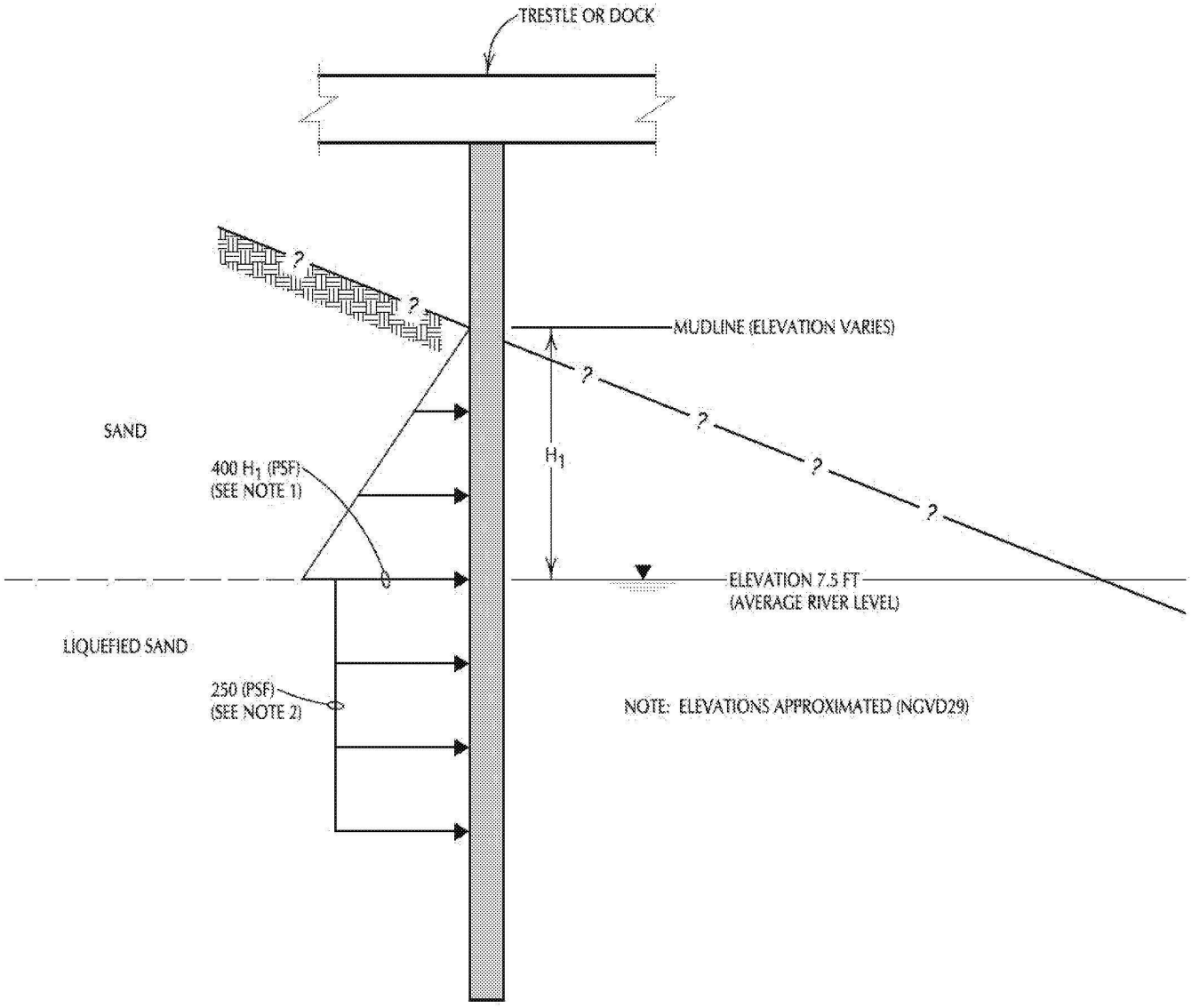

NOTES:

1) ACTS OVER TWO PILE DIAMETERS.

2) ACTS OVER ONE PILE DIAMETER. LATERAL SPREADING FORCES ARE ASSUMED TO ACT ON THE PILES TO THE DEPTH SHOWN ON FIGURE 3.

3) FORCES ARE FOR CONTINGENCY LEVEL (475 YEAR RETURN PERIOD) AND DESIGN EARTHQUAKE (⅔ MCE) HAZARD LEVELS.

4) THE LATERAL SPREADING FORCES INDICATED ABOVE ARE FOR TRESTLE AND DOCK PILES ONLY. LATERAL SPREADING FORCES ON THE TRESTLE ABUTMENT WILL DEPEND ON THE GROUND IMPROVEMENT DESIGN WHICH HAS NOT BEEN COMPLETED AT THIS TIME.

GRI BERGERABAM TSVEDT DOCK STRUCTURE

LATERAL SPREADING LOADS TRESTLE AND DOCK PILES

SEP. 2014 JOB NO. W1114-T3 FIG. 6

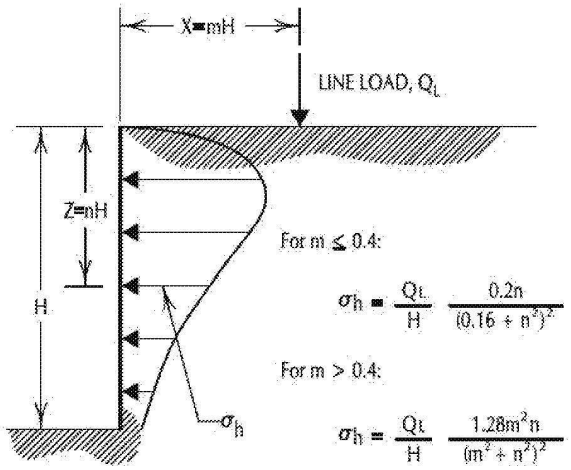

LINE LOAD PARALLEL TO WALL

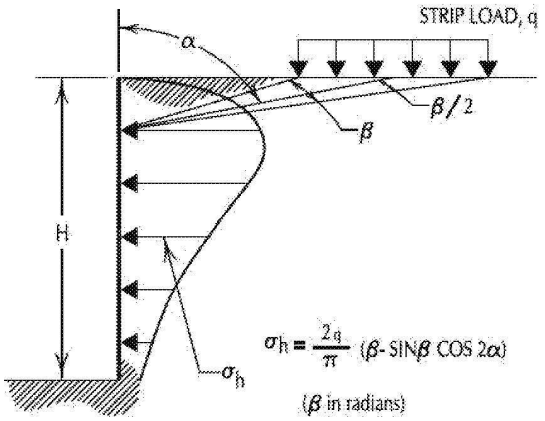

STRIP LOAD PARALLEL TO WALL

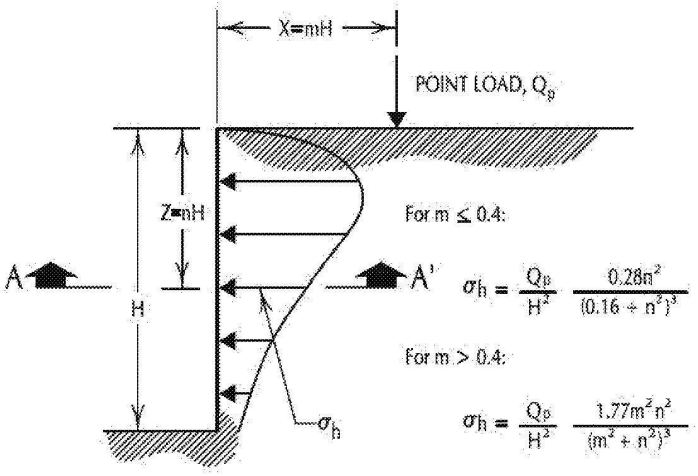

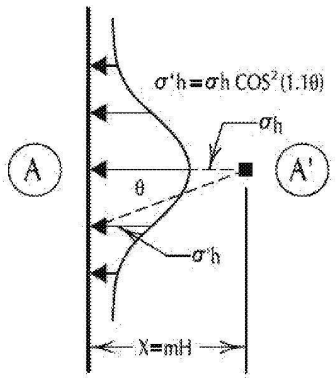

DISTRIBUTION OF HORIZONTAL PRESSURES

VERTICAL POINT LOAD

NOTES:

1. THESE GUIDELINES APPLY TO RIGID WALLS WITH POISSON'S RATIO ASSUMED TO BE 0.5 FOR BACKFILL MATERIALS.
2. LATERAL PRESSURES FROM ANY COMBINATION OF ABOVE LOADS MAY BE DETERMINED BY THE PRINCIPLE OF SUPERPOSITION.

GRI BERGERABAM TSVEDT DOCK STRUCTURE

SURCHARGE-INDUCED LATERAL PRESSURE

SEP. 2014 JOB NO. W1114-T3 FIG. 7

APPENDIX A

Field Explorations and Laboratory Testing

APPENDIX A

FIELD EXPLORATIONS AND LABORATORY TESTING

FIELD EXPLORATIONS

General

Subsurface materials and conditions in the marine terminal project area were investigated between July 29 and October 29, 2013 with four borings and one electric cone penetration test (CPT) probe. The approximate locations of the explorations are shown on Figure 2. An experienced geotechnical engineer from GRI directed the drilling and maintained a detailed log of the materials and conditions disclosed during the course of the work. The locations of the borings with respect to areas of the proposed facility are discussed below.

Borings

The borings were advanced to depths of approximately 80 to 104 ft with mud-rotary drilling methods. Borings B-23 through B-25 were completed using a truck-mounted drill rig provided and operated by Western States Soil Conservation of Hubbard, Oregon. Boring B-26 was completed using a track-mounted drill rig provided and operated by Hardcore Drilling Inc. of Dundee, Oregon. Disturbed and undisturbed soil samples were typically obtained at 2.5-ft intervals of depth in the upper 15 ft and at 5-ft intervals below this depth. Disturbed samples were obtained using a standard split-spoon sampler. At the time of sampling, the Standard Penetration Test was conducted. This test consists of driving a standard split-spoon sampler into the soil a distance of 18 in. using a 140-lb hammer dropped 30 in. The number of blows required to drive the sampler the last 12 in. is known as the standard penetration resistance, or N-value. The N-values provide a measure of the relative density of granular soils, such as sand or gravel, and the relative consistency, or stiffness, of cohesive soils, such as silt or clay. The split-spoon samples were carefully examined in the field and representative portions were saved in airtight jars. All samples were returned to our laboratory for further examination and physical testing.

Relatively undisturbed samples were obtained by pushing 3-in.-O.D. Shelby tubes into the undisturbed soil a maximum distance of 24 in. using the drill rig. The soils exposed in the ends of the Shelby tubes were examined and classified in the field. After classification, the ends of the tubes were sealed with plastic end caps and tape to preserve the natural moisture content of the soils. All samples were returned to our laboratory for further examination and testing.

Logs of the borings are provided on Figures 1A through 4A. Each log presents a descriptive summary of the various types of materials encountered in the boring and notes the depth at which the materials and/or characteristics of the materials change. To the right of the descriptive summary, the numbers and types of samples are indicated. Farther to the right, N-values are shown graphically, along with natural moisture contents and percent passing the No. 200 sieve. The terms used to describe the soils encountered in the borings are defined in Table 1A.

Electric Cone Penetration Test (CPT) Probes

One CPT probe, designated CPT-6, was advanced to practical refusal at a depth of about 83 ft below the ground surface using a truck-mounted Dutch Cone unit provided and operated by Vandehey Exploration,

Inc. of Banks, Oregon. The equipment is mounted on a truck and operated from within an enclosure on the back of the truck that houses the electrical equipment. The electrical cone probe has a cone and a sleeve that are similar to a mechanical probe, but the forces are measured electronically. In addition to the cone and sleeve transducers, a piezometer is fitted between the cone and the sleeve, which allows measurement of pore water pressure and rate of dissipation as the probe is advanced. An accelerometer can also be fitted within the electrical probe. The accelerometer is used to measure the arrival times of shear waves produced at the ground surface as the exploration is advanced. Using these measurements, the shear wave velocity of the soils penetrated can be estimated. The shear wave velocities characterize the soils for the purpose of seismic studies. Shear wave measurements were made during advancement of probe CPT-6. The terms used to describe the soils encountered in the CPT probes are defined in Table 2A. A log of the CPT probe is provided on Figure 5A.

LABORATORY TESTING

General

All samples obtained from the field were returned to our laboratory where the physical characteristics of the samples were noted, and the field classifications were modified where necessary. At the time of classification, the natural moisture content of each sample was measured. Additional testing included washed sieve analysis, sieve analysis, and dry unit weight determinations. The following sections describe the testing program in more detail.

Natural Moisture Content

Natural moisture content determinations were made in conformance with ASTM D 2216. The results are provided on Figures 1A through 4A.

Dry Unit Weight

The dry unit weight of four undisturbed samples was determined in the laboratory in accordance with ASTM D 2937 by cutting a cylindrical specimen of soil from a Shelby tube sample. The dimensions of the specimen were carefully measured, the volume calculated, and the specimen weighed. After oven-drying, the specimen was reweighed and the moisture content calculated. The dry unit weight was then computed. The dry unit weights are summarized below.

SUMMARY OF DRY UNIT WEIGHT DETERMINATIONS

Boring	Sample	Depth, ft	Natural Moisture Content, %	Dry Unit Weight, pcf	Soil Type
B-24	S-18	70	29	88	SAND; fine grained, trace silt
B-26	S-12	40	39	80	SAND; some silt, scattered wood debris
	S-14	45	34	81	SAND; some silt, scattered wood debris
	S-16	50	31	90	SAND; some silt, scattered wood debris

Grain Size Analysis

Washed-Sieve Method. Washed sieve analyses were performed on representative soil samples to assist in their classification. The test is performed by taking a sample of known dry weight and washing it over a No. 200 sieve. The material retained on the sieve is oven-dried and weighed, and the percentage of material passing the No. 200 sieve is calculated. The test results are shown on the Boring Logs, Figures 1A through 4A.

Dry Sieve Method. Sieve analyses were performed on five representative samples of sand in substantial conformance with ASTM D 6913. The test is performed by taking a sample of known dry weight and washing it over a No. 200 sieve. The material retained on the sieve is oven-dried and weighed, and the percentage of material passing the No. 200 sieve is calculated. The soil retained on the No. 200 sieve is then screened through a series of sieves of various sizes using a sieve shaker. The weight of each sieve is measured prior to and after the soil has been run through the shaker. The weight of the soil retained on each sieve is recorded and expressed as a percentage of the total sample weight. The test data are summarized on Figures 6A and 7A in the form of curves showing the percent of the total soil sample by weight finer versus sieve number or grain size in millimeters.

Table 1A: GUIDELINES FOR CLASSIFICATION OF SOIL

RELATIVE DENSITY FOR GRANULAR SOIL

Relative Density	Standard Penetration Resistance (N-values) blows per foot
very loose	0 - 4
loose	4 - 10
medium dense	10 - 30
dense	30 - 50
very dense	over 50

CONSISTENCY FOR FINE-GRAINED (COHESIVE) SOIL

Consistency	Standard Penetration Resistance (N-value) blows per foot	Torvane or Undrained Shear Strength, tsf
very soft	0 - 2	less than 0.125
soft	2 - 4	0.125 - 0.25
medium stiff	4 - 8	0.25 - 0.50
stiff	8 - 15	0.50 - 1.0
very stiff	15 - 30	1.0 - 2.0
hard	over 30	over 2.0

Sandy silt materials which exhibit general properties of granular soils are given relative density description.

Grain-Size Classification	Modifier for Subclassification	
	Adjective	Percentage of Other Material In Total Sample
Boulders > 12 in.		
Cobbles 3 - 12 in.	clean	0 - 2
Gravel	trace	2 - 10
1/4 - 3/4 in. (fine) 3/4 - 3 in. (coarse)	some	10 - 30
Sand No. 200 - No. 40 sieve (fine) No. 40 - No. 10 sieve (medium) No. 10 - No. 4 sieve (coarse)	sandy, silty, clayey, etc.	30 - 50
Silt/Clay - pass No. 200 sieve		

GRI

Table 2A

SOIL CLASSIFICATION BASED ON CONE PENETRATION TEST

Friction Ratio (Percent)	Soil Classification
0 to 2	Clean sand or slightly silty sand
2 to 5	Silty sand, clayey sand, or silt
> 5	Clayey silt, silty clay, or clay

COHESIVE SOILS

Sleeve Friction, tsf	Relative Consistency
<0.12	Very Soft
0.12 to 0.25	Soft
0.25 to 0.50	Medium Stiff
0.50 to 1.00	Stiff
1.00 to 2.00	Very Stiff
>2.00	Hard

COHESIONLESS SOILS

	Soil Type*			
	ML, SM	SM, SP, SW	SP, SW, GW	SW, GP
Relative Density	Cone Penetration Resistance, tsf			
Very Loose	0 - 8	0 - 14	0 - 20	0 - 24
Loose	8 - 20	14 - 35	20 - 50	24 - 60
Med. Dense	20 - 60	35 - 105	50 - 150	60 - 180
Dense	60 - 100	105 - 175	150 - 250	180 - 300
Very Dense	> 100	> 175	> 250	> 300

* Unified Soil Classification System

1) Friction ratio is equal to sleeve friction (tsf) divided by cone penetration (tsf) expressed as a percent.

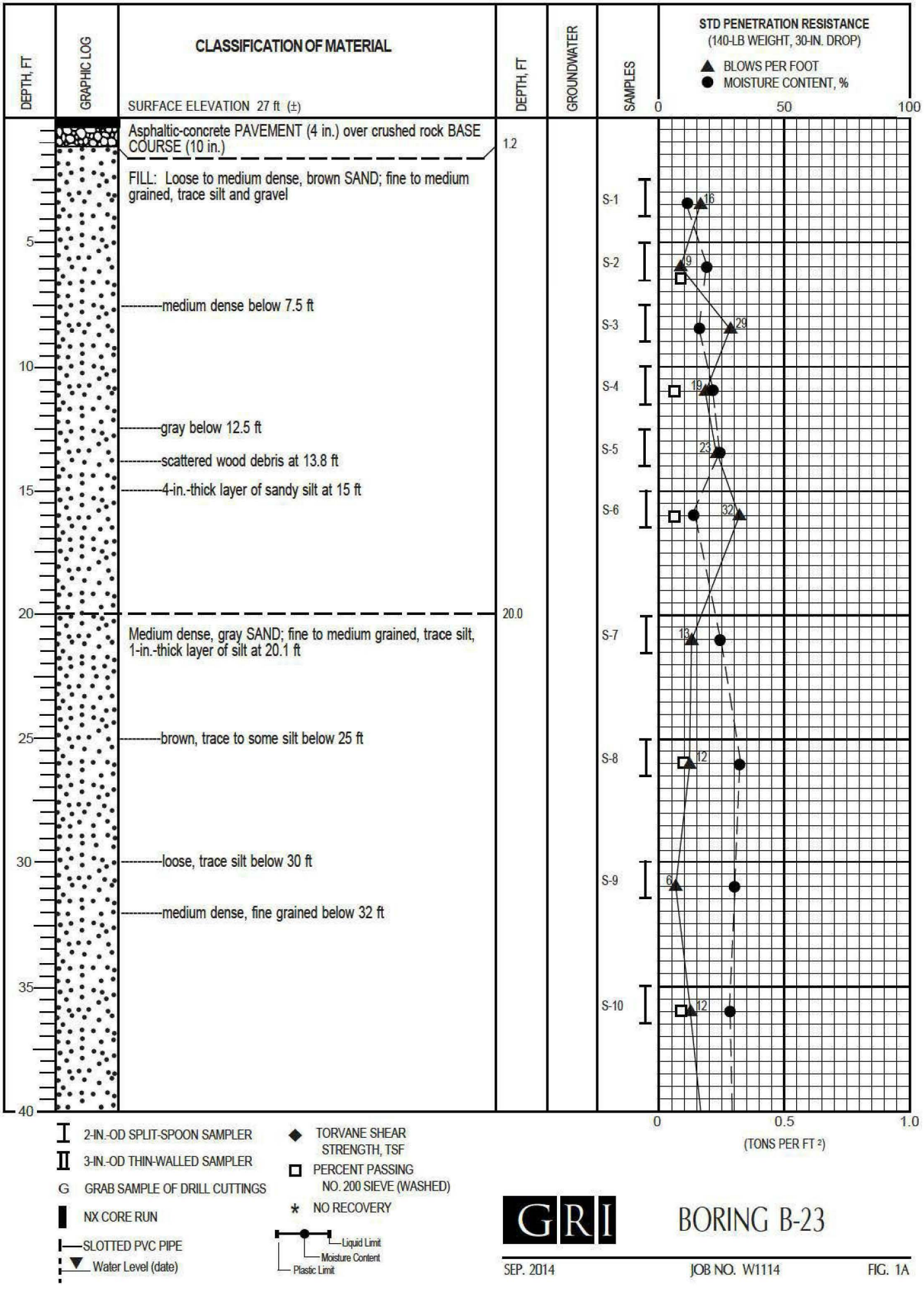

GRI

BORING B-23

SEP. 2014 JOB NO. W1114 FIG. 1A

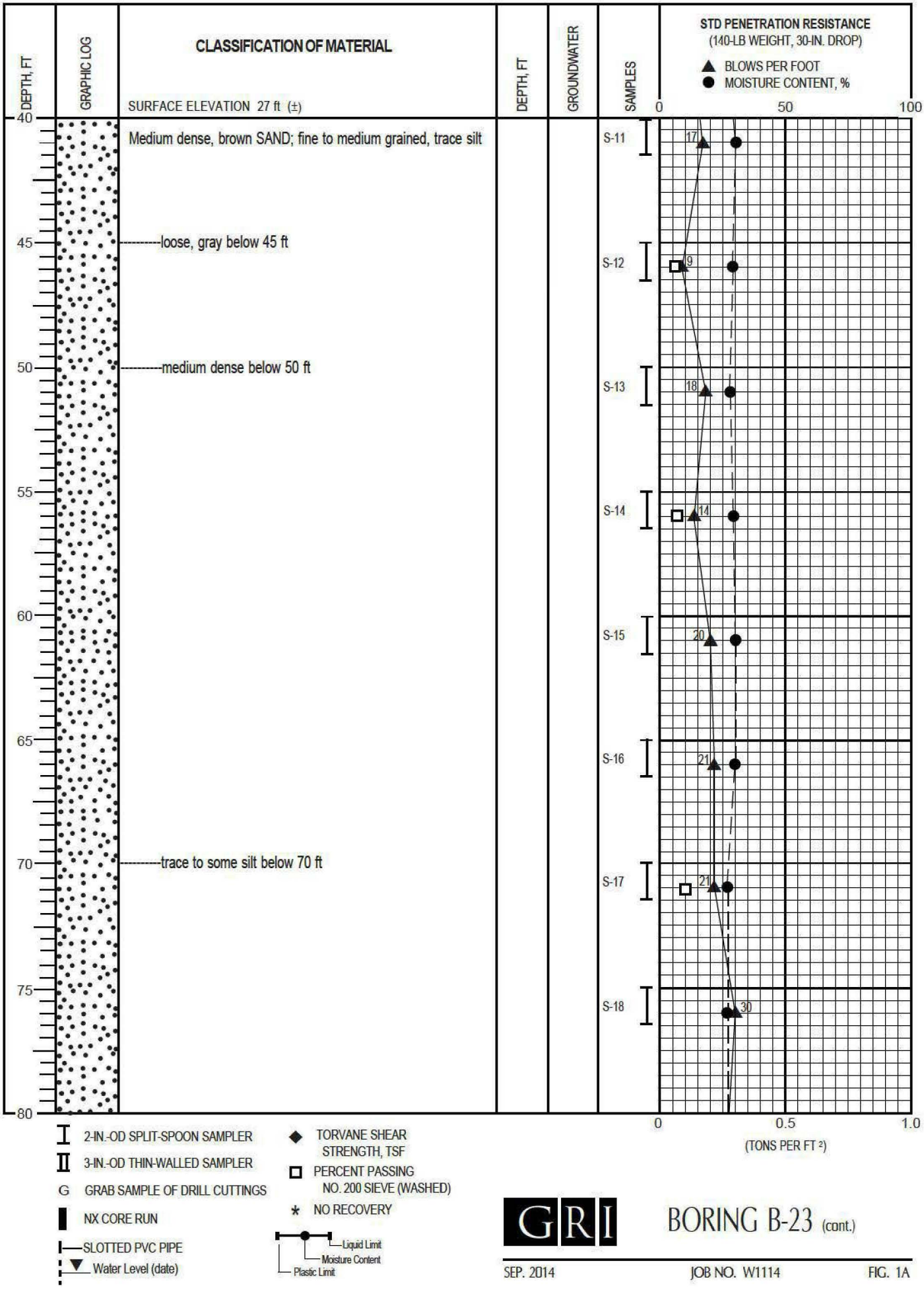

GRI

BORING B-23 (cont.)

SEP. 2014 JOB NO. W1114 FIG. 1A

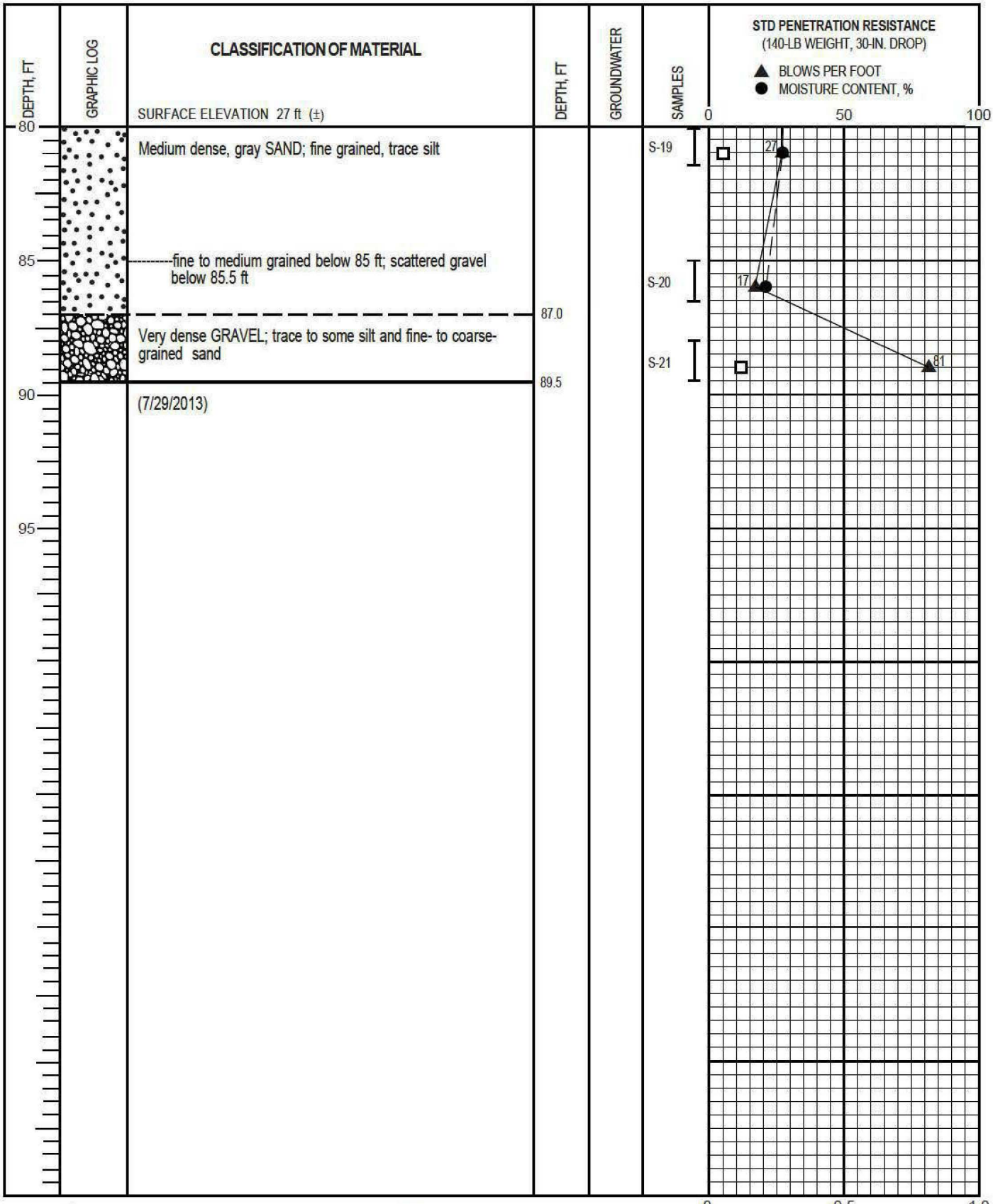

GRI

BORING B-23 (cont.)

SEP. 2014 JOB NO. W1114 FIG. 1A

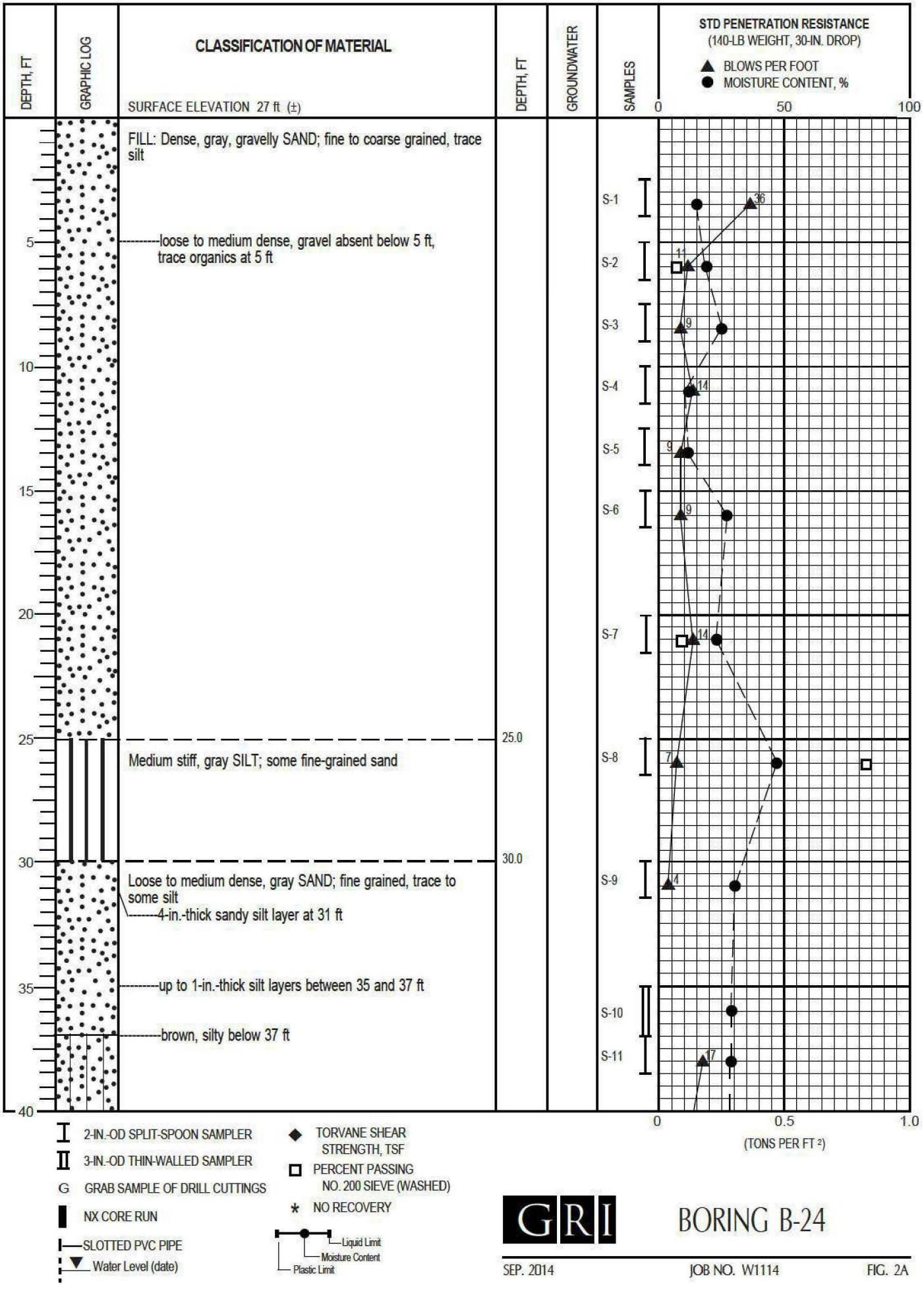

GRI

BORING B-24

SEP. 2014 JOB NO. W1114 FIG. 2A

EX-0188-000035-TSS

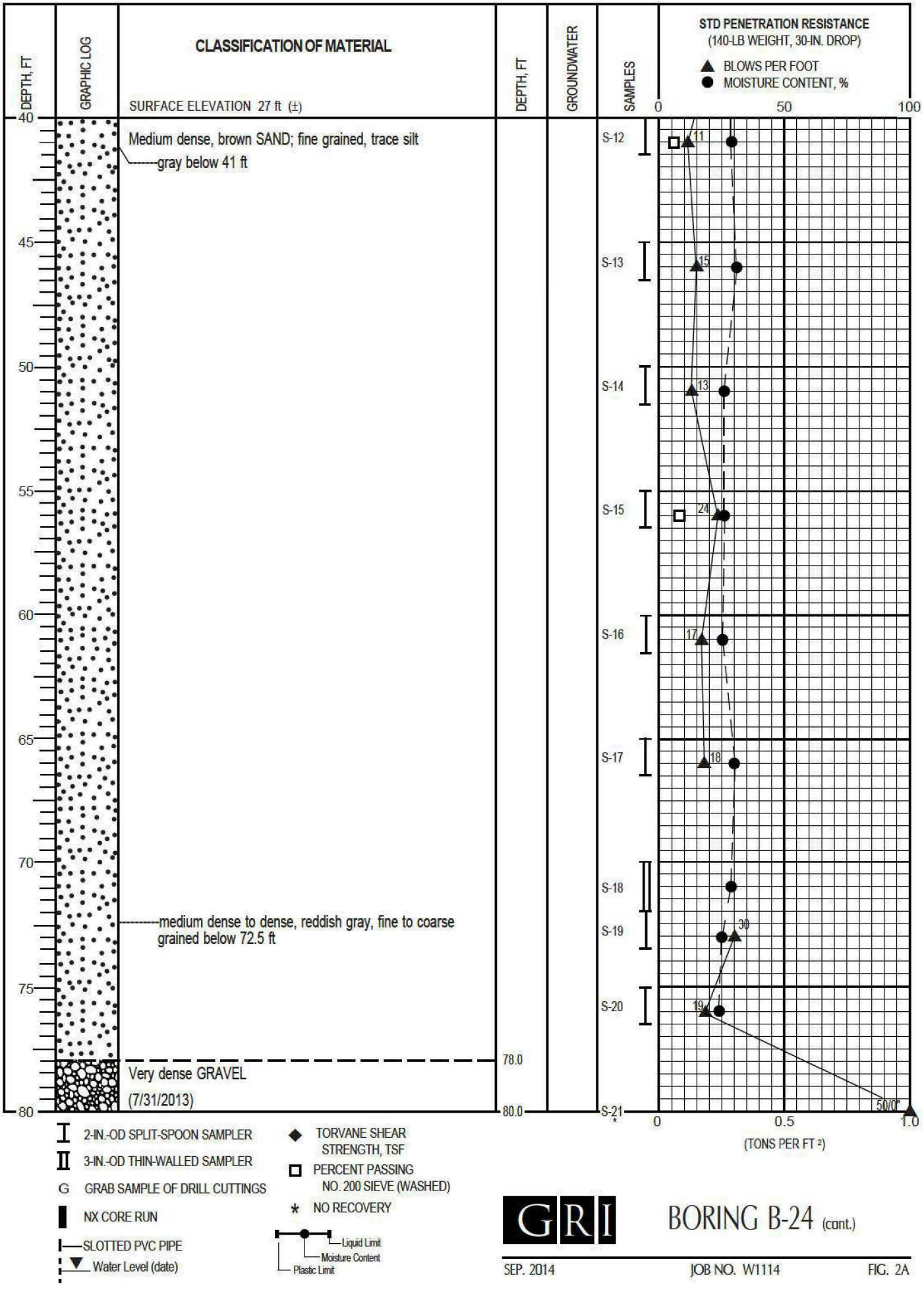

GRI

BORING B-24 (cont.)

SEP. 2014 JOB NO. W1114 FIG. 2A

EX-0188-000036-TSS

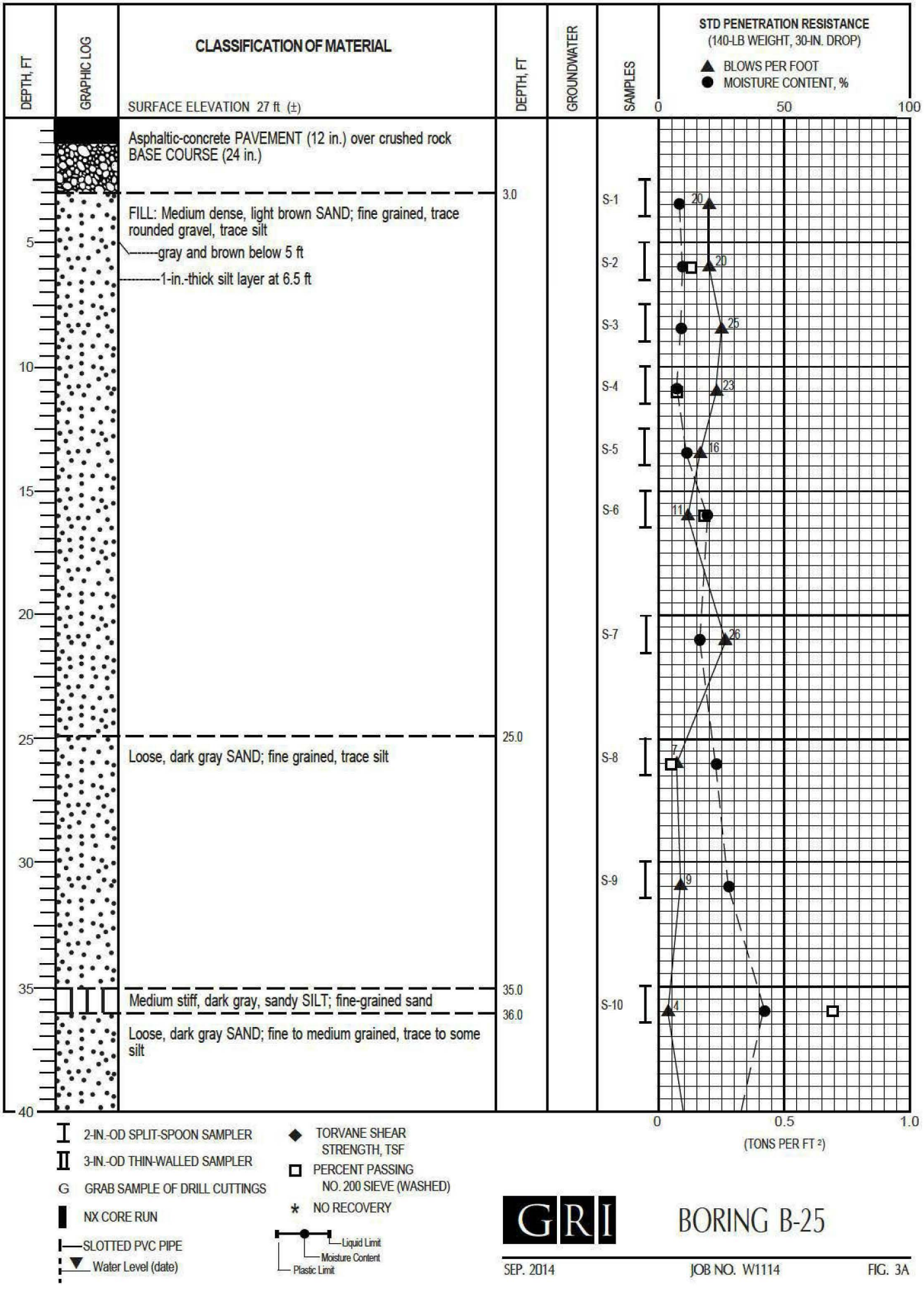

GRI

BORING B-25

SEP. 2014 JOB NO. W1114 FIG. 3A

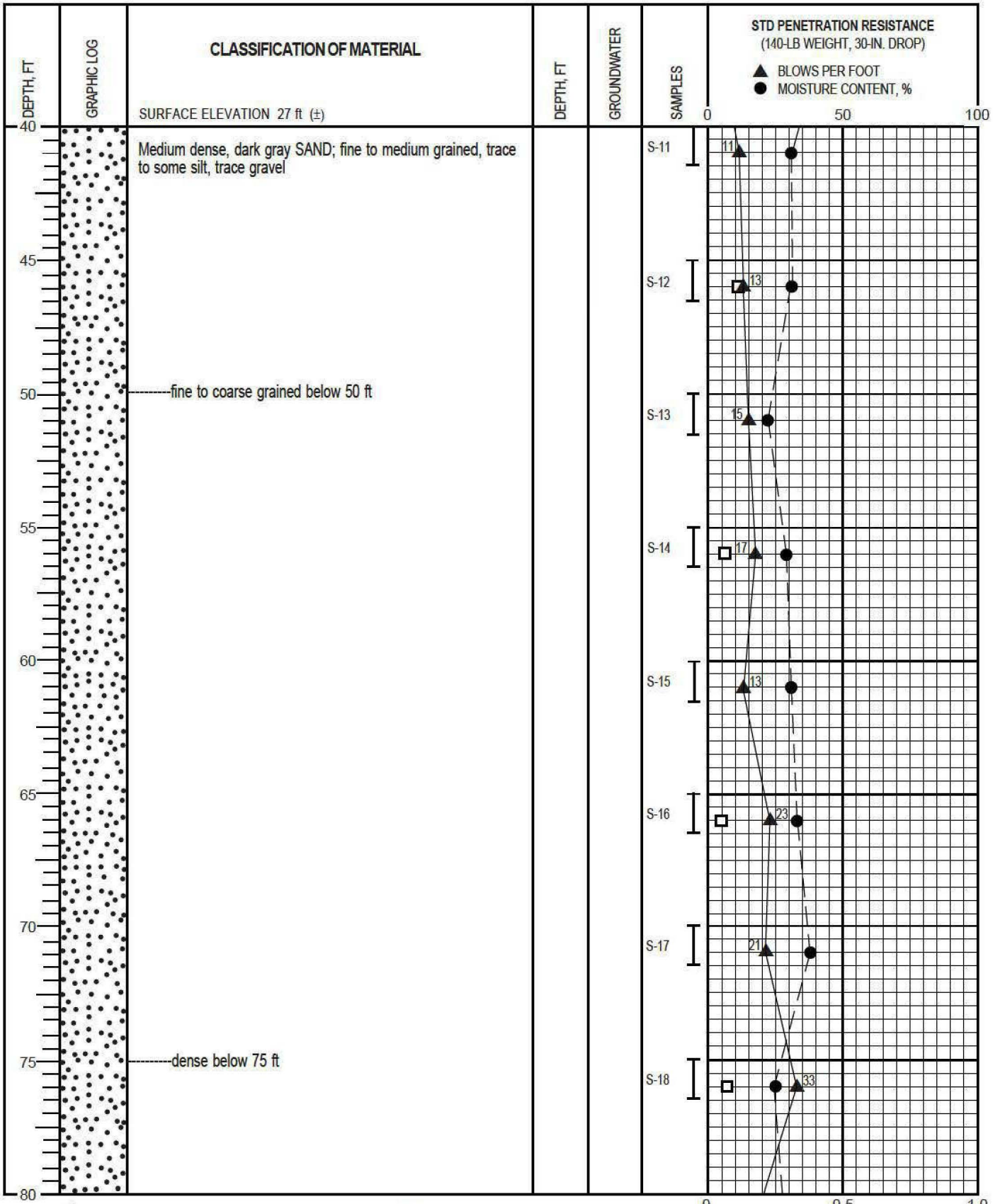

GRI

BORING B-25 (cont.)

SEP. 2014 JOB NO. W1114 FIG. 3A

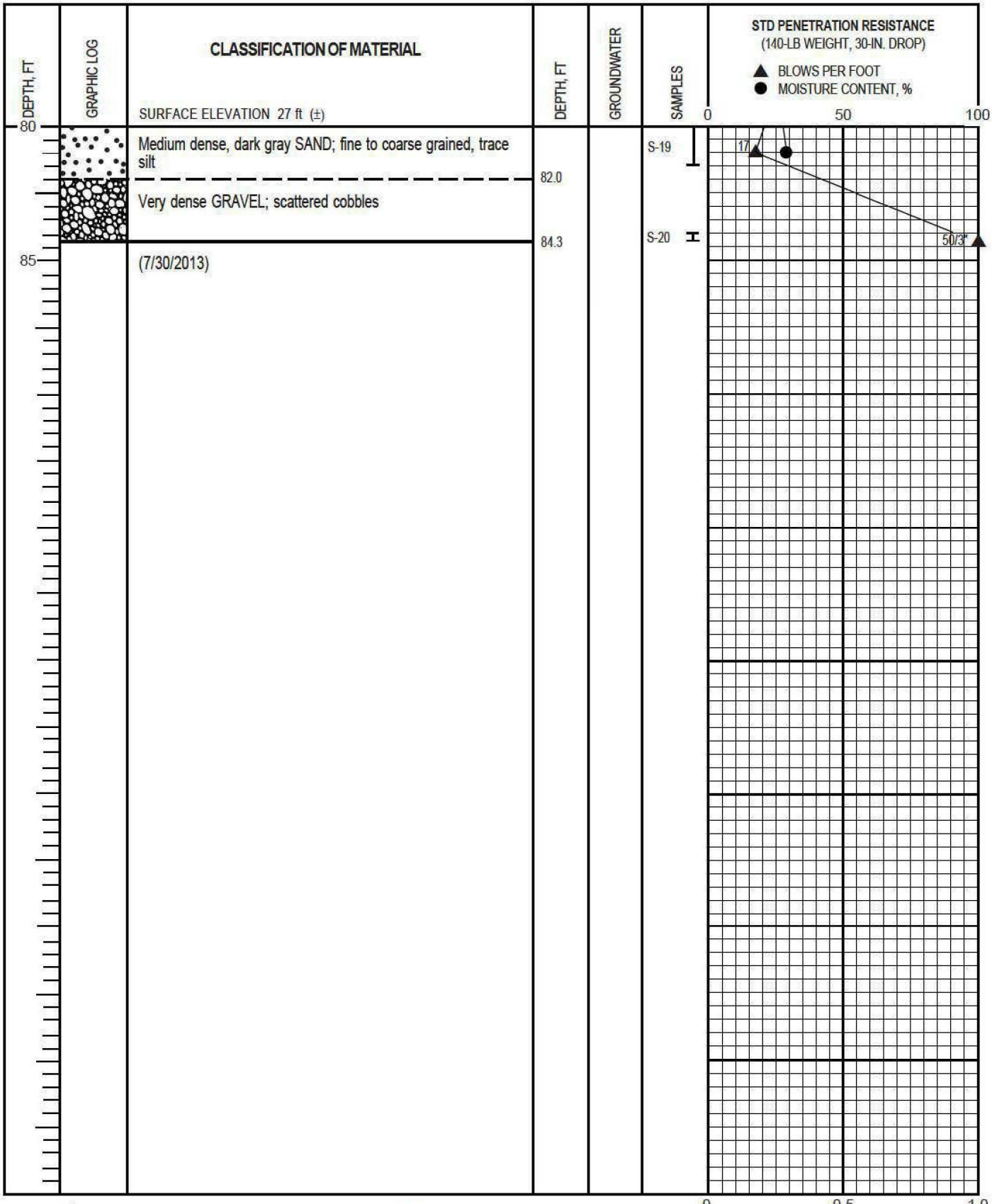

GRI

BORING B-25 (cont.)

SEP. 2014 JOB NO. W1114 FIG. 3A

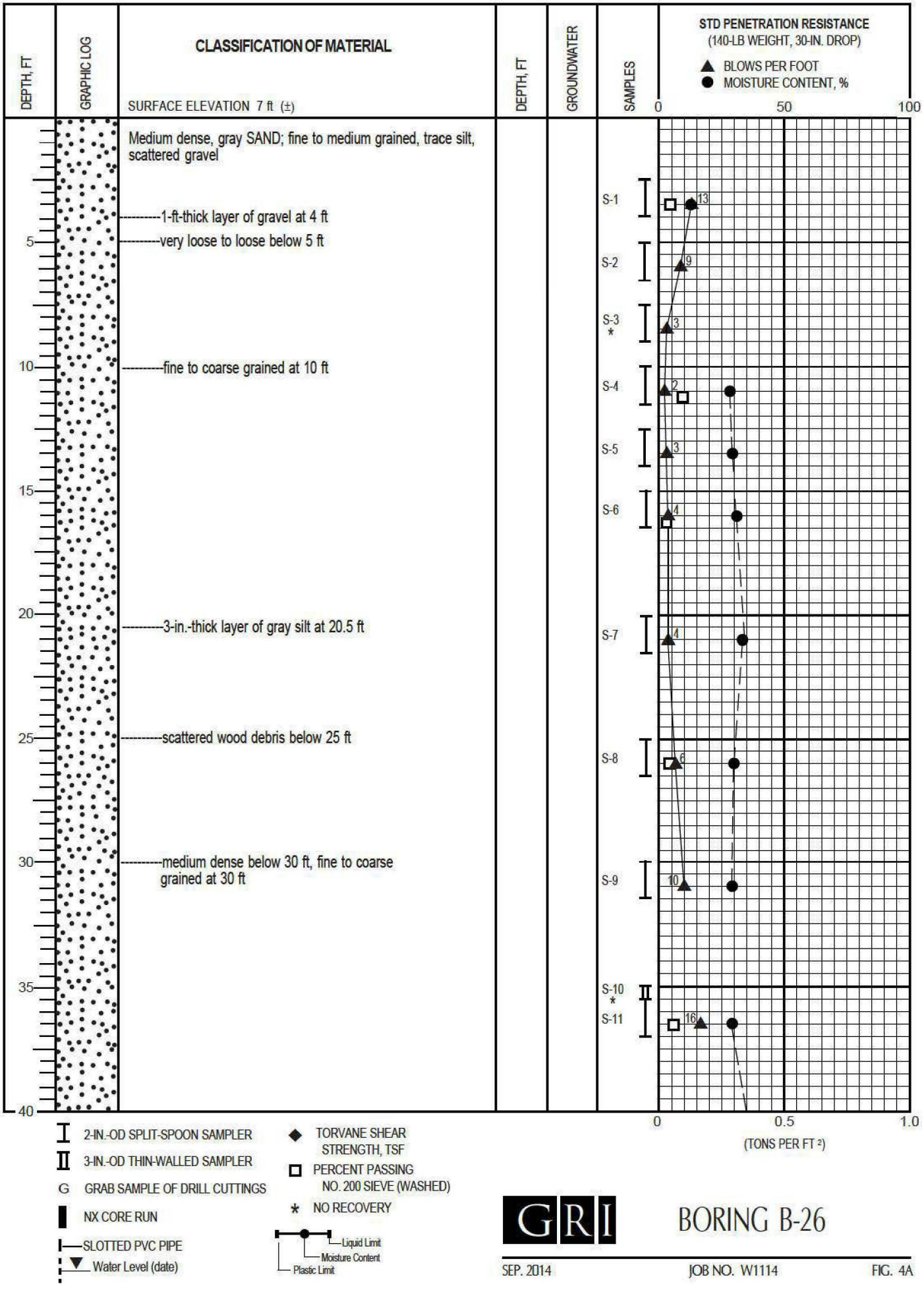

GRI

BORING B-26

SEP. 2014 JOB NO. W1114 FIG. 4A

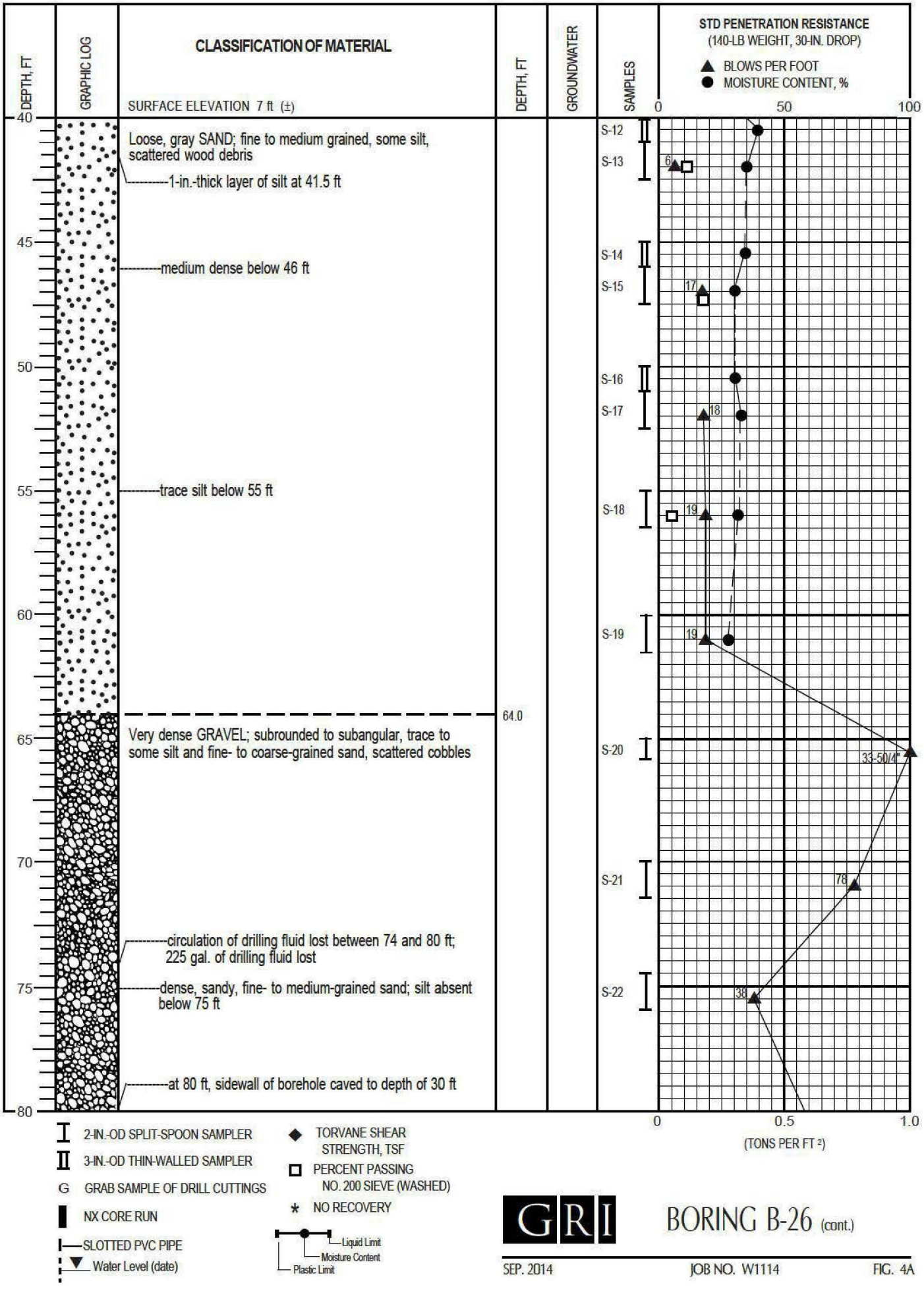

GRI

BORING B-26 (cont.)

SEP. 2014 JOB NO. W1114 FIG. 4A

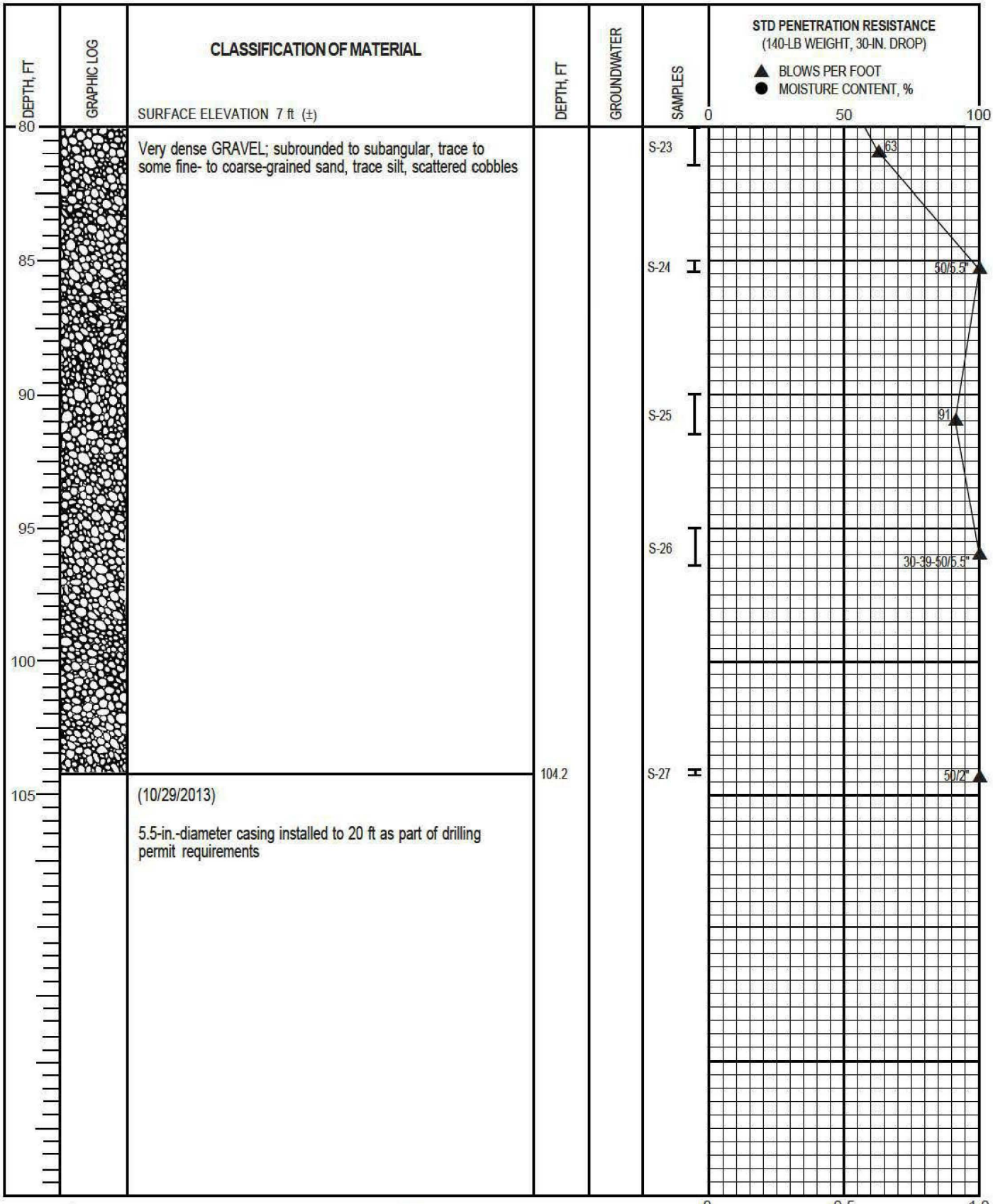

GRI

BORING B-26 (cont.)

SEP. 2014 JOB NO. W1114 FIG. 4A

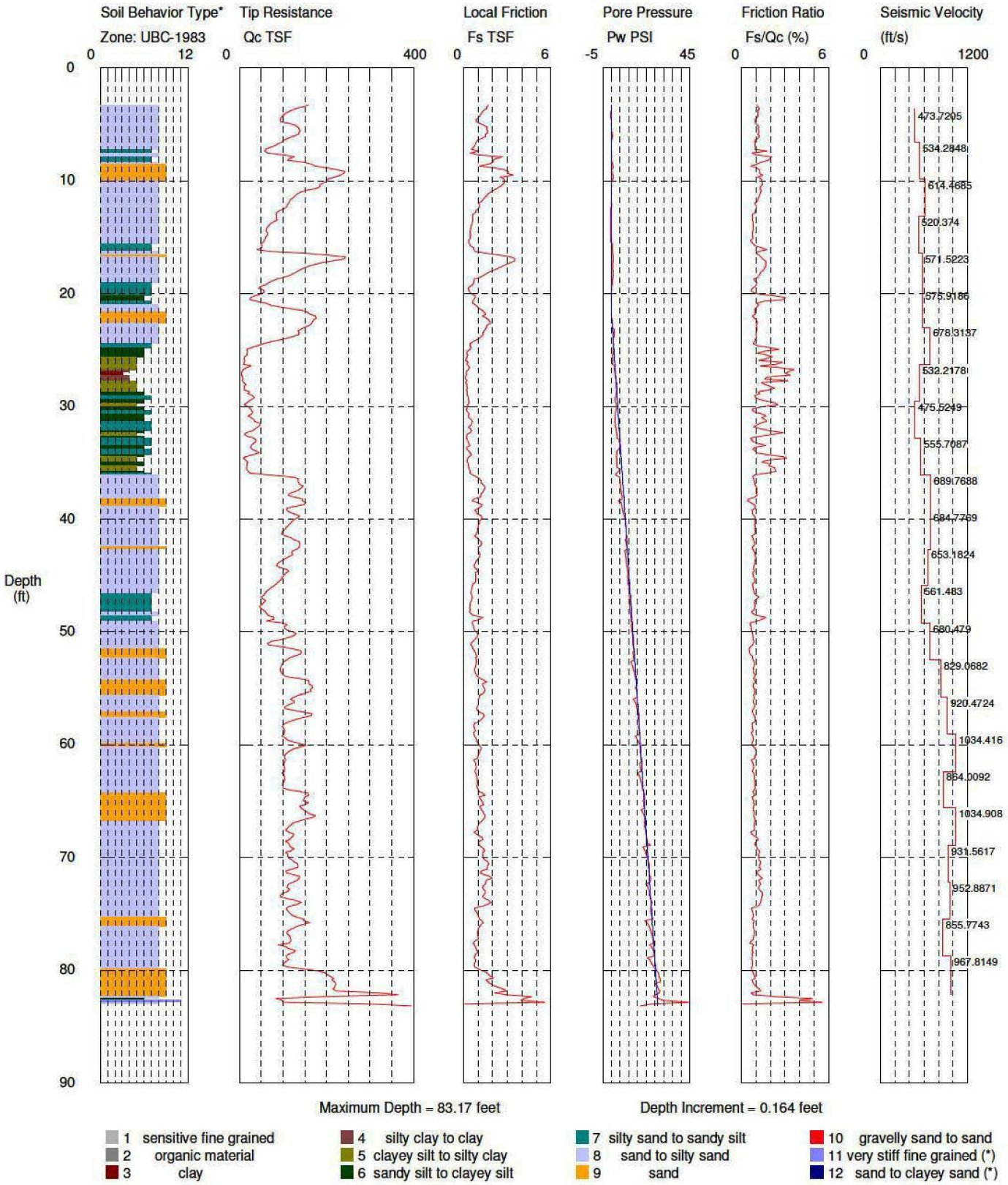

SURFACE ELEVATION = 27 FT

GRI

CONE PENETRATION TEST CPT-6

(WITH SEISMIC VELOCITY)

SEP. 2014 JOB NO. W1114 FIG. 5A

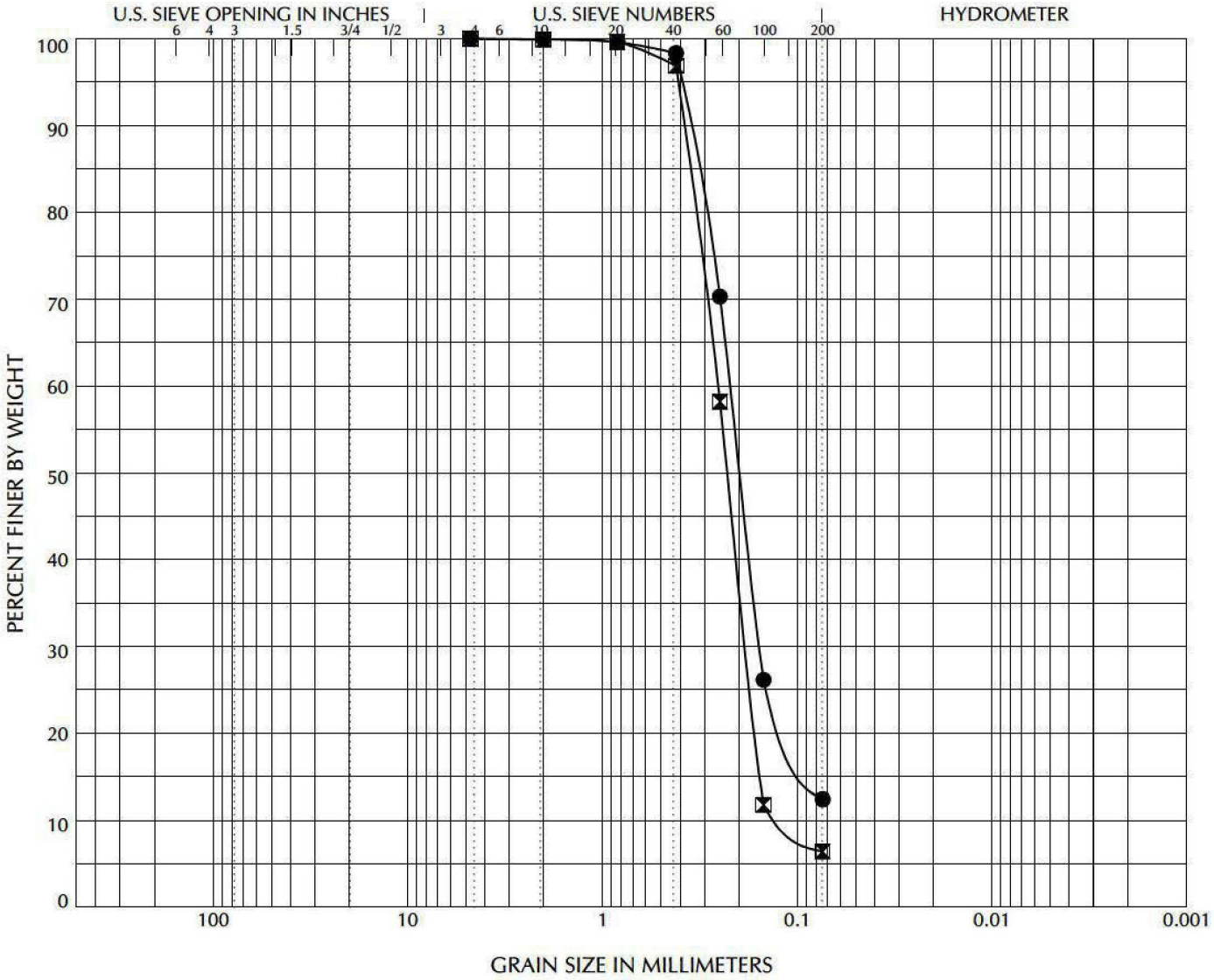

COBBLES	GRAVEL		SAND			SILT OR CLAY
	Coarse	Fine	Coarse	Medium	Fine	

	Location	Sample	Depth, ft	Classification	Gravel, %	Sand, %	Fines, %
●	B-23	S-8	25.0	SAND; fine to medium grained, some silt	0.0	87.3	12.7
⊠	B-23	S-12	45.0	SAND; fine grained, trace silt	0.0	93.5	6.5

GRI

GRAIN SIZE DISTRIBUTION

SEP. 2014 JOB NO. W1114 FIG. 6A

GRAIN SIZE GRI-TWO PER PAGE W1114-LAB.GPJ GRI DATA TEMPLATE.GDT 2/3/14

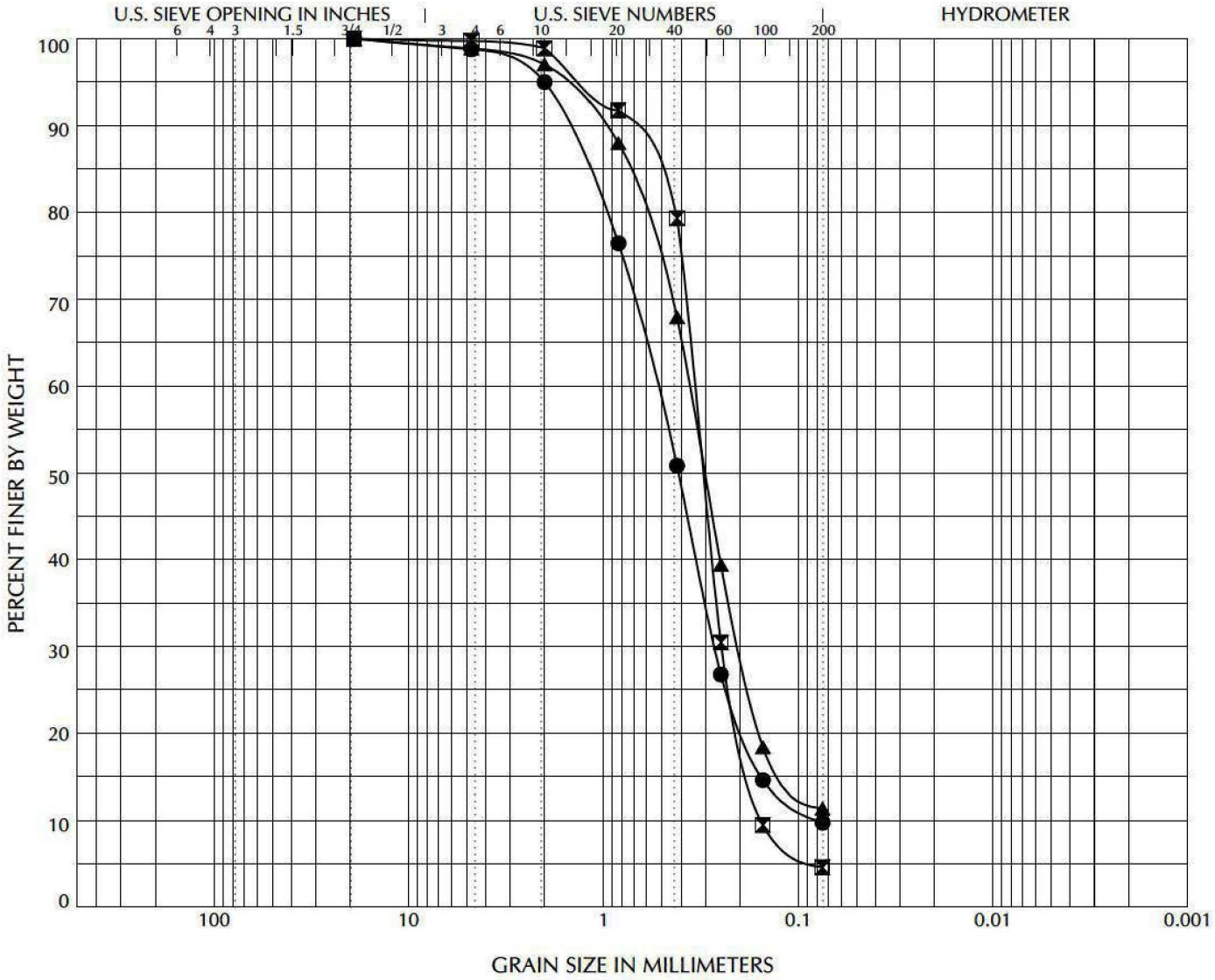

COBBLES	GRAVEL		SAND			SILT OR CLAY
	Coarse	Fine	Coarse	Medium	Fine	

	Location	Sample	Depth, ft	Classification	Gravel, %	Sand, %	Fines, %
●	B-26	S-4	10.0	Gray SAND; fine to coarse grained, trace silt	1.2	89.0	9.8
⧓	B-26	S-8	25.0	Gray SAND; fine to medium grained, trace silt, scattered wood debris	0.3	95.2	4.6
▲	B-26	S-13	41.0	Gray SAND; fine to medium grained, some silt, scattered wood debris	1.1	87.5	11.4

GRI

GRAIN SIZE DISTRIBUTION

SEP. 2014 JOB NO. W1114-T3 FIG. 7A

GRAIN SIZE GRI-THREE PER PAGE W1114-T3 LAB.GPJ GRI DATA TEMPLATE.GDT 6/4/14

APPENDIX B

Site-Specific Seismic Hazard Study

APPENDIX B

SITE-SPECIFIC SEISMIC HAZARD STUDY

General

GRI has completed a site-specific seismic hazard study for the docks at the proposed Tesoro Savage Vancouver Energy Distribution Terminal - Upland Facility (TSVEDT) in Vancouver, Washington. The purpose of the study was to evaluate the potential seismic hazards associated with regional and local seismicity. The site-specific hazard study is intended to meet the requirements of the upcoming American Society of Civil Engineers (ASCE) *Seismic Design of Pile-Supported Piers and Wharves* in compliance with the requirements of ASCE 7-05 Chapter 21. Our work was based on the potential for regional and local seismic activity, as described in the existing scientific literature, and on the subsurface conditions at the site, as disclosed by the geotechnical explorations completed for the project. Specifically, our work included the following tasks:

1) A detailed review of available literature, including published papers, maps, open-file reports, seismic histories and catalogs, and other sources of information regarding the tectonic setting, regional and local geology, and historical seismic activity that might have a significant effect on the site.

2) Compilation, examination, and evaluation of existing subsurface data gathered at and in the vicinity of the site, including classification and laboratory analyses of soil samples. This information was used to prepare a generalized subsurface profile for the docks on the TSVEDT property.

3) Identification of potential seismic sources appropriate for the site and characterization of those sources in terms of magnitude, distance, and acceleration response spectra.

4) Office studies, based on the generalized subsurface profile and the controlling seismic sources, resulting in conclusions and recommendations concerning:

    a) specific seismic events and characteristic earthquakes that might have a significant effect on the Docks;

    b) the potential for seismic energy amplification at the Docks; and

    c) site-specific acceleration response spectra for design of the Docks

This appendix describes the work accomplished and summarizes our conclusions and recommendations.

Geologic Setting

General. On a regional scale, the site lies within the Willamette-Puget Sound lowland trough of the Cascadia convergent tectonic system (Blakely et al., 2000). The lowland areas consist of broad north-south-trending basins in the underlying geologic structure between the Coast Range to the west and the Cascade Mountains to the east. The lowland trough is characterized by alluvial plains with areas of buttes and terraces. The site lies approximately 95 km inland from the down-dip edge of the seismogenic extent

of the Cascadia Subduction Zone (CSZ), an active convergent plate boundary along which remnants of the Farallon Plate (the Gorda, Juan de Fuca, and Explorer plates) are being subducted beneath the western edge of the North American continent. The subduction zone is a broad, eastward-dipping zone of contact between the upper portion of the subducting slabs and the over-riding North American Plate as shown on Figure 1B.

On a local scale, the site lies within the Portland Basin, a large, well-defined, northwest-trending structure characterized as a right-lateral pull-apart basin in the forearc of the CSZ. The Portland Basin is bounded by high-angle, northwest-trending, right-lateral strike-slip faults that are considered to be seismogenic; however, the relationship between specific earthquakes and individual faults in the area is not well understood since few of these faults are expressed clearly at the ground surface. A limited number of intrabasin faults have been mapped on the basis of stratigraphic offsets and geophysical evidence, and the site is located in close proximity to the inferred traces of the Portland Hills Fault and the East Bank Fault indicated on published geologic mapping (Personius et al., 2003). The distribution of these crustal faults relative to the site is shown on the Regional Geologic Map and Local Fault Map, Figures 2B and 3B, respectively. The locations of faults on the geologic map are inferred or approximate. Other faults may be present within the basin, but clear stratigraphic evidence regarding their location and extent is not presently available.

Because of the proximity of the site to the CSZ and its location within the Portland Basin, three seismic sources contribute to the potential for damaging earthquake motions at the site. Two of these sources are associated with tectonic activity related to the Cascadia Subduction Zone, the third is associated with movement on relatively shallow faults within and adjacent to the Portland Basin.

Site Soil and Geologic Conditions. The dock site is covered by alluvial sand and silt deposited by the Columbia River. The alluvium extends to variable depths, ranging from 16 ft at the T-section of the docks to 64 ft at pier 3 of the trestle. The sand and silt deposits are underlain by gravel associated with late Pleistocene catastrophic flood materials deposited by repeated Missoula Flood events that occurred between 13,500 and 15,000 years ago. Geologic investigations for the proposed Interstate 5 bridge replacement, about 3 miles upstream from the project site, indicate the gravel on the Washington side of the Columbia River can be up to 100 ft thick. The flood deposits are underlain by well-consolidated or cemented conglomerate and sandstone units of the Troutdale Formation (Pliocene), which are, in turn, underlain by the Sandy River Mudstone bedrock (Miocene to Pliocene; Beeson et al., 1991; Trimble, 1963).

Seismicity

General. The geologic and seismologic information available for identifying the potential seismicity at the site is incomplete, and large uncertainties are associated with estimates of the probable magnitude, location, and frequency of occurrence of earthquakes that might affect the site. The available information indicates the potential seismic sources that may affect the site can be grouped into three independent categories: *subduction zone events* related to sudden slip between the upper surface of the Juan de Fuca plate and the lower surface of the North American plate, *subcrustal (intraslab) events* related to deformation and volume changes within the deeper portion of the subducted Juan de Fuca plate, and *local crustal events* associated with movement on shallow, local faults within and adjacent to the Portland Basin. Based on our review of currently available information, we have developed parameters for each of these

potential seismic sources. The seismic sources are characterized by three important parameters: magnitude, distance to the subject site, and the peak horizontal bedrock accelerations produced by the controlling earthquake on the seismic source. The size of an earthquake is commonly defined by its moment magnitude Mw. Distance is measured using the closest horizontal distance to the surface projection of the rupture plane or the closest distance to the rupture plane, in kilometers. Peak horizontal bedrock accelerations are expressed in units of gravity (1 g = 32.2 ft/sec^2 = 981 cm/sec^2).

Subduction Zone Event. Written Japanese tsunami records provide evidence that a great CSZ earthquake occurred in January 1700. Geological studies show that great megathrust earthquakes have occurred repeatedly in the past 7,000 years (Atwater et al., 1995; Clague, 1997; Goldfinger, 2003; and Kelsey et al., 2005), and geodetic studies (Hyndman and Wang, 1995; Savage et al., 2000) indicate rate of strain accumulation consistent with the assumption that the CSZ is locked beneath offshore northern California, Oregon, Washington, and southern British Columbia (Fluck et al., 1997; Wang et al., 2001). Numerous geological and geophysical studies suggest the CSZ may be segmented (Hughes and Carr, 1980; Weaver and Michaelson, 1985; Guffanti and Weaver, 1988; Goldfinger, 1994; Kelsey and Bockheim, 1994; Mitchell et al., 1994; Personius, 1995; Nelson and Personius, 1996; Witter, 1999), but the most recent studies suggest that for the last great earthquake in 1700, most of the subduction zone ruptured in a single Mw 9 earthquake (Satake et al., 1996; Atwater and Hemphill-Haley, 1997; Clague et al., 2000). Published estimates of the probable maximum size of subduction zone events range from moment magnitude Mw 8.3 to >9.0. Numerous detailed studies of coastal subsidence, tsunamis, and turbidites yield a wide range of recurrence intervals, but the most complete records (>4,000 years) indicate average intervals of 350 to 600 years between great earthquakes on the CSZ (Adams, 1990; Atwater and Hemphill-Haley, 1997; Witter, 1999; Clague et al., 2000; Kelsey et al., 2002; Kelsey et al., 2005; Witter et al., 2003). Tsunami inundation in buried marshes along the Washington and Oregon coast and stratigraphic evidence from the Cascadia margin support these recurrence intervals (Kelsey et al., 2005; Goldfinger, 2003).

The USGS probabilistic analysis assumes four potential locations for the eastern edge of the earthquake rupture zone for the CSZ, as shown in Figure 4B. The 2008 USGS mapping effort indicates two rupture scenarios are assumed to represent these megathrust events: 1) Mw 9.0±0.2 events that rupture the entire CSZ every 500 years and 2) Mw 8.0 to 8.7 events with rupture zones that occur on segments of the CSZ and occur over the entire length of the CSZ during a period of about 500 years (Petersen et al., 2008). The assumed distribution of earthquake magnitudes is shown on Figure 5B. This distribution assumes the larger Mw 9.0 earthquakes likely occur more often than the smaller segmented ruptures. Therefore, for our deterministic analysis, we have chosen to represent the subduction zone event by a design earthquake of Mw 9.0 at a focal depth of 15 km and a rupture distance of 86 km. This corresponds to a sudden rupture of the entire length of the Juan de Fuca-North American plate interface with an assumed rupture zone along the coastline due west of Vancouver. Based on an average of the attenuation relationships published by Zhao (2006), Atkinson and Macias (2009), and Abrahamson, et al. (2012), a subduction zone earthquake with these parameters would result in an average peak bedrock acceleration of approximately 0.19 g at the project site.

Subcrustal Event. There is no historic earthquake record of subcrustal, intraslab earthquakes in Southwest Washington. Although both the Puget Sound and Northern California regions have experienced many of these earthquakes in historic times, Wong (2005) hypothesizes that due to subduction zone geometry, geophysical conditions and local geology, Southwest Washington/Oregon may not be subject to intraslab

earthquakes. In the Puget Sound area, these moderate to large earthquakes are deep (40 to 60 km) and over 200 km from the deformation front of the subduction zone. Offshore, along the Northern California coast, the earthquakes are shallower (up to 40 km) and located along the deformation front. Estimates of the probable magnitude, distance, and frequency of subcrustal events in Southwest Washington are generally based on comparisons of the CSZ with active convergent plate margins in other parts of the world and on the historical seismic record for the region surrounding Puget Sound, where significant events known to have occurred within the subducting Juan de Fuca plate have been recorded. Published estimates of the probable maximum size of these events range from moment magnitude Mw 7.0 to 7.5. The 1949, 1965, and 2001 documented subcrustal earthquakes in the Puget Sound area correspond to Mw 7.1, 6.5, and 6.8, respectively. Published information regarding the location and geometry of the subducting zone indicates that a focal depth of 50 km is probable (Weaver and Shedlock, 1989). We have chosen to represent the subcrustal event by a characteristic earthquake of moment magnitude Mw 7.0 at a focal depth of 50 km and a rupture distance of 50 km. Based on the attenuation relationships published by Zhao (2006), and Atkinson and Boore (2003), and Abrahamson, et al. (2012), a subcrustal earthquake of this magnitude and distance would result in a peak horizontal bedrock acceleration of approximately 0.14g at the site.

Local Crustal Event. Sudden crustal movements along relatively shallow, local faults in the southwest Washington area, although rare, have been responsible for local crustal earthquakes. The precise relationship between specific earthquakes and individual faults is not well understood, since few of the faults in the area are expressed at the ground surface, and the foci of the observed earthquakes have not been located with precision. The history of local seismic activity is commonly used as a basis for determining the size and frequency to be expected of local crustal events. Although the historical record of local earthquakes is relatively short (the earliest reported seismic event in the area occurred in 1920), it can serve as a guide for estimating the potential for seismic activity in the area.

Based on fault mapping conducted by the U.S. Geological Survey (USGS, 2008), the Portland Hills Fault is the closest mapped crustal fault to the site that is considered active in the probabilistic hazard maps. The Portland Hills Fault is located approximately 7 km from the site and has a characteristic earthquake magnitude of Mw 7.0. A crustal earthquake of this magnitude and distance would result in a peak horizontal bedrock acceleration of approximately 0.33g at the site based on an average of the NGA ground motion relations developed by the Pacific Earthquake Engineering Research (PEER) by Boore and Atkinson (2008), Campbell and Bozorgnia (2008), Idriss (2008) and Chiou and Youngs (2008).

Other Seismic Hazards. Based on the presence of loose sands and soft silts below the water table at the site, there is a high risk of liquefaction and lateral spreading during a design-level earthquake. More detailed discussions regarding liquefaction and lateral spreading are provided in the Seismic Considerations section of the report. Although detailed tsunami modeling of the Columbia River due to a Cascadia Subduction Zone earthquake has not been completed, we anticipate the risk of upland damage by tsunami at the site is low due to the distance from the coast. River fluctuations may result from a tsunami generated by a CSZ earthquake. Due to the proximity of the Columbia River, there is a risk of seiche. Unless occurring on a previously unmapped fault, it is our opinion the risk of ground rupture at the site is very low.

Deterministic Earthquake Parameters

As discussed above, three distinctly different seismic sources affect seismicity in the project area. Deterministic evaluation of the earthquake sources using published attenuation relations provides estimates of peak bedrock accelerations and response spectra for each seismic source. These deterministic estimates are not associated with a relative hazard level or probability of occurrence like probabilistic estimates, but simply provide an estimate of the ground motion parameters for each seismic source at a given distance from the site. The basic parameters of each earthquake source are as follows:

TABLE 1B: DETERMINISTIC EARTHQUAKE PARAMETERS

Earthquake Source	Attenuation Relationships	Magnitude, M_w	Rupture Distance, km	Focal Depth, km	Median Peak Bedrock Acceleration, g	Average Median Peak Bedrock Acceleration, g
Subduction Zone	Zhao (2006)	9.0	86	15	0.19	
	Atkinson and Macias (2009)	9.0	86	15	0.17	0.19
	Abrahamson (2012)	9.0	86	15	0.23	
Subcrustal	Zhao (2006)	7.0	50	50	0.15	
	Atkinson and Boore, (2003)	7.0	50	50	0.10	0.14
	Abrahamson (2012)	7.0	50	50	0.18	
Local Crustal	Campbell and Bozorgnia (2008)	7.0	7	NA	0.32	
	Chiou and Youngs (2008)	7.0	7	NA	0.36	0.33
	Boore and Atkinson (2008)	7.0	7	NA	0.27	
	Idriss (2008)	7.0	7	NA	0.38	

The values summarized in Table 1B represent the average of median peak bedrock accelerations for the characteristic earthquake on the controlling faults. The upcoming ASCE *Seismic Design of Pile-Supported Piers and Wharves* references ASCE 7-05 which requires an evaluation of 150 percent of the largest median spectral response acceleration taking into account the characteristic earthquakes on all known active faults within the region. Figure 6b compares 150% of these median deterministic spectral values with the deterministic lower limit on MCE response spectrum, in accordance with Figure 21.2-1 of ASCE 7-05 to develop the deterministic Maximum Considered Earthquake (MCE) bedrock spectra. Figure 6B shows that the individual fault deterministic response spectra are lower than the deterministic lower limit on MCE response spectrum. Per Section 21.2.2 of ASCE 7-05, the deterministic spectrum shall be the greater of the 150% deterministic spectrum and the deterministic lower limit spectrum of Figure 21.2-1. Therefore, the deterministic lower limit response spectrum is selected to represent the bedrock deterministic MCE response spectrum.

Probabilistic Considerations

The probability of an earthquake of a specific magnitude occurring at a given location is commonly expressed by its return period, i.e., the average length of time between successive occurrences of an earthquake of that size or larger at that location. The return period of a design earthquake is calculated once a project design life and some measure of the acceptable risk that the design earthquake might occur or be exceeded are specified. These expected earthquake recurrences are expressed as a probability of exceedance during a given time period or design life. The ASCE standard *Seismic Design of Pile-Supported Piers and Wharves* defines three seismic hazard levels: the Operating Level Earthquake (OLE),

the Contingency Level Earthquake (CLE), and the Design Earthquake (DE). The OLE is defined by 50% probability of exceedance in 50 years, which corresponds to an earthquake with an expected recurrence interval of 72 years, and represents a performance level with minimal structural damage. The CLE is defined by 10% probability of exceedance in 50 years, which corresponds to an earthquake with an expected recurrence interval of 475 years, and represents a performance level of controlled and repairable structural damage. The DE is defined per ASCE 7-05 which develops the response spectra based on ground motions associated with the MCE. The MCE is represented by a probabilistic earthquake with a 2% probability of exceedance in 50 years (return period of 2,475years), except where subject to deterministic limitations (Leyendecker et al., 2000). The Design Earthquake (DE) response spectrum is obtained by taking two-thirds of the MCE level ground motions.

For the Dock site, located at the approximate latitude and longitude coordinates of 45.65°N and 122.71°W, the spectral acceleration values corresponding to the 72, 475 and 2,475 years of return periods were obtained for Site Class B from the 2008 USGS hazard curves and uniform-hazard maps. These spectral accelerations for the three hazard levels are plotted on Figure 7B, and the values are presented on Table 2B.

TABLE 2B: RESPONSE SPECTRA FOR DIFFERENT PROBABILISTIC HAZARD LEVELS

	Spectral Acceleration, g		
Period, seconds	**72 Years**	**475 Years**	**2,475 Years**
0	0.05	0.20	0.41
0.1	0.09	0.39	0.86
0.2	0.11	0.45	0.96
0.3	0.10	0.38	0.83
0.5	0.07	0.29	0.64
1	0.03	0.16	0.37
2	0.01	0.07	0.19
3	0.01	0.04	0.10
4	0.00	0.02	0.07
5	0.00	0.02	0.04

Deaggregation of the 2008 USGS data suggests that the Cascadia Subduction Zone, subcrustal events, and local crustal faults all contribute to the seismic hazard at the site.

Development of Target Bedrock Spectra

The site-specific analysis requires developing a bedrock target spectrum prior to selecting and scaling input acceleration time histories. The bedrock target spectra are developed for all three seismic hazard levels, which are previously discussed in the probabilistic consideration section. The target spectra for the OLE and CLE conditions can be directly represented by the site–specific probabilistic uniform hazard curves which correspond to the ground motion with 50% probability of exceedance in 50 years and 10% probability of exceedance in 50 years, respectively. The target bedrock spectrum for the DE is developed as per the requirements of ASCE 7-05. According to Chapter 21 of ASCE 7-05, the controlling target spectrum is developed by comparing the deterministic and probabilistic MCE response spectra, and taking the lower of the two spectra to represent the site-specific MCE bedrock response spectrum. The

comparison of the MCE probabilistic and deterministic response spectra are shown in Figure 8B for the dock site. The probabilistic MCE spectrum is lower than the deterministic spectrum and, therefore, based on the above criterion, the probabilistic spectrum is defined to be the MCE bedrock spectrum.

Site Response Modeling

The effect of a specific seismic event on the site is related to the type and thickness of soil overlying the bedrock at the site and the type and quantity of seismic energy delivered to the bedrock beneath the site by the earthquake. Site response analysis was completed to estimate this site-specific behavior in accordance with ASCE standard for Pile-Supported Piers and Wharves. The site response analysis consisted of three components: 1) selection of target bedrock response spectrum, 2) numerical modeling to analyze the site-specific behavior of the soils using horizontal ground motion acceleration time histories scaled to the approximate level of the target bedrock response spectrum over the periods of interest, and 3) calculation of the ratio of the surface response spectra values to the bedrock response spectra values, at each spectral period, to develop a recommended ground surface response spectrum.

The site response modeling was completed using the D-MOD2000 program by GeoMotions, LLC. D-MOD2000 is a one-dimensional non-linear, time–domain site response modeling program capable of capturing the nonlinear- hysteretic soil behavior during cyclic seismic loading and unloading. The program computes the dynamic response of a layered soil profile to vertically propagating shear waves using total stress or effective stress analyses. The effective stress option provides a means to evaluate the influence of excess pore pressure development and cyclic degradation of soil strength/stiffness (i.e., pore water pressure generation, and pore water pressure dissipation and redistribution) on the dynamic response of the soil profile. D-MOD2000 uses the hyperbolic modified Kodner and Zelasko (MKZ) model to characterize the nonlinear stress-strain soil behavior. The MKZ parameters are generally obtained by fitting the hyperbolic model to published empirical curves.

Within the D-MOD2000 program, the user creates a discretized soil profile and inputs a variety of soil modeling parameters derived from field and laboratory testing and established correlations in the geotechnical literature. A suite of scaled earthquake records are input into the program and propagated up through the soil column to the ground surface. From the modeled ground surface response for a particular soil profile, a Spectral Acceleration Ratio (SAR) can be determined for each earthquake record as the ratio of ground surface to bedrock spectral acceleration ($SA_{surface}/SA_{bedrock}$) at selected periods.

Input Parameters

For the Dock, D-MOD2000 based total and effective stress analyses were performed for evaluating the seismic response and performance of the soil underlying the site. First, a generalized subsurface profile for the site was developed based on our subsurface explorations. Two shear wave velocity profiles at the T-section of the Dock and Pier 3 of the Trestle were estimated based on boring B-26 drilled at Pier 3 and CPT-6 measurements located in the upland area. The ratio of the effective overburden stresses to the one-fourth power, $(\sigma'_{v,\ Dock}/\ \sigma'_{v,\ CPT\text{-}6})^{0.25}$, was used as an adjustment factor to derive the shear wave velocity profiles from CPT-6 measurements. The assumed soil profiles at the T-section of the Dock and Pier 3 of the Trestle are tabulated below in Tables 3B and 4B, respectively.

TABLE 3B: SUBSURFACE PROFILE AT T-SECTION OF DOCK

Material	Thickness, ft	Total Unit Weight, pcf	Estimated Shear Wave Velocity, ft/sec
SAND	3	110	400
SAND	3	110	450
SAND	3	110	500
SAND	4	110	500
SAND	3	110	600
Very dense GRAVEL	5	125	850
Very dense GRAVEL	5	125	950
Very dense GRAVEL	5	125	1,100
Very dense GRAVEL	5	125	1,150
Very dense GRAVEL	10	125	1,200
Very dense GRAVEL	10	125	1,250
Very dense GRAVEL	10	125	1,300
Very dense GRAVEL	10	125	1,350
Very dense GRAVEL	10	125	1,400
Very dense GRAVEL	10	125	1,450
Very dense GRAVEL	10	125	1,500
Very dense GRAVEL	10	125	1,550
Very dense GRAVEL	10	125	1,600
Very dense GRAVEL	10	125	1,650
Very dense GRAVEL	10	125	1,700
Very dense GRAVEL	10	125	1,750
Very dense GRAVEL	10	125	1,800
Very dense GRAVEL	10	125	1,900
Very dense GRAVEL	10	125	2,100
Very dense GRAVEL	10	125	2,200
Troutdale	10	130	2,500

TABLE 4B SUBSURFACE PROFILE AT PIER 3 OF TRESTLE

Material	Thickness, ft	Total Unit Weight, pcf	Estimated Shear Wave Velocity, ft/sec
Loose SAND	3	110	300
Loose SAND	3	110	400
Loose SAND	4	110	350
Loose SAND	3	110	350
Loose SAND	3	110	400
Medium dense SAND	4	110	500
Medium dense SAND	3	110	550
Medium dense SAND	3	110	500
Medium dense SAND	3	110	450
Medium dense SAND	4	110	550
Medium dense SAND	3	110	700

Material	Thickness, ft	Total Unit Weight, pcf	Estimated Shear Wave Velocity, ft/sec
Medium dense SAND	3	110	750
Medium dense SAND	3	110	850
Medium dense SAND	4	110	750
Medium dense SAND	3	110	900
Medium dense SAND	3	110	800
Medium dense SAND	3	110	850
Medium dense SAND	4	110	750
Medium dense SAND	3	110	900
Very dense GRAVEL	5	125	1,100
Very dense GRAVEL	5	125	1,200
Very dense GRAVEL	5	125	1,300
Very dense GRAVEL	5	125	1,350
Very dense GRAVEL	10	125	1,400
Very dense GRAVEL	10	125	1,450
Very dense GRAVEL	10	125	1,500
Very dense GRAVEL	10	125	1,550
Very dense GRAVEL	10	125	1,600
Very dense GRAVEL	10	125	1,650
Very dense GRAVEL	10	125	1,700
Very dense GRAVEL	10	125	1,750
Very dense GRAVEL	10	125	1,800
Very dense GRAVEL	10	125	1,850
Very dense GRAVEL	10	125	1,900
Very dense GRAVEL	10	125	2,000
Very dense GRAVEL	10	125	2,100
Very dense GRAVEL	10	125	2,200
Very dense GRAVEL	10	125	2,300
Very dense GRAVEL	10	125	2,400
Troutdale	10	130	2,500

The material properties and boundary conditions were specified in D-MOD2000 for the Dock site. The unit weights for each of the soil profile were estimated based on the laboratory unit weight test results. The sand and gravel layers encountered throughout the soil profile were assigned the depth- dependent EPRI (1993) sand and rock modulus reduction and damping curves, which accounts for the effects of confining pressure. The representative pore-pressure generation parameters for the sand layers were selected based on grain size distribution curve matching procedures with D-MOD2000. The grain size distribution curve for the sand layer was compared to the liquefiable sands and silts curves within D-MOD2000 database, and the Santa Monica Beach (SMB) sand was selected to approximate the pore-pressure generation parameters. The half-space boundary condition at the base of the model was represented by a visco-elastic boundary with a unit weight of 130 pounds per cubic foot (pcf) and a shear wave velocity of 2,500 feet per second.

Ground Motion Selection and Scaling

The target bedrock response spectrum for the site was developed for Site Class B, or rock site, conditions in accordance with the method outlined in the Target Bedrock Spectrum section of this report for OLE, CLE and MCE hazard levels. A series of earthquake acceleration-time histories have been selected and scaled to the target bedrock spectrum. From the available records, corrected free-field and basement/ground floor accelerograms were selected for input as bedrock time histories. Wherever possible, earthquakes of similar magnitude and duration to the characteristic earthquakes were selected. These records were checked for obvious errors, missing data points, and other anomalies and were transformed into a uniform data format. The selected strong-motion records are tabulated below in Table 5B.

TABLE 5B SELECTED STRONG-MOTION RECORDS

Earthquake	Recording Station	Magnitude	Rupture Distance, km	Peak Bedrock Acceleration, g
Loma Prieta (1989)	San Jose - Santa Teresa Hills	6.9	14.7	0.28
Nisqually (2001)	Olympia, WSDOT Test Lab	6.8	18.3	0.22
Chile (2010)	Curico	8.8	65.1	0.47
Chile (2010)	Hualane	8.8	50	0.46
Japan (2011)	Kuroiso (TCG001)	9	102	0.42
Japan (2011)	Yamatsuri (FKS 014)	9	76	0.23
Japan (2011)	Hachinohe (AOM 012)	9	99	0.19

The selected acceleration time histories were then scaled to reasonably match the bedrock target spectrum at periods of interest including the site fundamental period for the OLE, CLE and MCE hazard levels. The scaling process involves selecting a single factor and multiplying the acceleration time history by this factor so that its pseudo acceleration response spectrum more closely matches the target spectrum at the period of interest.

Site Response Results

Using the generalized subsurface profiles (i.e., at the T-section of the Dock and Pier 3 of the Trestle), the target spectra developed at the bedrock, and the strong ground motion records listed in the preceding tables, pseudo acceleration response spectra were computed for the Dock site with the D-MOD2000 nonlinear model. The ground surface response spectra were developed at 5% of critical damping. The ground surface spectra were compared to the input rock spectra to quantify amplification and/or attenuation through the soil column at the site. The ratio of ground surface to bedrock spectral accelerations, defined as the spectral amplification ratio (SAR), is shown on Figure 9B and Figure 10B for the CLE and MCE conditions, respectively. To estimate ground surface site response throughout the range of spectral periods, the target response spectra is multiplied by the SAR to determine the ground surface response spectrum. The results of the site-specific response modeling are shown on Figures 11B and 12B for the CLE and MCE hazard levels, respectively. Figures 11B and Figure 12B also include the code-based spectrum (i.e., for example Site Class D and Site Class E), developed using site amplification factors based on the appropriate Site Class type. The code-based spectrum is typically derived based on the 0.2 and 1 second spectral accelerations values at the bedrock and site coefficients (i.e., F_a and F_v) provided in Table 11.4-1 and Table 11.4-2 of ASCE 7-05. The code-based site coefficients and the spectral values corresponding to 0.2 and 1 second periods are provided on Table 6B for the OLE, CLE and MCE hazard

levels. The two spectral values are obtained from the map of spectral acceleration parameters provided in Chapter 22 of ACSE 7-05 for the MCE condition while the spectral values corresponding to 72- and 475-year return periods are obtained from USGS data for the OLE and CLE conditions, respectively.

TABLE 6B: SITE COEFFICIENTS AND SPECTRAL VALUES

Hazard Level, Ss and S1 Values	Site Class	F_a	F_v
OLE S_s=0.11 g, S_1=0.03 g	D	1.6	2.4
	E	2.5	3.5
CLE S_s=0.45 g, S_1=0.16 g	D	1.44	2.17
	E	1.87	3.33
MCE S_s=0.94 g, S_1=0.41 g	D	1.12	1.59
	E	0.97	2.40

The site is generally designated as Site Class D based on the average shear wave velocity (Vs_{100}) in the upper 100 ft per Section 20.4 of ASCE 7-05. For the OLE hazard level the degree of ground shaking is insufficient to cause liquefaction of the soil. Therefore, the code-based Site Class D depicted on Figure 13B is recommended for the OLE condition to estimate the ground response spectral acceleration.

For the CLE and MCE hazard levels, our analyses indicate the soil may liquefy and the site is designated as Site Class F in accordance with section 20.3.1 of ASCE 7-05. A site response analyses is required for Site Class F designations. Structures with a fundamental period less than 0.5 second are exempted from this requirement, and the response spectrum may be developed based on the appropriate Site Class for non-liquefied site conditions. Research by Youd and Carter (2005) indicates that code–based response spectra for non-liquefied conditions may be conservatively extended to represent the response spectra for structures with fundamental periods less than 1.0 sec for liquefied conditions. Per Section 21.3 of ASCE 7-05, the ground surface response spectra developed from site response analysis for Site Class F may not be less than 80% of the Site Class response spectrum values assuming no liquefaction.

The calculated and recommended site specific ground surface response spectra at the T-section of the dock and at Pier 3 of the trestle are shown on Figures 11B and 12B for the CLE and MCE, respectively. The calculated values presented on the figures are based on total stress analysis. However, effective stress analyses were also completed for comparison. As anticipated, the effective stress analyses resulted in a "softening" of the soil response and generally lower response values than the total stress analyses. The trends associated with the effective stress analyses were considered in selecting the recommended spectra. The recommended response spectra are also intended to conservatively envelope the estimated response for both the T-section of the dock and the Pier 3 location of the trestle. It should be noted that Figures 11B and 12B also include a spectra based on 80% of Site Class E in addition to site class D spectral values due to liquefaction and code considerations for liquefiable profiles.

CLE Hazard Level. The estimated CLE ground surface response spectra at periods greater than 0.5 second are less than or equal to 80% of the Site Class E response spectrum which is the minimum allowed by the code for periods in this range of interest. At periods less than 0.5 second, the code allows the use of the non-liquefied site class D spectrum. We have recommended a slight increase from the site class D spectrum at short periods to match 80% of the site class E spectrum to account for the shorter period

amplification observed in the total stress analyses of the T-section of the dock. Considering the range of analyses and uncertainties, we have recommended a single CLE hazard level response spectrum at all periods for both the dock and trestle structure. This spectrum based on 80% of the Site Class E response spectrum is shown on Figure 11B.

DE Hazard Level. The estimated MCE ground surface response spectra from the total stress analysis typically exceed either the Site Class D or 80% of Site Class E spectra at periods less than 1.8 seconds. However, total stress parameters do not account for reductions in the response due to softening of the liquefied soils observed in our effective stress analyses, particularly at short periods. At the MCE hazard level, the site class D spectrum is more conservative than the site class E spectrum and we have recommended the site class D spectrum in accordance with the recommendations in ASCE7-05. At periods between 0.89 and 1.8 seconds we conservatively recommend the design spectrum include an increase above Site Class D and E to transition to longer periods and envelop the estimated site specific ground surface response. At periods greater than approximately 1.8 seconds, the site-specific response spectrum is less than 80% of Site Class E, which is the minimum spectral amplification allowed by ASCE 7-05 for liquefied conditions. Plots of our recommended response spectra are shown on the Figure 12B for the MCE. The design earthquake (DE) response spectrum is determined by taking two-thirds of the MCE response spectrum and is shown on Figure 14B.

Conclusions

The site-specific response modeling for the Dock site was completed using total and effective stress parameters based on the generalized subsurface profiles developed at the T-section of the Dock and Pier 3 of the Trestle. The site response modeling was performed for three seismic hazard levels (i.e., OLE, CLE and DE) to meet the requirements of ASCE standard *Seismic Design of Pile-Supported Piers and Wharves*.

For the OLE hazard level, we recommend the code-based Site Class D response spectrum as shown on Figure 13B. For the CLE hazard level, the recommended spectrum is based on 80% of the code based Site Class E response spectrum. For the DE hazard level, the code-based Site Class D response spectrum is recommended for periods less than 0.89 second. At longer periods the recommended response spectrum envelopes the site-specific spectral response values and 80% of the Site Class E response spectrum. The recommended spectra for CLE and DE are shown on Figures 11B and 14B, respectively.

References

Abrahamson, N., Gregor, N., and Addo, K., 2012, BC Hydro Ground Motion Prediction Equations for Subduction Earthquakes, submitted for publication, Bulletin of the Seismological Society of America.

Adams, J., 1990, Paleoseismicity of the Cascadia subduction zone: Evidence from turbidites off the Oregon-Washington margin: Tectonics, v. 9, no. 4, p. 569-583.

ASCE 7-05, 2005, Minimum design loads for buildings and other structures: American Society of Civil Engineers.

ASCE, Proposed Seismic Design of Pile-Supported Piers and Wharves

Atkinson, G.M., and Boore, D.M., 2003, Empirical ground motion relations for subduction zone earthquakes and their application to Cascadia and other regions: Seismological Research Letters, v. 93, no. 4, pp. 1703-1729.

Atkinson, G.M. and Macias, M., 2009, Bulletin of the Seismological Society of America, vol. 99, no. 3, pp. 1552-1578.

Atwater, B.F., and Hemphill-Haley, E., 1997, Recurrence intervals for great earthquakes of the past 3,500 years at northeastern Willapa Bay, Washington: U.S. Geological Survey Professional Paper 1576, 108 p.

Atwater, B.F., Nelson, A.R., Clague, J.J., Carver, G.A., Yamaguchi, D.K., Bobrowsky, P.T., Bourgeois J., Darienzo, M.E., Grant, W.C., Hemphill-Haley, E., Kelsey, H.M., Jacoby, G.C., Nishenko, S.P., Palmer, S.P., Peterson, C.D., and Reinhart, M.A., 1995, Summary of coastal geologic evidence for past great earthquakes at the Cascadia subduction zone. *Earthquake Spectra*, 11:1, 1-18.

Beeson, M.H., Tolan, T.L., and Madin, I.P., 1991, Geologic map of the Portland quadrangle, Multnomah and Washington counties, Oregon and Clark County, Washington: Oregon Department of Geology and Mineral Industries, Geologic Map Series GMS-75.

Blakely, R.J., Wells, R.E., Tolan, T.L., Beeson, M.H., Trehu, A.M., and Liberty, L.M., 2000, New aeromagnetic data reveal large strike-slip(?) faults in the northern Willamette Valley, Oregon: Geological Society of America Bulletin, v. 112, p. 1225–1233.

Boore, D.M., and Atkinson, G.M., February 2008, Ground-motion prediction equations for the average horizontal component of PGA, PGV, and 5%-damped PSA at spectral periods between 0.01 s and 10.0 s: Earthquake Engineering Research Institute, Earthquake Spectra, vol. 24, no. 1, pp 99-138.

Campbell, K.W., and Bozorgnia, Y., February 2008, NGA ground motion model for the geometric mean horizontal component of PGA, PGV, and PGD and 5%-damped linear elastic response spectra for periods ranging from 0.01 to 10 s: Earthquake Engineering Research Institute, Earthquake Spectra, vol. 24, no. 1, pp 139-171.

Chiou, S.J., and Youngs, R.R., 2008, NGA Model for Average Horizontal Component of Peak Ground Motion and Response Spectra: Pacific Earthquake Engineering Research Center, PEER 2008/09, November 2008.

Clague, J.J., 1997, Evidence for large earthquakes at the Cascadia subduction zone: Reviews of Geophysics, v. 35, no. 4, p. 439-460.

Clague, J.J., Atwater, B.F., Wang, K., Wang, Y., and Wong, I., 2000, Penrose conference report–Great Cascadia earthquake tricentennial: GSA Today, v. 10, no. 11, p. 14-15.

Electric Power Research Institute (EPRI), 1993, Guidelines for determining design basis of ground motions. Final Report No. TR-102293, Palo Alto, California.

Fluck, P., Hyndman, R.D., and Wang, K., 1997, Three-dimensional dislocation model for great earthquakes of the Cascadia subduction zone: Journal of Geophysical Research, v. 102, no. B9, p. 20,539-20,550.

GeoMotions, 2007, D-MOD2000, A Computer Program for Seismic Response Analysis of Horizontally Layered Soil Deposits, Earthfill Dams and Solid Waste Landfills.

Goldfinger, C., 1994, Active deformation of the Cascadia Forearc–Implications for great earthquake potential in Oregon and Washington: Oregon State University, unpublished Ph.D. dissertation, 246 p.

_____, 2003, Great earthquakes in Cascadia: a who dunnit success story: presentation at 2003 EERI national conference, Portland, Oregon.

Guffanti, M., and Weaver, C.S., 1988, Distribution of Late Cenozoic volcanic vents in the Cascade Range–Volcanic arc segmentation and regional tectonic considerations: Journal of Geophysical Research, v. 93, no. B6, p. 6513-6529.

Hughes, J.M., and Carr, M.J., 1980, Segmentation of the Cascade volcanic chain: Geology, v. 8, p. 15-17.

Hyndman, R.D., and Wang, K., 1995, The rupture zone of Cascadia great earthquakes from current deformation and the thermal regime: Journal of Geophysical Research, v. 100, no. B11, p. 22,133-22,154.

Idriss, I.M., 2008, An NGA Empirical Model for Estimating the Horizontal Spectral Values Generated by Shallow Crustal Earthquakes, Earthquake Spectra, Volume 24, Number 1, pp. 217-242.

Kelsey, H.M., and Bockheim, J.G., 1994, Coastal landscape evolution as a function of eustasy and surface uplift rate, Cascadia margin, southern Oregon: Geological Society of America Bulletin, v. 106, p. 840-854.

Kelsey, H.M., Witter, R.C., and Hemphill-Haley, E, 2002, Pl.-boundary earthquakes and tsunamis of the past 5500 yr, Sixes River estuary, southern Oregon: Geological Society of America Bulletin, v. 114, no. 3, p. 298-314.

Kelsey, H.M., Nelson, A.R., Hemphill-Haley, E., Witter, R.C., 2005, Tsunami history of an Oregon coastal lake reveals a 4600 yr record of great earthquakes on the Cascadia subduction zone: GSA Bulletin, v. 117 p 1009-1032.

Leyendecker, E.V., and Frankel, A.D., February 2000, Development of maximum considered earthquake ground motion maps, in Earthquake Spectra, vol. 16, no. 1.

Mitchell, C.E., Vincent, P., Weldon, R.J., III, and Richards, M.A., 1994, Present-day vertical deformation of the Cascadia margin, Pacific Northwest, United States: Journal of Geophysical Research, v. 99, no. B6, p. 12,257-12,277.

Nelson, A.R., and Personius, S.F., 1996, Great-earthquake potential in Oregon and Washington–An overview of recent coastal geologic studies and their bearing on segmentation of Holocene ruptures, central Cascadia subduction zone, in Rogers, A.M., Walsh, T.J., Kockelman, W.J., and Priest, G.R., eds., Assessing earthquake hazards and reducing risk in the Pacific Northwest: U.S. Geological Survey Professional Paper 1560, v. 1, p. 91-114.

Personius, S.F., 1995, Late Quaternary stream incision and uplift in the forearc of the Cascadia subduction zone, western Oregon: Journal of Geophysical Research, v. 100, no. B10, p. 20,193-20,210.

Personius, S. F., Dart, R. L., Bradley, Lee-Ann, and Haller, K. M., 2003, Map and data for Quaternary faults and folds in Oregon: U.S. Geological Survey Open-File Report 03-095.

Petersen, M. D., Frankel, A. D., Harmsen, S. C., Mueller, C. S., Haller, K. M., Wheeler, R. L., Wesson, R. L., Zeng, Y, Boyd, O. S., Perkins, D. M., Luco, N., Field, E. H., Wills, C. J., and Rukstales, K. S., 2008, Documentation for the 2008 update of the United States National Seismic Hazard Maps: U.S. Geological Survey Open-File Report 2008-1128.

Satake, K., Shimazaki, K., Tsuji, Y., and Ueda, K., 1996, Time and size of a giant earthquake in Cascadia inferred from Japanese tsunami records of January 1700: Nature, V.379, pp. 246-249, 18 January.

Savage, J.C., Svarc, J.L., Prescott, W.H., and Murray, M.H., 2000, Deformation across the forearc of the Cascadia subduction zone at Cape Blanco, Oregon: Journal of Geophysical Research, v. 105, no. B2, p. 3095-3102.

Trimble, D.E., 1963, Geology of Portland, Oregon, and adjacent areas: U.S. Geological Survey Bulletin 1119.

U.S. Geological Survey, 2013, Probabilistic hazard lookup by latitude, longitude, accessed 6/12/13, from USGS website: https://geohazards.usgs.gov/deaggint/2008/

Wang, Y., He, J., Dragert, H., and James, T.S., 2001, Three-dimensional viscoelastic interseismic deformation model for the Cascadia subduction zone: Earth, Planets and Space, v. 53, p. 295-306.

Weaver, C.S., and Shedlock, K.M., 1989, Potential subduction, probable intraplate and known crustal earthquake source areas in the Cascadia Subduction Zone: U.S. Geological Survey Open-File Report 89-465, p. 11-26.

Weaver, C.S., and Michaelson, C.A., 1985, Seismicity and volcanism in the Pacific Northwest–Evidence for the segmentation of the Juan de Fuca Pl.: Geophysical Research Letters, v. 12, no. 4, p. 215-218.

Witter, R.C., 1999, Late Holocene Paleoseismicity, tsunamis and relative sea-level changes along the south-central Cascadia subduction zone, southern Oregon: University of Oregon, unpublished Ph.D. dissertation, 178 p.

Witter, R.C., Kelsey, H.M., Hemphill-Haley, E., 2003. Great Cascadia earthquakes and tsunamis of the past 6700 years, Coquille River estuary, southern coastal Oregon. Geological Society of America Bulletin 115, 1289–1306.

Wong, I., 2005, Low potential for large intraslab earthquakes in the central Cascadia Subduction Zone: Bulletin of the Seismological Society of America, vol. 95, no. 5.

Youd, T.L., and. Carter, B.L., 2005, Influence of soil softening and liquefaction on spectral acceleration, J. Geotech. Geoenviron. Eng., 131, 811–825.

Zhao J.X., Zhang, J., Asano, A., Ohno, Y., Oouchi, T., Takahashi, T., Ogawa, H., Irikura, K., Thio, H., Somerville, P., Fukushima, Y., and Fukushima, Y., 2006, Attenuation relations of strong ground motion in Japan using site classification based on predominant period: Bulletin of the Seismological Society of America, v. 96, p. 898–913.

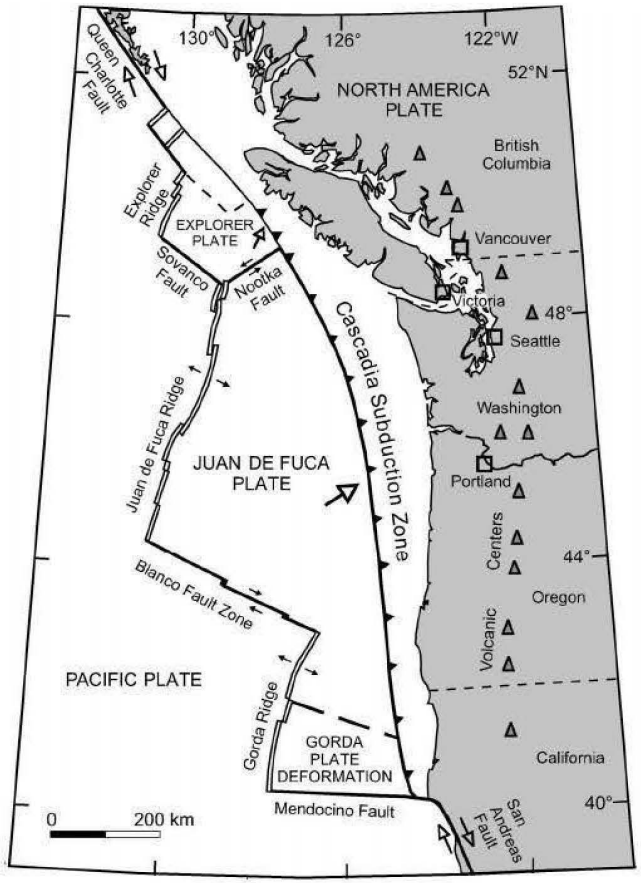

A) TECTONIC MAP OF PACIFIC NORTHWEST, SHOWING ORIENTATION AND EXTENT OF CASCADIA SUBDUCTION ZONE (MODIFIED FROM DRAGERT AND OTHERS, 1994)

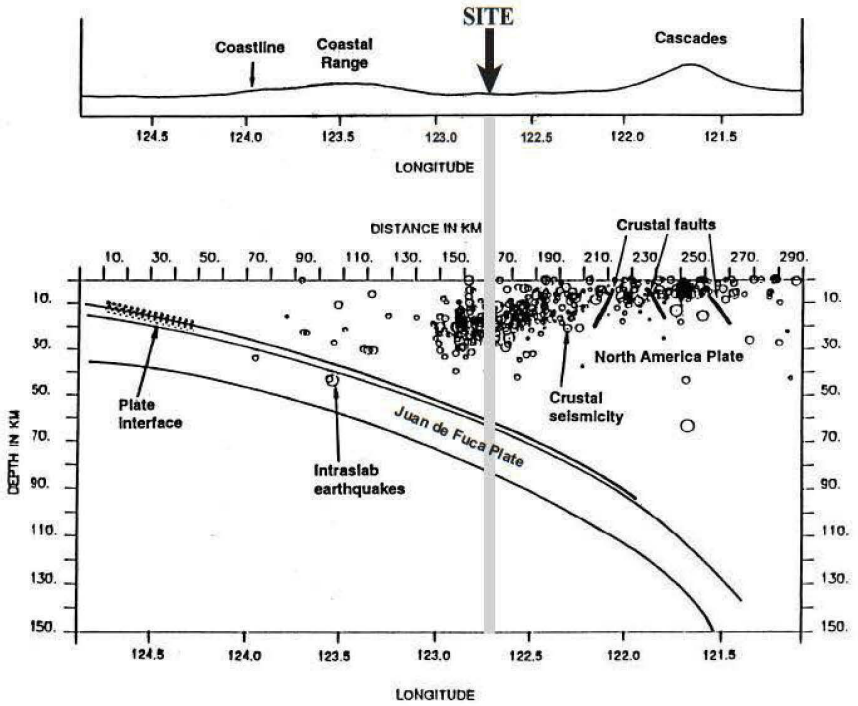

B) EAST-WEST CROSS-SECTION THROUGH WESTERN OREGON AT THE LATITUDE OF PORTLAND, SHOWING THE SEISMIC SOURCES CONSIDERED IN THE SITE-SPECIFIC SEISMIC HAZARD STUDY (MODIFIED FROM GEOMATRIX, 1995)

GRI

TECTONIC SETTING SUMMARY

SEP. 2014 JOB NO. W1114-T3 FIG. 1B

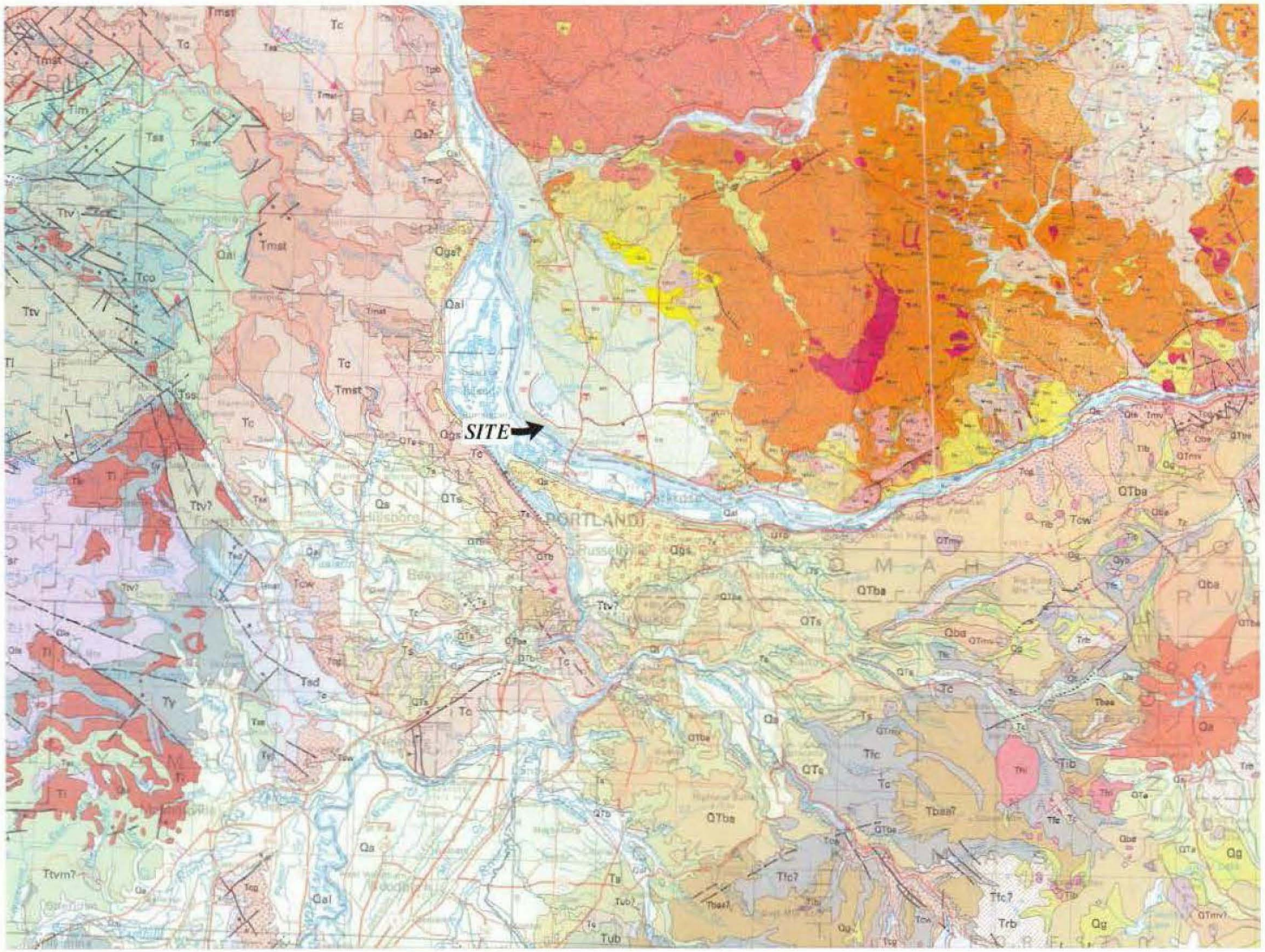

Contact — Approximately located

Fault — Dashed where inferred; dotted where concealed; queried where doubtful; ball and bar on downthrown side

Thrust fault — Dashed where inferred; dotted where concealed; queried where doubtful; sawteeth on upper plate

Strike and dip of bed

FROM:

WALSH, T.J., KOROSEC, M.A., PHILLIPS, W.M., LOGAN, R.L., AND SCHASSE, H.W., 1987, GEOLOGIC MAP OF WASHINGTON-SOUTHWEST QUADRANT; 1:250,000: WASHINGTON DIVISION OF GEOLOGY AND EARTH RESOURCES, 6M-34

WALKER, G.W., AND MACLEOD, N.S., 1991, GEOLOGIC MAP OF OREGON: U.S. GEOLOGICAL SURVEY

North

0 10 20 MILES

0 10 20 KILOMETERS

GRI

REGIONAL GEOLOGIC MAP

SEP. 2014 JOB NO. W1114-T3 FIG. 2B

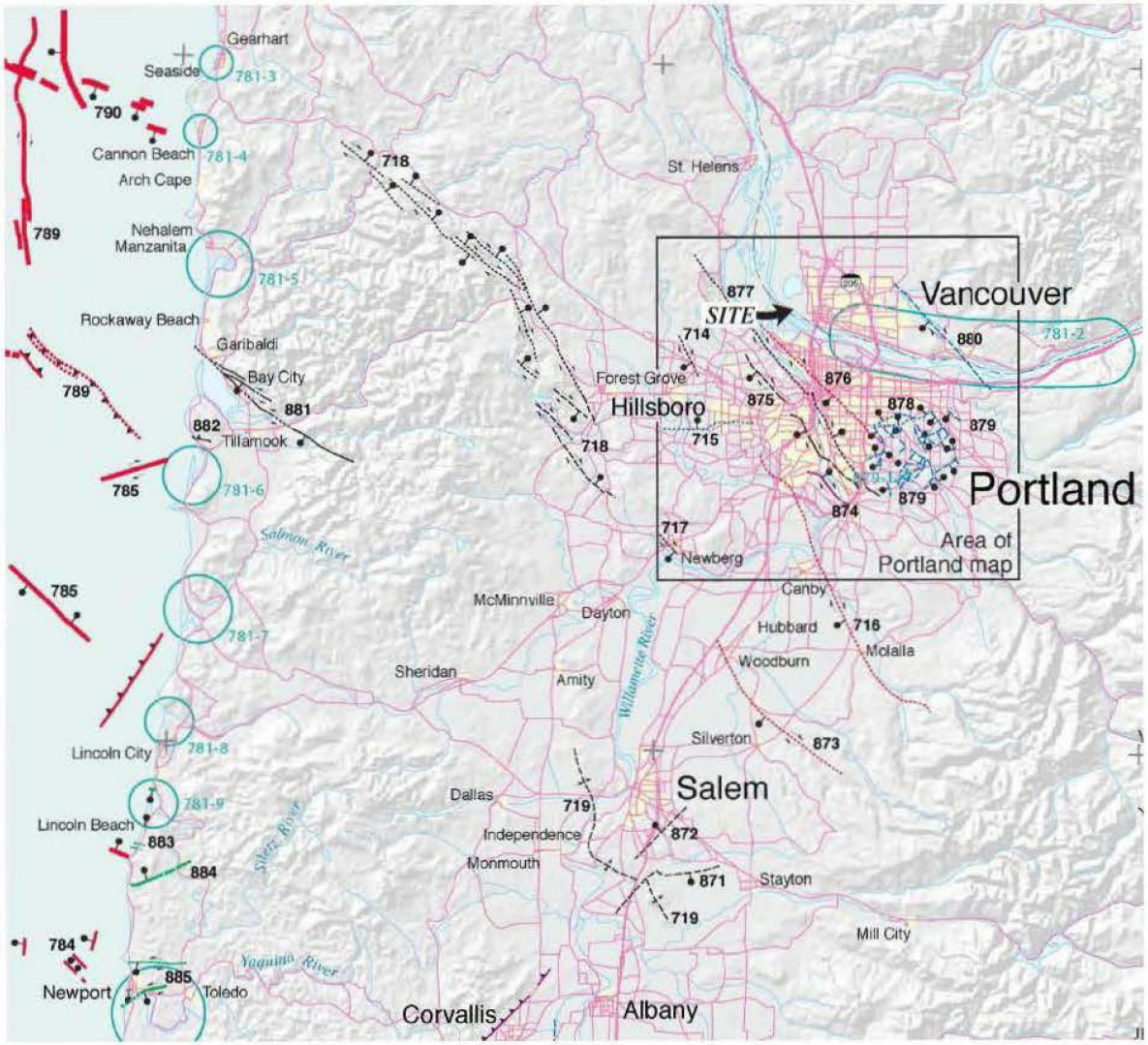

MAP EXPLANATION

TIME OF MOST RECENT SURFACE RUPTURE
- Holocene (<10,000 years) or post last glaciation (<15,000 years; 15 ka); no historic ruptures in Oregon to date
- Late Quaternary (<130,000; post penultimate glaciation)
- Late and middle Quaternary (<750,000 years; 750 ka)
- Quaternary, undifferentiated (<1,600,000 years; <1.6 Ma)
- Class B structure (age or origin uncertain)

SLIP RATE
- >5 mm/year
- 1.0-5.0 mm/year
- 0.2-1.0 mm/year
- <0.2 mm/year

TRACE
- Mostly continuous at map scale
- Mostly discontinuous at map scale
- Inferred or concealed

STRUCTURE TYPE AND RELATED FEATURES
- Normal or high-angle reverse fault
- Strike-slip fault
- Thrust fault
- Anticlinal fold
- Synclinal fold
- Monoclinal fold
- Plunge direction of fold
- Fault section marker

DETAILED STUDY SITES
- Trench site
- Subduction zone study site

CULTURAL AND GEOGRAPHIC FEATURES
- Divided highway
- Primary or secondary road
- Permanent river or stream
- Intermittent river or stream
- Permanent or intermittent lake

FAULT NUMBER	NAME OF STRUCTURE
876	EAST BANK FAULT
877	PORTLAND HILLS FAULT
880	LACAMAS LAKE FAULT
878	GRAND BUTTE FAULT

FROM: PERSONIUS, S.F., AND OTHERS, 2003, MAP OF QUATERNARY FAULTS AND FOLDS IN OREGON, USGS OPEN FILE REPORT OFR-03-095.

North

0 5 10 MILES

0 5 10 KILOMETERS

GRI

LOCAL FAULT MAP

SEP. 2014 JOB NO. W1114-T3 FIG. 3B

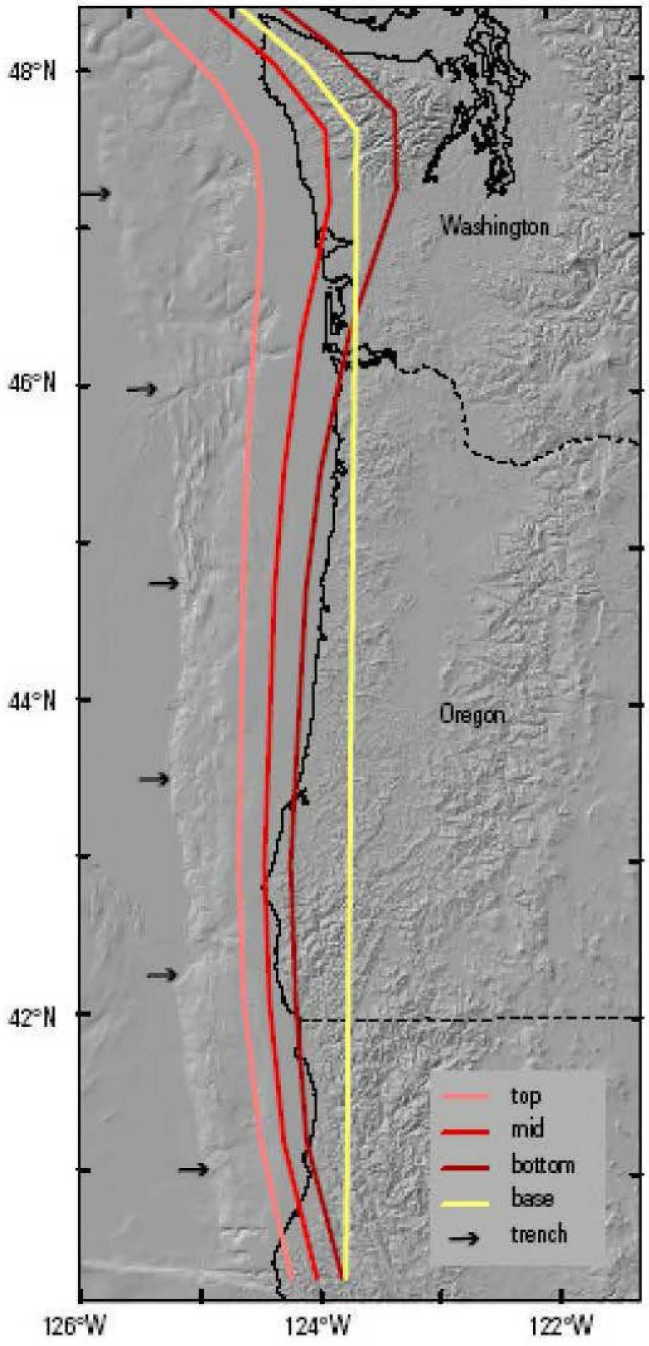

Figure 21. Location of the eastern edge of earthquake-rupture zones on the Cascadia subduction zone for the various models used in this study relative to the surficial expression of the trench: top, base of the elastic zone; mid, midpoint of the transition zone; bottom, base of the transition zones; base, base of the model that assumes ruptures extend to about 30-kilometers depth. Figure provided by Ray Weldon.

FROM: PETERSEN, MD, FRANKEL, AD, HARMSEN, SC, AND OTHERS, 2008, DOCUMENTATION FOR THE 2008 UPDATE OF THE UNITED STATES NATIONAL SEISMIC HAZARD MAPS: US GEOLOGICAL SURVEY, OPEN FILE REPORT 2008-1128

GRI

ASSUMED RUPTURE LOCATIONS
(CASCADIA SUBDUCTION ZONE)

SEP. 2014 JOB NO. W1114-T3 FIG. 4B

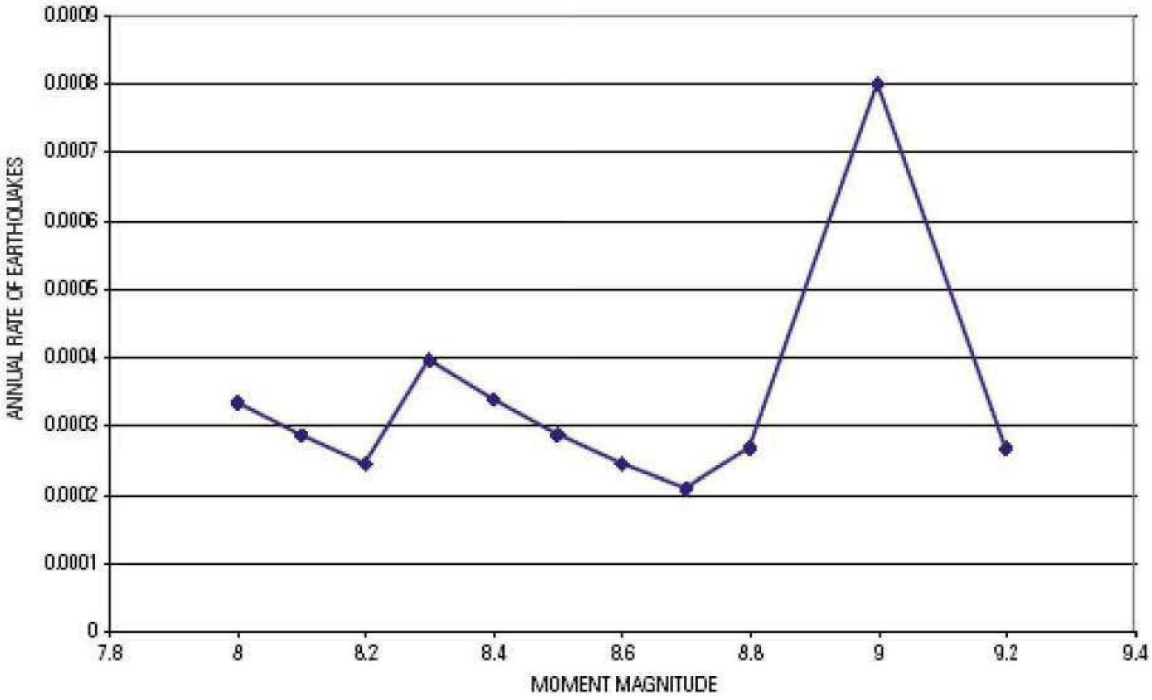

Figure 22. Magnitude-frequency distribution of the Cascadia subduction zone.

FROM: PETERSEN, M, FRANKEL, A, HARMSEN, S, AND OTHERS, 2008, DOCUMENTATION FOR THE 2008 UPDATE OF THE UNITED STATES NATIONAL SEISMIC HAZARD MAPS: US GEOLOGICAL SURVEY, OPEN FILE REPORT 2008-1128

GRI

ASSUMED MAGNITUDE-FREQUENCY DISTRIBUTION

(CASCADIA SUBDUCTION ZONE)

SEP. 2014 JOB NO. W1114-T3 FIG. 5B

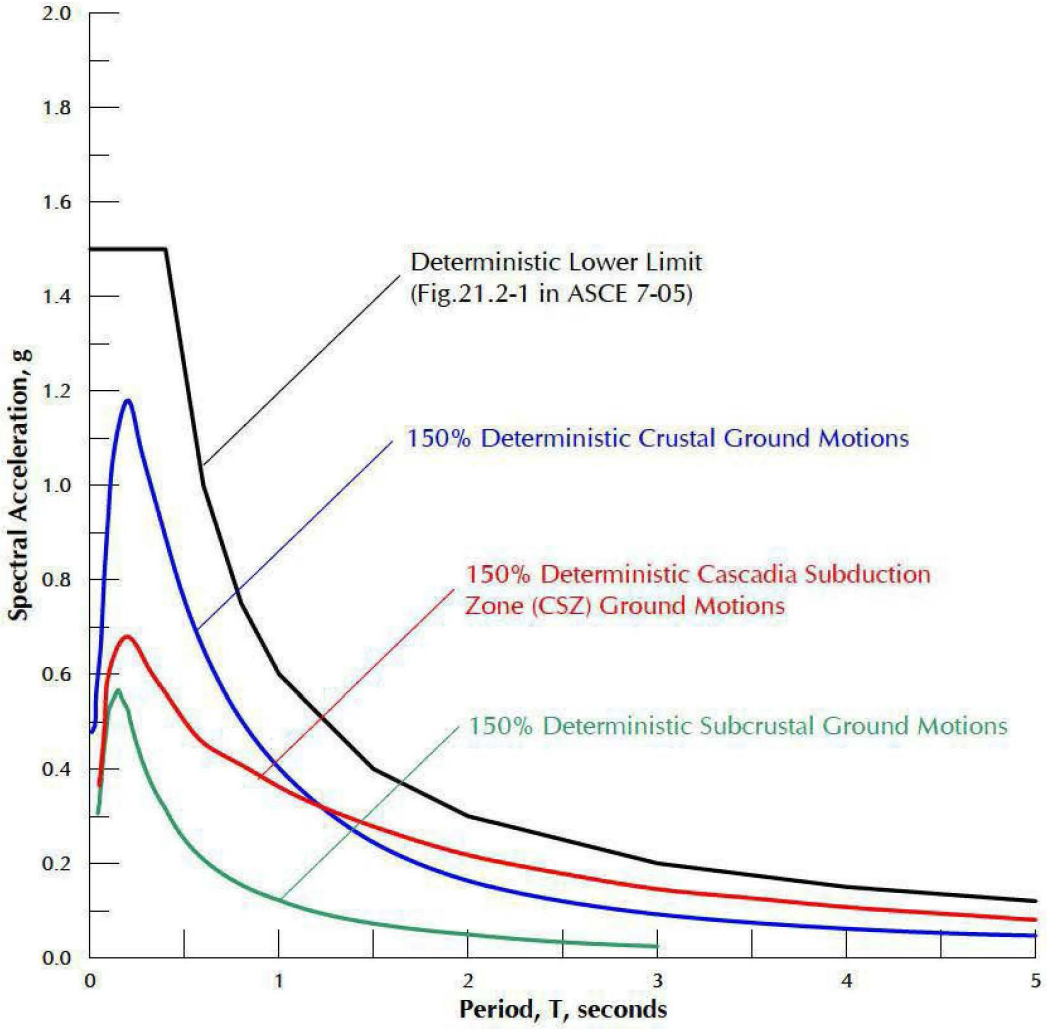

GRI

DETERMINISTIC MCE
BEDROCK RESPONSE SPECTRA COMPARISON
(5% DAMPING)

SEP. 2014 JOB NO. W1114-T3 FIG. 6B

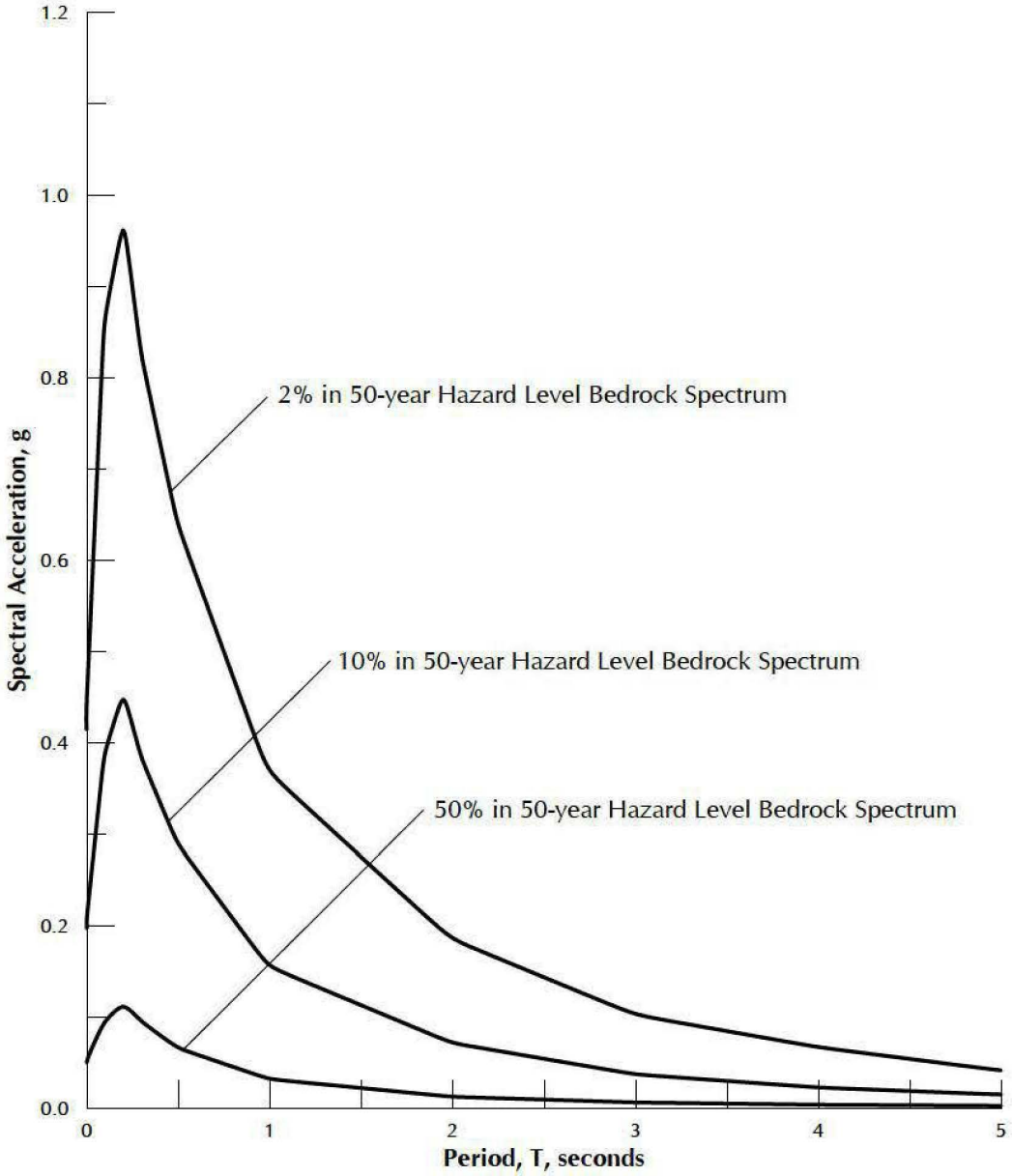

GRI

BEDROCK RESPONSE SPECTRA FOR
DIFFERENT PROBABILISTIC HAZARD LEVELS
(5% DAMPING)

SEP. 2014 JOB NO. W1114-T3 FIG. 7B

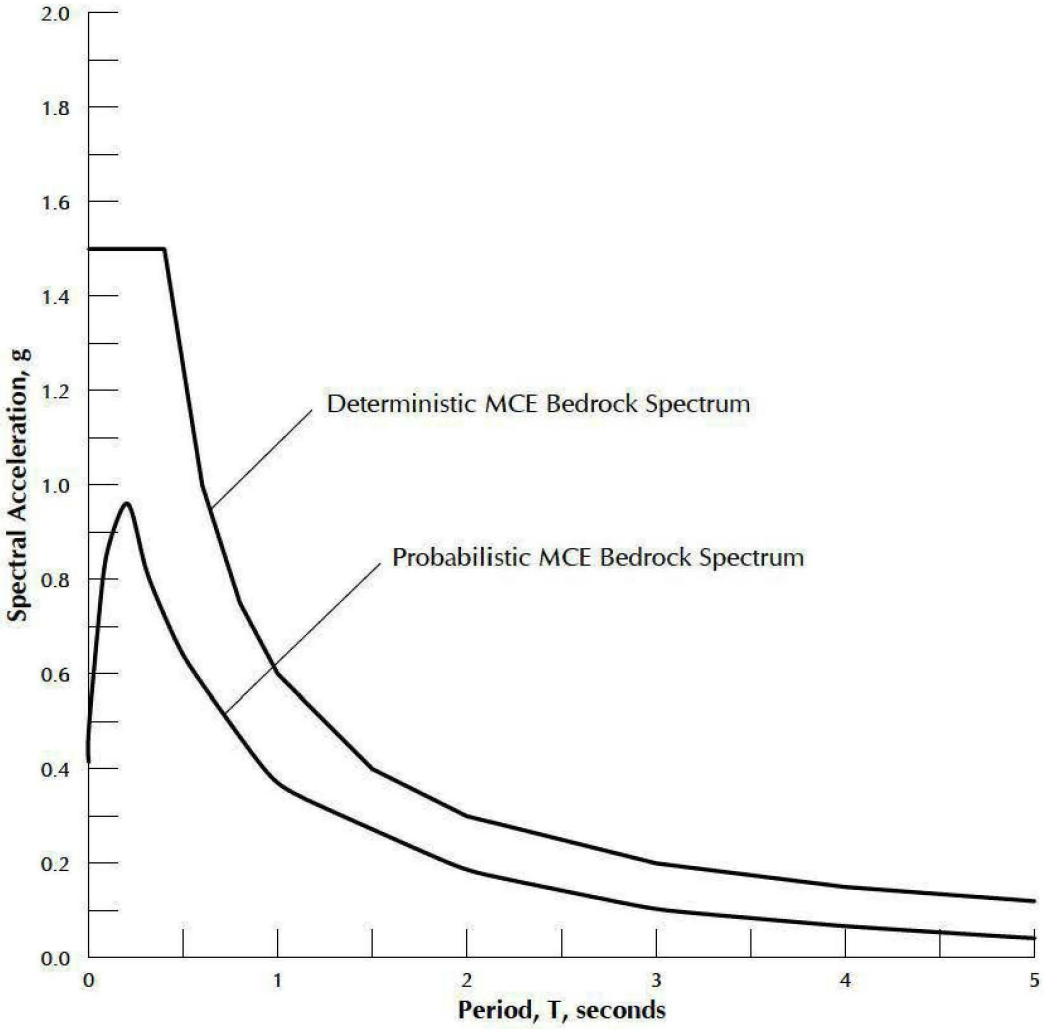

GRI

DETERMINISTIC AND PROBABILISTIC MCE
BEDROCK RESPONSE SPECTRA COMPARISON
(5% DAMPING)

SEP. 2014 JOB NO. W1114-T3 FIG. 8B

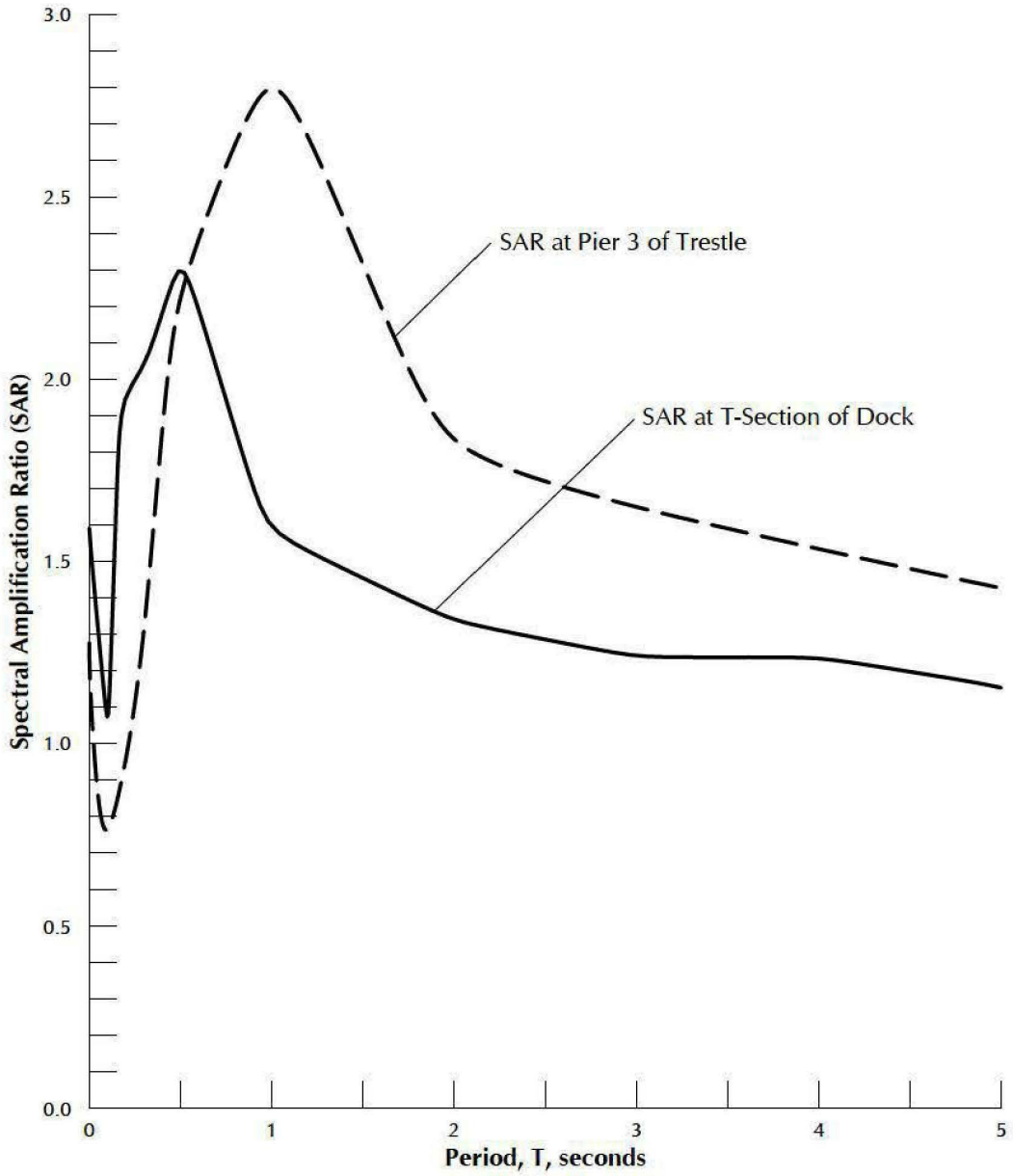

GRI

SPECTRAL AMPLIFICATION RATIO (SAR)
FOR CLE (475-YEAR) HAZARD LEVEL

SEP. 2014 JOB NO. W1114-T3 FIG. 9B

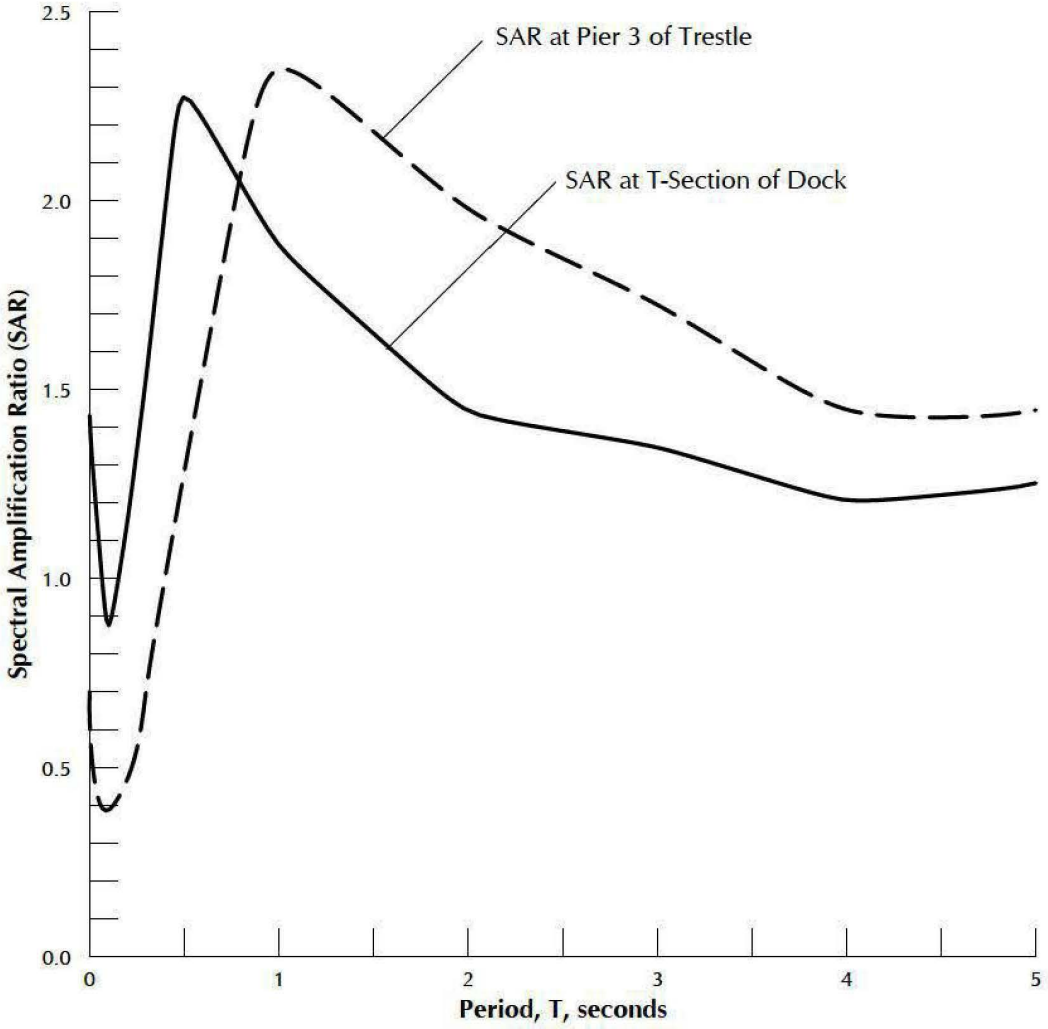

GRI

SPECTRAL AMPLIFICATION RATIO (SAR)
FOR MCE (2,475-YEAR) HAZARD LEVEL

SEP. 2014 JOB NO. W1114-T3 FIG. 10B

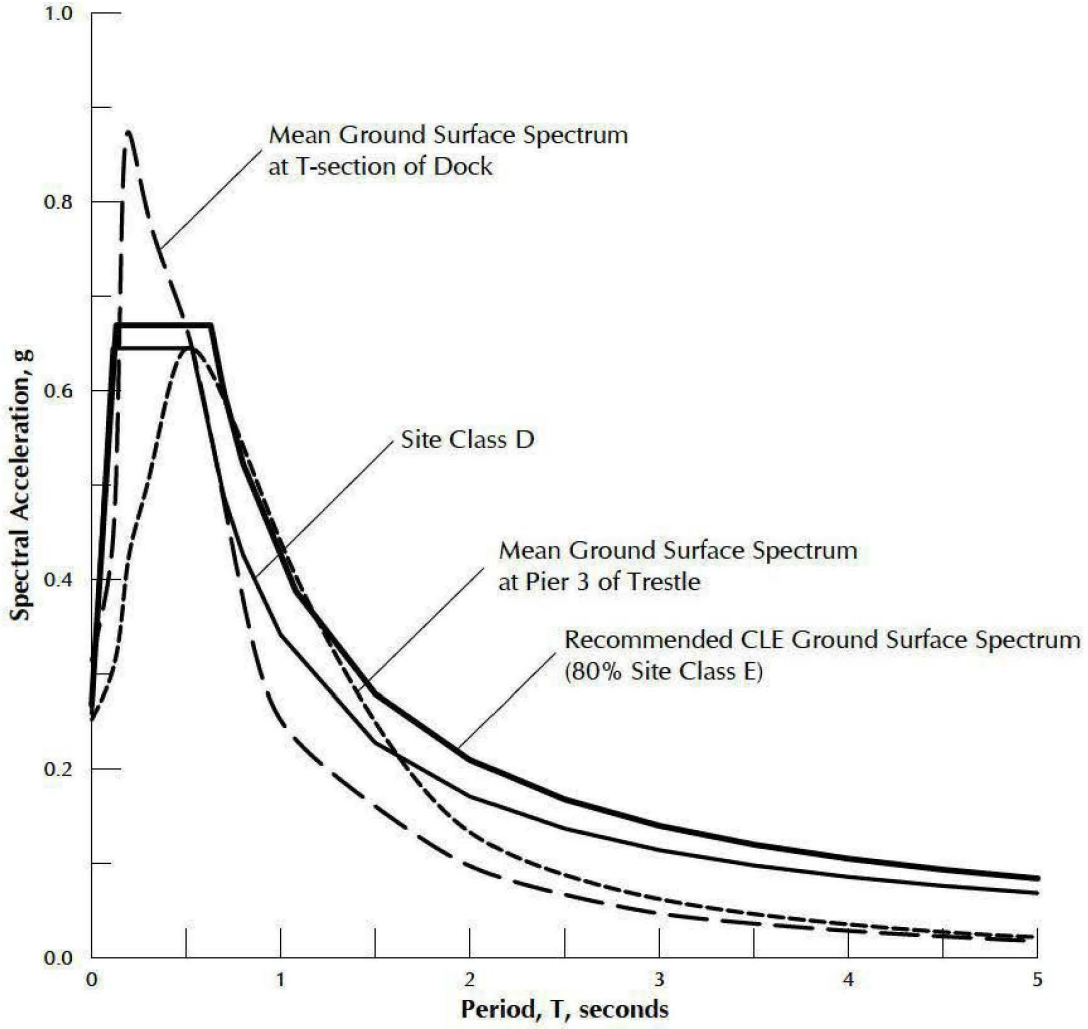

GRI

CLE GROUND SURFACE RESPONSE SPECTRA

(5% DAMPING)

SEP. 2014 JOB NO. W1114-T3 FIG. 11B

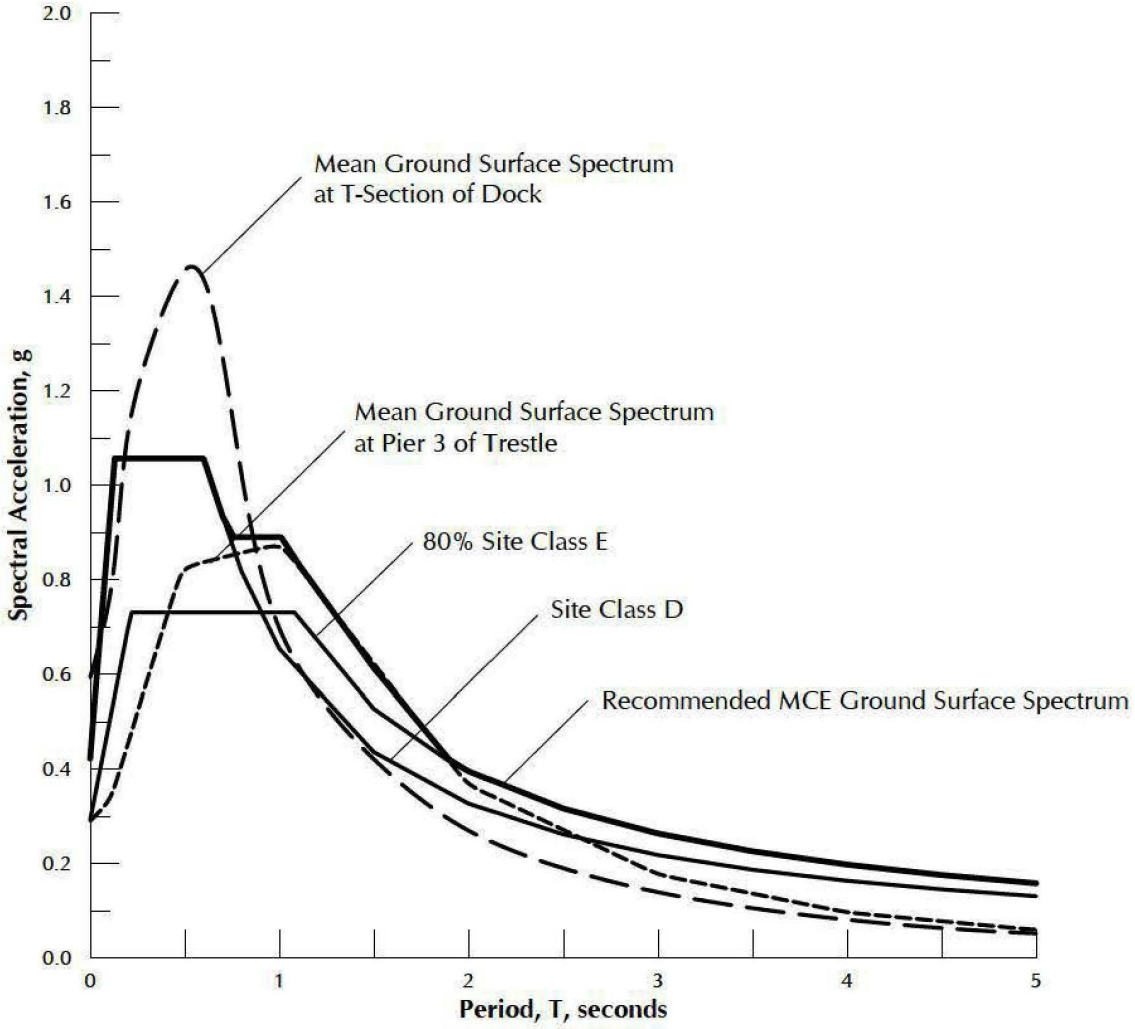

GRI

MCE GROUND SURFACE
RESPONSE SPECTRA
(5% DAMPING)

SEP. 2014 JOB NO. W1114-T3 FIG. 12B

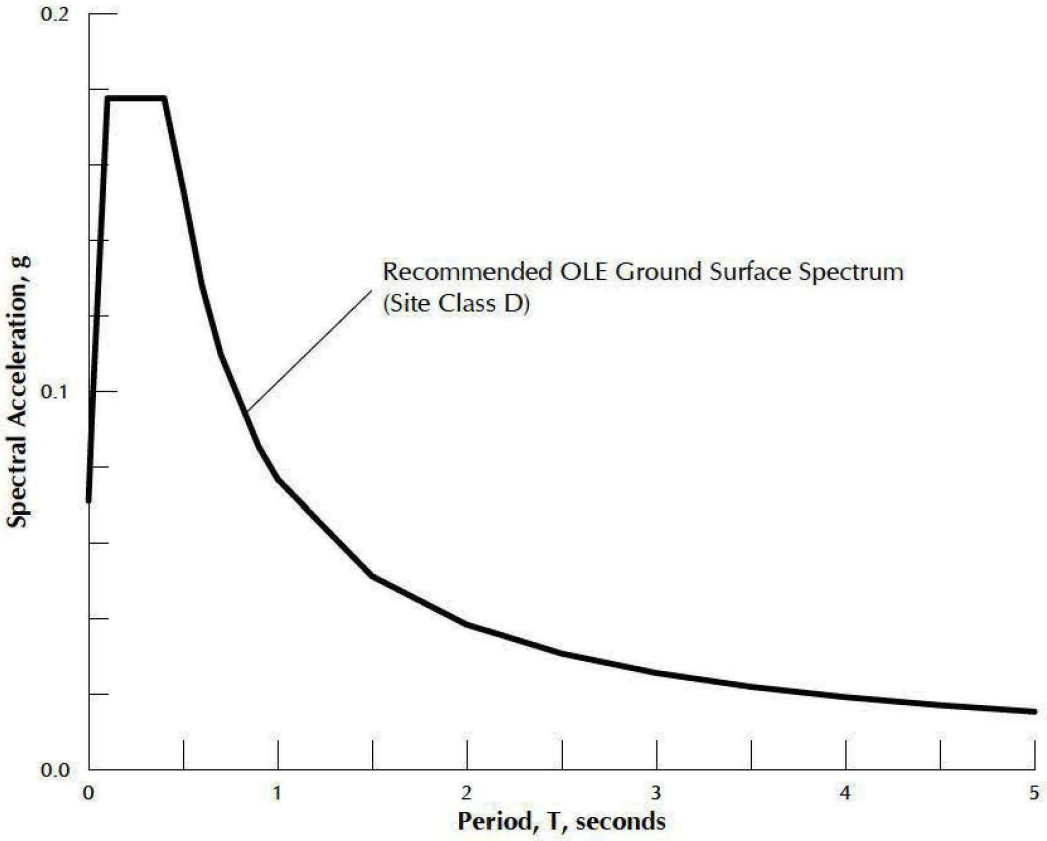

GRI

OLE GROUND SURFACE
RESPONSE SPECTRUM
(5% DAMPING)

SEP. 2014 JOB NO. W1114-T3 FIG. 13B

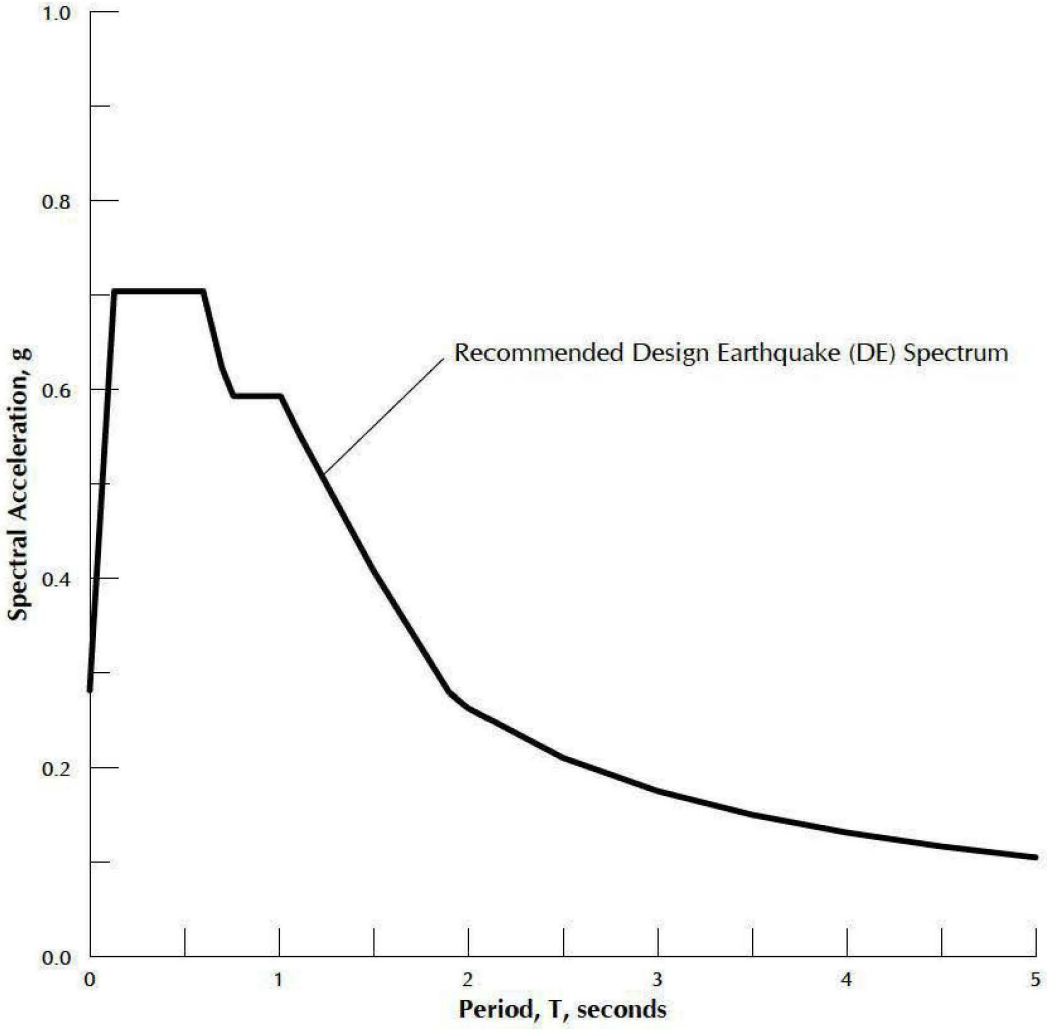

GRI

DE (2/3 MCE) GROUND SURFACE RESPONSE SPECTRUM
(5% DAMPING)

SEP. 2014 JOB NO. W1114-T3 FIG. 14B